Max-Planck-Institut
für Meteorologie

REPORT No. 191

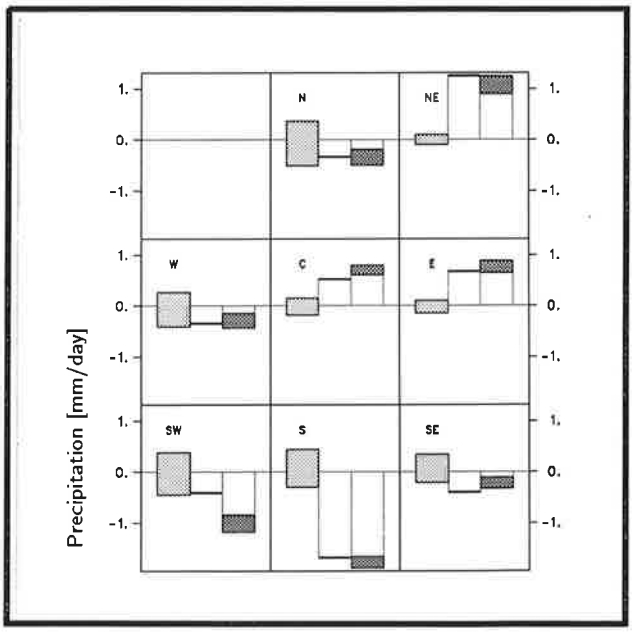

VALIDATION OF PRESENT-DAY REGIONAL CLIMATE SIMULATIONS OVER EUROPE: NESTED LAM AND VARIABLE RESOLUTION GLOBAL MODEL SIMULATIONS WITH OBSERVED OR MIXED LAYER OCEAN BOUNDARY CONDITIONS

by

Bennert Machenhauer • Martin Windelband • Michael Botzet
Richard G. Jones • Michel Déqué

HAMBURG, February 1996

AUTHORS:

Bennert Machenhauer
Martin Windelband
Michael Botzet

Max-Planck-Institut
für Meteorologie

Richard G. Jones

Hadley Centre
for Climate Prediction and Research
Meteorological Office
London Road
Bracknell, Berkshire
RG 12 2SZ
GB

Michel Déqué

Météo-France
Centre National de Recherches Météorologiques
42, Avenue Gustave Coriolis
F - 31057 Toulouse Cedex
France

MAX-PLANCK-INSTITUT
FÜR METEOROLOGIE
BUNDESSTRASSE 55
D-20146 Hamburg
F.R. GERMANY

Tel.: +49-(0)40-4 11 73-0
Telefax: +49-(0)40-4 11 73-298
E-Mail: <name> @ dkrz.de

REPb 191

ISSN 0937 – 1060

Validation of present-day regional climate simulations over Europe: nested LAM and variable resolution global model simulations with observed or mixed layer ocean boundary conditions

Bennert Machenhauer, Martin Windelband, Michael Botzet

Max Planck Institute for Meteorology, Germany,

Richard G. Jones

Hadley Centre for Climate Prediction and Research, Meteorological Office, UK

and

Michel Déqué

Météo-France, Centre National de Recherches Meteorologiques, France

ISSN 0937-1060

Hamburg, February 1996

Abstract

Multi-year high resolution present-day climate simulations were made with two limited area models (LAMs) at UKMO and MPI and with a global variable resolution spectral model at Météo-France. We shall refer to these models as the regional climate models (RCMs). Together with the RCM simulations we verify the similar multi-year simulations made with the corresponding coarse resolution global models. We refer to these models as the GCMs. They are the two coarse resolution GCMs whose output were used for boundary conditions to the LAM simulations and a homogeneous coarse resolution version (T42) of the Météo-France GCM. In the Météo-France and the MPI simulations observed (AMIP) SST and sea-ice distributions were used whereas in the UKMO simulations we used SST and sea-ice distributions determined from a mixed layer ocean model coupled to the GCM.

In the present assessment the main emphasis is put on the validation of precipitation and surface air temperature simulations. The relatively large biases or systematic errors in these parameters in both the GCM and RCM simulations seem in most cases to be explained as the result of systematic errors in the surface pressure (or the low level flow) and in the cyclone activity. In most remaining cases they seem to be due to defects in specific physical parameterization schemes.

The UKMO and Météo-France simulations are 10-year integrations whereas the MPI simulations are integrations of 46-months only. For the MPI GCM simulation it is shown, however, that the 46-month integration is representative of a 10-year one. It is argued that the same most likely is the case also for the MPI RCM simulation. It is furthermore demonstrated for the MPI GCM that the bigger biases found represent what may be called "long term systematic errors", i.e. biases which will appear also in integrations over several decades and thus are not just due to decadal variations. It is argued that most likely this is the case also for the other simulations considered.

As expected increased resolution gives generally improved orographic precipitation. Also synoptic systems seem more realistic in the high resolution simulations with sharper fronts and often deeper lows. As evidenced from maps of standard deviations of band-pass filtered 500 hPa heights the cyclone activity increases with resolution. This is generally an improvement. The validation has shown, however, that a regional increase of resolution alone does not solve the problems. Before useful local and regional simulations can be produced certain parameterization schemes involved must be improved. Equally important is a reduction of the dynamical systematic errors, i. e. systematic errors in fields characterising the large scale general circulation, which are also causing large regional and local scale biases in temperature and precipitation. A large integration area for the MPI RCM simulations was chosen to allow a possible reduction of these dynamical errors. Only in winter do we find slight improvements in the biases of surface pressure with increasing resolution, while there were insignificant changes or even small deteriorations in the other seasons. Similar results were found for the Météo-France simulations. The too low pressure in the UKMO simulations was found to decrease further with resolution consistent with the increase in cyclone activity. The increase of cyclone activity with increasing resolution was a deterioration for the UKMO simulations as it was already too high in the GCM simulation, whereas for the MPI and partly also for the Météo-France simulations it was an improvement.

The systematic errors in temperature and precipitation are of the same order of or larger than the changes expected due to increase in greenhouse gas concentrations (at least to the 2xCO2 level). Therefore, at the present state of development it seems that the high resolution climate change scenarios that can be produced by the dynamical regionalization techniques tested here are not yet accurate enough to be directly used for impact studies.

1.0 Introduction

For meaningful climate change impact studies realistic simulations of the local climate are needed. Of particular importance in this context is the simulation of severe weather phenomena. A prerequisite for an accurate numerical simulation of the local climate is that the numerical model used explicitly resolves physiographic features, as the land-sea distribution and the detailed orography, which are of importance for the local climate. This requires a high resolution. A high resolution is also needed to simulate accurately the development of weather systems, and in particular those which give rise to severe weather phenomena. Due to limited computer power the resolution that can be used in the global coupled atmosphere-ocean models (CGCMs) used for long climate simulations (at present T42) is far from sufficient. Therefore different approaches to obtain simulations of higher resolution are presently being developed. Each of these approaches build on the time-slice technique in which a certain period (say 10 years) in a long CGCM simulation is being repeated using a high resolution atmospheric model which takes initial and sea surface boundary conditions from the CGCM simulation.

- The first approach is to use a higher resolution global model, an AGCM.
- A second approach is to use a variable resolution global model in which the highest resolution is over an area of interest.
- A third approach is to use a high resolution limited area model (LAM) centred over an area of interest and taking also lateral boundary conditions from the low resolution CGCM simulation.

Presently it is possible by the first approach to reach a resolution of T106 (maximum grid length in the transform grid, dmax=125 km) (e.g. Wild et al., 1995b and Déqué and Piedelievre, 1995).

In a specific experiment the second approach has so far been used to get resolutions which vary between T220 and T106 over Europe (dmax between 60 and 125 km) and decreases down to T18 (dmax=740km) in the southern Pacific Ocean. With the available computer power the 60 km grid length is about the maximum resolution that can be achieved using this approach.

The third approach was pioneered by Dickinson et al. (1989) and it was used in the first regional climate change experiments for Europe by Marinucci and Giorgi (1992) and Giorgi et al.(1992). With boundary fields from a T42 spectral model (or an equivalent grid point model) LAM simulations with grid lengths (dmax) between 50 and 60 km are presently being produced. Using boundary conditions from such LAM simulations (J. Hesselbjerg Christensen, personal communication) or from T106 time-slice simulations (Marinucci et al.,1994) experiments indicate that higher resolution LAM simulations (grid lengths 20-30 km on a smaller integration area) are feasible. Thus by this nested LAM approach the highest resolutions can be achieved.

In the EC project "Regionalization" (1 January 1993 - 31 March 1995) and its follow-on project "Regionalization of Anthropogenic Climate Change Simulations" (1 May 1994 - 30 April 1996), both coordinated by Bennert Machenhauer, 8 European institutions started tests of the second and the third approach aiming specifically at climate simulations for Europe. The main objective of the projects was to further develop and test these dynamical regionalization tech-

niques, utilizing a series of high resolution LAMs and the variable resolution global model referred to above. The performance of different LAMs and different boundary relaxation techniques should first be tested with "perfect" boundary forcing fields (ECMWF analyses) by validation against the analyses and surface observations from the period in question. These tests might reveal model deficiencies which one should then try to remove. Accordingly several LAMs have been tested and tuned in this way using boundary conditions from a common period, 1 January 1990 - 31 August 1991. The common validation over Europe of all the simulations was performed at the Danish Meteorological Institute, DMI (Christensen et al.,1996). A second step should be to perform high resolution present-day climate simulations with the LAMs nested in AMIP GCM simulations (Gates,1992).The variable resolution global model should also be tested with such "perfect" ocean boundary conditions. These regional simulations should then be evaluated against available climatological data, i.e. analyses (gridded data) and if necessary surface station data. The estimated accuracy would constitute first estimates of upper bounds of the accuracy that can be expected in regionalization of CGCM climate change simulations, with the same dynamical techniques. This validation might reveal further deficiencies of the regional models which should then, if possible, be eliminated before they were utilized in the third project step. This third and final project step should be to make high resolution regional simulations with time-slice lateral and/or lower boundary conditions from new (T42 or equivalent grid point resolution) CGCM climate change scenarios, i.e. in each case a time-slice from a control simulation and a time-slice from a transient simulation at the time of an equivalent 2xCO2 greenhouse gas concentration. Second estimates of upper bounds of the accuracy of the regionalization of CGCM climate change simulations should then be made by a validation of the control simulations against the available climatological data.

The present report deals with the second project step presenting a validation and inter-comparison of regional climate simulations for Europe performed with more or less "perfect" ocean boundary conditions. Multi-year high resolution simulations have been made with two LAMs at UKMO and MPI and with a global variable resolution spectral model at Metéo-France. We shall refer to these models as the regional climate models (RCMs). Together with the RCM simulations we consider the similar multi-year simulations made with the corresponding coarse resolution global models. We refer to these models as the GCMs. They are the two coarse resolution GCMs whose output were used for boundary conditions to the LAM simulations and a homogeneous coarse resolution version (T42) of the Metéo-France GCM. In the Météo-France and the MPI simulations observed (AMIP) SST and sea-ice distributions were used whereas in the UKMO simulations we used SST and sea-ice distributions determined from a mixed layer ocean model coupled to the GCM.

The common validation over Europe which includes all six simulations, three RCM and three GCM simulations, were performed at the coordinating institute, MPI.

In the remaining part of the present section the model versions used, the simulations performed and the climatological data used will be described. In Section 2 the simulated precipitation and surface air temperature will be presented and their relation to resolution, physical parameterization and systematic errors in surface pressure and cyclone activity will be discussed. Finally, Section 3 contains further discussions of the results and our conclusions.

1.1 Models

The UKMO models are described in some detail in Jones et al. (1995), hence only a brief description will be given. The RCM is a limited area atmospheric model covering a domain shown in Figure 1.2 (the hatched area in the uppermost map). The corresponding GCM is a global atmospheric model which is coupled to a mixed layer ocean model. Both the RCM and the GCM belong to the UKMO Unified Forecast / Climate Model (UM) system. Their physical and dynamical formulations are thus identical, apart from certain details of the diffusion and filtering. The atmospheric component of the UM is a primitive equation grid point model using a terrain-following hybrid vertical coordinate (Simons and Burridge,1981). There are 19 levels. The horizontal coordinate system is the spherical latitude-longitude system. The RCM domain is placed around the Equator in a rotated system in order to have a quasi-homogeneous grid. (Therefore no filtering of short wave lengths along latitude circles near the poles are needed, as in the GCM where a Fourier filtering must be performed to keep reasonable length of time steps). The horizontal resolution of the GCM is 2.75° x 3.75° (250 km spacing at 50° N) and that of the RCM is 0.44° x 0.44° (50 km spacing). The models use the same comprehensive physical parameterization package including all the usual processes. Generally the parameterization schemes used are different from the corresponding ones used at Metéo-France and MPI. The following differences might be of special interest. Firstly, the UM uses fractional coverage of sea-ice in a grid cell whereas the other models use either full or no ice coverage in a cell. Thus in the UM formulation the effect of sub-grid scale leads in the ice pack may be taken into account, this is not possible in the formulations of the other models. Secondly, no moisture convergence closure is used in the UM convective precipitation scheme as in that of the other models. The occurrence of convection is determined solely by the static stability. A convective precipitation scheme with a similar closure has been implemented in a newer version of the MPI physical package (ECHAM4) than the one (ECHAM3) which is used in the present simulations and the introduction of fractional ice coverage is considered for implementation in the next version. In the present UKMO simulations, the atmospheric GCM is run coupled to a 50 m mixed layer ocean model and a thermodynamic sea-ice model. The latter models predict SST, ice concentration, ice depth and depth of snow at each ocean grid point. In a one-way nesting technique, the RCM is driven at its lateral and lower sea surface boundaries by time series of data archived from a previous integration of the coupled GCM. At the lateral boundaries the relaxation to the GCM values of the prognostic variables are made with linearly decreasing weight inward over a zone of four grid length. The GCM values used at the lateral boundaries are obtained by linear interpolation in time from values saved every six hours. The values used at the sea point lower boundaries are interpolated from fields saved every 5 days.

The Météo-France GCM is a climate version of the spectral ARPEGE-IFS model developed by Météo-France and ECMWF (Déqué et al., 1994). It is a primitive equation model using the same horizontal and vertical coordinates as the UKMO models. The physical parameterization package is mainly that of the Météo-France operational model, with some additions such as treatment of the ozone concentration as a 3-D prognostic variable, a higher vertical resolution in the stratosphere (20 levels out of the 30 are above 200hPa) and a soil-vegetation scheme with rainfall interception. This model offers the possibility of varying the horizontal resolution by a stretching which maintains local isotropy, i.e. the angles are preserved. A pole of stretching de-

termines the point of maximum resolution and a stretching factor how much the resolution is increased in this point. The Météo-France RCM used here is a stretched version of the ARPEGE climate model with a T63 resolution, pole of stretching in the Tyrrherian sea (40° N, 12° E) and a stretching factor of 3.5. The resulting horizontal resolution is shown in Figure 1.2 (the middlemost map). It varies between T106 and T 220 over Europe and decreases down to T18 in the southern Pacific. The grid length in the transform grid varies between about 60 km at the pole of stretching and 750 km at the antipole. When we refer to "the corresponding GCM" we mean a usual homogeneous T42 resolution version of the ARPEGE model with a grid length in the transform grid of about 300 km. A more detailed description of the Météo-France models used in the present experiments may be found in Déqué and Piedelievre(1995).

The GCM of MPI, called ECHAM, is also a spectral primitive equation model. The horizontal and vertical coordinates used is as in the other models. The horizontal resolution is T42 and it has 19 levels. It has a comprehensive physical parameterization package including all the usual processes. The version used in the present simulations is ECHAM3, which is described in Roeckner et al. (1994) and documented in more details in DKRZ (1994). The RCM of MPI is called HIRHAM. It combines the adiabatic part of the HIRLAM model, developed by the Nordic, Dutch and Irish meteorological services, with the ECHAM3 physical parameterization package (Christensen and Meijgaard, 1992). It is a limited area primitive equation grid point model. The vertical hybrid coordinate, the vertical levels and the vertical finite difference schemes are the same as in ECHAM3. Like the UKMO RCM the HIRHAM uses a rotated latitude-longitude grid. The resolution is 0.51°x0.51° corresponding to a grid length of about 55 km. The domain covered is shown in Figure 1.2 (lower map). As in the UKMO RCM the HIRHAM prognostic fields are relaxed to those of an ECHAM simulation in a boundary zone. The standard width of this zone is 10 grid lengths and the fractional weight given to the ECHAM fields in this zone is shown in Figure 1.3. The ECHAM boundary fields are interpolated in space and time from 6-hourly output of an ECHAM simulation made in advance. A short description of the HIRHAM model version used here is given in Christensen et al. (1996) and more detailed descriptions of the adiabatic part are given in Machenhauer(1988) and Källberg (1989).

1.2 Climate simulations

In the present assessment we present results from six multi-year present-day climate simulations. The simulations are made with the above described GCMs and RCMs of UKMO, Météo-France and MPI.

Results from a 10-year integration of their RCM under present-day conditions (1 x CO2) and from the corresponding 10-year integration of the driving GCM were supplied by UKMO. The SST and sea-ice distributions in the coupled mixed-layer-ocean/atmosphere GCM simulation, and hence also in the RCM simulation, were found to be very similar to the observed seasonally varying climatological fields (Jones et al.,1995).

The integrations with the ARPEGE model, which were supplied by Météo-France, were two 10-year integrations, one with the T63 stretched model version and one with the T42 version. In both integrations AMIP sea surface conditions were used (the observed mean monthly SST

and sea-ice fields from the period 1979-1988).

The integrations supplied by MPI to the present assessment are a 46-month HIRHAM integration and the corresponding integration with the driving T42 ECHAM3 model. Both models have used the first 46 months of the AMIP data as lower boundary sea surface conditions. The HIRHAM version used here differs somewhat from the "large area" version described in Christensen et al. (1996). The same large area (Fig. 1.2) was used here but whereas the standard 10-point boundary relaxation zone has been used in Christensen et al. (1996) the present version used a 30-point zone. The 30 point zone was introduced in order to avoid an unrealistic increase of total mass in the integration domain which occurred in some preliminary winter month simulations when using the original 10-point zone. After the completion of the 46-month integration it was discovered that the spurious increase in total mass were due to an error in the procedure used to prepare the ECHAM boundary fields. The ECHAM velocity fields should have been multiplied by 1/cos(phi) where phi is the latitude in the rotated coordinate system. As a consequence the magnitude of the imposed velocities have been slightly smaller than they should have been, up to about 10% at the northern and southern boundaries. The fractional weights used in the 30-point zone is shown in Figure 1.3. Note that the weights decrease rapidly to very small values over the last 10-20 points. The preliminary experiments had shown that with this 30-point relaxation zone the spurious increase in the total mass, which apparently was due to the small but in some cases systematic errors in the ECHAM velocities, could be controlled. We believe that also other possible effects of the errors in the boundary field are negligible when using the 30-point zone. This was the case at least for the first month of the integration which was repeated with correct ECHAM velocity fields applied in the boundary relaxation. Another difference between the present HIRHAM version and the version used by Christensen et al. (1996) is that here no corrections to simulate diffusion of moisture along pressure surfaces are included in the linear fourth order horizontal diffusion scheme. This older diffusion scheme was used also in the small area integration with "perfect" boundary conditions presented in Christensen et al. (1996) and it was speculated that it could have caused the excessive July precipitation in mountain areas found in that integration. Finally it should be mentioned that the following changes were introduced in the ECHAM3 soil-vegetation scheme in both the present large area HIRHAM version and the one used in Christensen(1995). The soil moisture holding capacity were increased from 20 cm to 35 cm and new "forest" and "vegetation" fields (with substantially reduced values of coverage) were introduced. These changes anticipate changes which have been introduced in the new ECHAM4 soil-vegetation scheme and they were made in order to counteract an excessive drying out and heating of the surface in summer over central Europe which were found in a previous test integration.

1.3 Climatological data

Simulated surface pressure and upper air fields will be evaluated against climatology derived from ECMWF analyses. Except for relative humidity this climatology is based on 14 years of data (1979, 1981-1993). For relative humidity 6 years of data (1981-1986) is used.

The main emphasis will be put on the validation of simulations of precipitation and surface air temperature. Here we evaluate against new climatological data for Europe produced by the Climate Research Unit (CRU) of University of East Anglia, Hulme et al. (1995). A preliminary

version of these data was kindly made available by the Climate Impacts LINK Project. The data covers land points in Europe in a 0.5° x 0.5° latitude-longitude grid (in the following referred to as the CRU grid). Here land points are defined as grid cells with a non-zero fraction of land, whereas in the models land points are defined as grid cells with more than 50% land. This climatology is based on data from the period 1961-90, for temperature and precipitation using 1500 and 2300 stations, respectively. Interpolation of the station data to the CRU grid was done by fitting a partial thin plate smoothing spline (e.g. Hutchinson, 1991), in which elevation is included along with latitude and longitude as a predictor of the climate surface. For each parameter the data in each grid cell are given for a minimum, an area mean and a maximum value of the height of the surface topography. We have, however, used only the data determined for the mean height of the orography. This mean orography, shown in Figure 1.1, most closely matches the orography of the models which are shown also in the figure. The model orographies in Figure 1.1 were plotted from values in the CRU grid obtained by interpolations from the model grids. This may have introduced some smoothing of the RCM orographies. The land-sea masks used in this and subsequent figures were obtained by interpolating the model land sea masks (fields of fractions of land having the value 1 in land points and 0 in sea points) to the CRU grid and then selecting as land points only those points with more than 50% land which are also land points in the CRU data. Actually daily minimum and maximum temperature were analysed by Hulme et al.(1994) and from these the daily mean surface air temperature we are using was defined as a simple average.

For each variable Hulme et al. (1994) validated the performance of their method of analysis at 100 independent observation sites. They found for January and July that the mean absolute error (MAE) for maximum and minimum temperature was between 0.5°C and 0.8°C and for precipitation between 9% and 12%. For precipitation they also compared the mean-elevation CRU climatology with the Legates/Willmott climatology (the version not corrected for gauge-undercatch; Legates and Willmott, 1990). The Legates/Willmott climatology has previously often been used for validation of regional climate simulations (e.g. Jones et al.,1995 and Déqué and Piedelievre, 1995). Over most lowland areas of "greater Europe" the agreement is generally good between Legates and the mean-elevation CRU fields, over many of the larger mountainous areas, however, both large absolute and relative differences are apparent, in all cases the CRU climatology being wetter than Legates. This is broadly as expected, since in upland areas where precipitation is generally largest, gauge locations are biased towards lower elevations (Legates had no elevation dependency in his interpolation scheme therefore could not correct for this bias). Hulme et al. (1994) concludes that the CRU estimates for many of the mountain areas in mainland Europe (e.g. the Alps, Norway, the Balkans) are likely to be more realistic than those of Legates.

For monthly mean temperatures and precipitation the CRU data set includes also fields of anomalies in the same 0.5° x 0.5° grid over the "greater European" area for each month in the 30 year period 1961 to 1990 (Barrow et al., 1993). They are based on previous more coarse mesh global analyses (for temperature at 5° latitude by 5° longitude resolution (Jones, 1994) and for precipitation at 2.5° latitude and 3.75° longitude resolution (Hulme, 1994)). They will be used in the following to define the observed (or natural) decadal variability in certain sub-areas of Europe against which time-slice biases can be compared.

2.0 Precipitation and surface air temperature biases and their relation to resolution, physical parameterization and systematic errors in surface pressure and cyclone activity

We shall consider in this section fields of seasonally averaged systematic errors or biases. When referring to a systematic error or a bias for a given season we mean an average over the years in the integration period of the deviation of the seasonal mean from the ECMWF or the CRU climatology. All fields will be shown on the domain used in Figure 1.1, our common verification area, which we shall refer to as the CRU domain.

In Figures 2.1 - 2.8 we present for each season (DJF, MAM, JJA, and SON) the ECMWF climatology and values from the six model simulations of the averaged mean sea level pressure (MSLP) and the standard deviation of band pass filtered (2.5 - 6 days) 500 hPa heights. The latter fields give an indication of the position of the cyclone tracks and the level of cyclone activity (Blackmon, 1976). Included in the figures are also maps of the seasonally averaged systematic errors in MSLP for the six simulations.

Figure 3.1 shows for the four seasons vertical profiles of the ECMWF climatological temperature and relative humidity averaged over the CRU domain. Figures 3.2 - 3.5 show profiles of the seasonal biases (or systematic errors) in these variables for the UKMO and the MPI simulations (such profiles are not available for the Météo-France simulations). Finally, Figures 3.6 and 3.7 show profiles of differences between the biases in the RCM and the GCM simulations.

Maps showing the CRU seasonal averaged climatological precipitation and surface air temperature over land are included in Figures 4.1 - 4.8 (the top-most maps). Below these maps in the same figures are shown the seasonally averaged systematic errors in precipitation and surface air temperature for the six simulations. In order to be able to compare better the observed CRU values of surface air temperature and the various simulated values of this variable, each of which refers to different orographies (i.e. Figure 1.1), they have all been reduced to mean sea level (MSL) using a laps rate of 0.65 K per 100 m.

The European land area within the CRU domain has been divided in 9 sub-areas as shown in Figure 5.1. In Tables 1.1 and 1.2 are listed the magnitude of the mean seasonal systematic errors in reduced surface air temperature and precipitation, respectively, averaged over the land points in each of the 9 sub-areas and over all land points in Europe. Finally, Figures 5.2 - 5.5 show the seasonal variation, month by month, of land point precipitation and reduced surface air temperature for each of the 9 sub-areas for the six simulations and for the CRU climatology.

We shall see that the systematic errors in precipitation and surface air temperature to a large extent can be explained by a too coarse resolution orography, especially in the GCMs, errors connected to systematic errors in surface pressure, the level of cyclone activity, the position of cyclone tracks and defects in certain physical parameterization schemes, i.e. those of vegetation-soil processes and possibly radiation.

2.1 Effects of coarse resolution orography

Typical error patterns which are due to lack of resolution in the model orographies are seen in many of the precipitation error maps of all three GCMs (Figures 4.1, 4.3, 4.5 and 4.7). The po-

sition of the narrow maxima in the CRU climatological precipitation are clearly related to the location of the main mountain chains, situated at the up-slope or at the tops of the CRU mountains, shown in Figure 1.1. In the GCM the corresponding maxima are smooth large scale patterns, often with less extreme values. When the CRU precipitation is subtracted from the smooth GCM simulated patterns the narrow CRU maxima show up in the difference map as narrow minima, often with negative values, surrounded by one or more maxima due to the orographic precipitation which is simulated in the GCM and not compensated by the CRU maxima. As an example consider the systematic errors in precipitation simulated by ECHAM in the spring season, Figure 4.3. The narrow maximum in the CRU precipitation over the Alps and the former Yugoslavia (the top-most map, left column) appears as a negative pattern in the ECHAM - CRU precipitation map and here we see also three large scale maxima, one northwest of, one north of and one north-east of the mountain chain, each of which are situated on up-slope sides of the smooth ECHAM mountains. Other examples are the autumn precipitation errors over UK in all three GCM simulations shown in Figure 4.7.

In the RCM simulations higher resolution orographies, which fit the CRU orography more closely, have been used. We should therefore expect that the above described error patterns would be more or less absent or at least reduced in the error maps of the RCMs (even the RCM orographies are generally of a coarser resolution than the CRU orography (Fig. 1.1) and furthermore the smallest scales are damped more or less by diffusion in the models). There is a clear tendency of reduced errors in the RCM simulations. Examples can be seen by comparing the error fields of the above mentioned GCM simulations with those of the corresponding RCM simulations in Figures 4.4 and 4.8, respectively. In most cases the errors have been reduced substantially. It is, of course, not enough to have an improved orography. Often other errors, e. g. in the mean low level flow or the level of cyclone activity, influence the simulation of orographic precipitation and prevent the benefits of the higher resolution from being realised.

There is a clear tendency of too much precipitation at the mountain tops in all three RCM simulations when the surrounding air at low levels is not too dry. Examples are the RCM simulations of precipitation in spring shown in Figure 4.4. The error patterns are seen to be highly correlated with the orographies in Figure 1.1. The reason for these errors is most likely that the horizontal diffusion of moisture, which is performed at the terrain following model levels, transport moisture from the low levels to the mountain tops. As mentioned previously the horizontal diffusion scheme in a newer version of HIRHAM has been modified in order to eliminate this spurious moisture flux.

In the temperature error maps of the GCMs and to some extent also in those of the RCMs relative minima and even negative values are often seen at the positions where the model and the CRU orographies differ the most. Examples can be seen in the GCM spring temperature error maps in Figure 4.3 in the Alp-Balkan region. These errors may not be real as they may be caused by the reduction to MSL of the surface air temperatures. We may have used a too simple or even unrealistic procedure in the reduction to MSL. If a representative lapse rate in reality is (numerically) smaller than the 6.5°C per km we have used even perfect simulations would have error patterns similar to those found here.

2.2 Effects of systematic errors in surface pressure, cyclone activity and physical parameterization

The systematic errors in precipitation and reduced surface air temperature in Figures 4.1 - 4.8 can in many cases be related to the systematic errors in MSLP (Figures 2.1 - 2.8). Figure 2.1 shows for the winter season the MSLP systematic errors of the GCMs (right hand column). The pattern of errors is seen to be somewhat similar for the three models. For the UKMO model we see a saddle pattern with too high pressure in the northern and southern part and a belt of relatively low pressure between a western and an eastern minimum. In the ARPEGE simulation the southern maximum is stronger and more eastward and the western minimum is shifted north-eastward and intensified considerably compared with the UKMO simulation. For the ECHAM model the southern maximum is shifted north-east and too high pressure prevails over most of Europe between the southern and northern maximum.

In the MSLP systematic error patterns the western minimum is connected with a southward or south-eastward displaced and in some cases too deep Icelandic low. The eastern minimum corresponds to a too deep and/or too easterly placed eastern European trough. The southern maximum is due to a weakened or even a reversed Mediterranean low, or in other words a subtropical high pressure instead in this area. The northern maximum corresponds to a weakening of the north-eastward extension of the Icelandic low.

For the other seasons similar patterns of systematic MSLP errors are found for the GCMs. In each season each RCM has a systematic error pattern which resembles that of the corresponding GCM. The differences between the GCMs (or between the RCMs) of different institutions are much larger than between each GCM and the corresponding RCM. For each model the pattern varies in form and in amplitude from season to season, with the largest amplitude in winter and the smallest in summer. In the maps of MSLP (in the left hand columns of Figures 2) the isobars of the MSLP may approximately be taken as stream lines for the seasonally averaged low level flow (above the boundary layer, assuming approximate geostrophic balance). The systematic errors in the MSLP imply systematic errors in this flow, in both strength and direction, and consequently they imply systematic errors in the advection of moisture and heat into Europe, in particular from the Atlantic. We shall see that in many cases such systematic errors in advection seem to explain the systematic errors in precipitation and surface air temperature.

This is the case for all the models considered here but in particular for the ARPEGE models. For both these models a characteristic error pattern, all year round, is too strong advection from the Atlantic. Another important MSLP error pattern is a pattern with too high pressure over southern Europe, i.e. an extreme northerly position and large values of "the southern maximum". For the MPI model simulations in particular this error pattern significantly influences precipitation and temperature in the winter and adjacent seasons. In the winter time the Mediterranean low is more or less eliminated in these simulations. Instead of relatively unstable conditions the atmosphere is stabilized by subsidence and the usual winter rain is suppressed.

A third error pattern, which is characteristic for the UKMO models, is a pattern with a connection between the "eastern" and "the western minimum" giving too low pressure in a belt across Europe. As this pattern is accompanied with too high cyclone activity excessive precipitation is simulated in this belt.

2.2.1 The Météo-France simulations

The most clear relation between systematic errors in the dynamic fields and those in precipitation and temperature is found in the ARPEGE simulations. They have throughout the year the largest systematic errors in MSLP.

Starting with the T42 simulation for the winter season (Fig. 2.1) we see that for this simulation the systematic errors in MSLP imply that the gradient south of about 60° N is much larger than in the climatology and consequently that the westerly flow is much too strong. The too strong mean advection of warm moist air from the relatively warm Atlantic results in excessive precipitation and temperature over most of Europe (Fig. 4.1).The cyclone track is seen to be shifted southward (5-7 degrees of latitude) compared to the climatology and cyclone activity is reduced over most Europe. In spite of the reduced cyclone activity the much too strong westerlies lead to too much precipitation. Sub-area biases go up to about 4.6°C and 102% of the climatological precipitation as seen in Table 1.2 and 1.1, respectively.

In the corresponding RCM we see (Figure 2.2) that the pattern of the MSLP systematic errors is rather similar to that of the T42 simulation. The extreme values have been reduced slightly, i.e. the southern maximum from 9 to 7 hPa and the western minimum from -19 to -17 hPa, and they have been shifted eastward and northward, respectively. As a consequence of these changes to the systematic errors in the surface pressure the too strong westerlies are situated somewhat more northerly. This is the case also for the cyclone track now extending deeper into Europe at latitudes of southern Scandinavia. The track is still too southerly in the sense that the branch extending north-eastward over the Norwegian Sea in the climatology is not simulated by the T63s model. The level of activity has increased but is still in the T63s inferior to that in the climatology. Due to the increased strength of the westerly flow the resulting systematic errors in precipitation and temperature (Figure 4.2) is again too much precipitation and too high temperatures over most Europe. The magnitude of the errors have, however, generally decreased compared to those in the T42 simulation. The largest sub-area biases are 4.6°C and 89%. Due to an almost realistic representation of the Scottish mountains and the too strong westerly flow the precipitation here is now slightly overestimated. At the northern part of the Norwegian west coast there is slightly less precipitation than observed. The reason could be that the averaged flow, as was the case in the T42 simulation, is approximately parallel to the mountain range, with a slight component across the range from the eastern side. The southern maximum in MSLP systematic error is moved west-north-westward in the T63s simulation and covers all the countries around the Mediterranean. As a consequence, due to the stabilizing effect of too much subsidence, too little precipitation is simulated at many places here.

In spring the ARPEGE T42 simulated pressure is too high over the Mediterranean and too low in a belt along approximately 60° N (Fig. 2.3). Between these extremes the westerly flow is much too strong and north of about 60° N the flow is easterly, almost opposite to the observed. The cyclone track is situated too far south and extends, with increased level of activity compared to the climatology, over Europe at about 50°N.The too strong westerlies and the enhanced cyclone activity explain the excessive precipitation at the mid-latitudes (here referring to the belt between approximately 45° and 60° N). Note that the two main maxima in excess precipitation are situated at the up-slope side of the maxima in the model orography which sup-

ports their explanation by the excessive advection. Except for some areas which are too cold the deviations from the CRU climatological temperatures are relatively small. This is in agreement with the fact that a westerly flow should not advect heat from the Atlantic at mid-latitudes at this time of the year (as indicated in the CRU mean temperature map in Figure 4.3 since the 10° C isotherm follows closely the 50° N latitude circle). The pattern of the cold areas resembles that of the difference between the orography of the model and the CRU data. Therefore it could be caused by the way we have reduced the temperatures to MSL. North of about 60° N the errors in precipitation and temperature may be explained by the erroneous easterlies if we assume that cold, relatively dry air is being advected from the east in the model. The cold temperatures in the north-eastern area might also be due to late snow melt in the area resulting from too much winter snow. The peak values of sub-area averaged biases are 1.4°C and 111%.

In the corresponding ARPEGE T63s simulation (Figures 2.4 and 4.4) the pattern of systematic errors in MSLP has changed somewhat. The southern maximum has increased and has moved northward and the belt of too low pressure is now situated at the northern boundary of the map. As a consequence the belt of too strong westerlies has moved northward and is now centred at latitudes around Denmark. The cyclone activity has increased with a cyclone track across Europe at about the same latitudes. As expected from this picture southern Europe gets too little precipitation and northern Europe too much. As mentioned above the advection of heat from the Atlantic this time of the year should be small. In agreement with that we see that the temperatures simulated are close to the observed over most western Europe though they are too cold over eastern Europe. Over north-east Europe this may, as suggested be due to late snow melt. The peak values of sub-area averaged biases are close to those of the T42 simulation.

In summer the ARPEGE T42 systematic errors in the MSLP (Figure 2.5) imply too strong westerlies in a belt between approximately 45° N and 65° N. In agreement with this too much precipitation and too low temperatures are simulated (Fig.4.5).The maxima in excess precipitation in central Europe are again situated on the up-slope of the T42 mountains. East of these model mountains an area with too little precipitation and too high temperatures may be noted. This is probably caused by an unrealistic drying out of the soil as discussed below for the T63 simulation for which it is even more pronounced. The cyclone activity is slightly reduced but this time of the year the convective precipitation should dominate over the large scale frontal rain connected mostly with the cyclones. The magnitude of the sub-area averaged biases go up to -3.7°C and 90%.

In the ARPEGE T63s simulation the pressure error maximum over southern Europe has intensified and moved northwards as has the northern error minimum (Fig. 2.6). Consequently, the area affected by the anomalous westerlies are now north of about 50° N whereas the area south of this is influenced by the too high pressure. The cyclone activity has increased and become higher than in the climatology over northern Europe. In agreement with this pattern it is too wet and too cold in the northern part (sub-area "N" has biases of -3.3°C and 110%) and too dry and at many places too warm in the southern part of Europe (sub-area "SE" has biases of 0°C and -41%). Note that the most excessive dry and warm areas in south-east are situated south and east of the model mountains and thus are areas sheltered from the moist and cold air from the Atlantic. The surface pressure is only slightly too high in this area and thus excessive subsid-

ence is not likely to explain the deficit of precipitation and the high temperatures here. Most likely the cause is a drying out of the soil in the model as explained in more details below in connection with the MPI simulations.

In autumn the ARPEGE T42 systematic errors in MSLP (Fig. 2.7) imply again too strong westerlies over most of Europe (north of the Alps) and we find (Fig. 4.7) in agreement with this too much precipitation (up to a bias of 49% in sub-area "NE") even though the cyclone activity is slightly reduced. As in the spring we should in the autumn expect neither cold nor warm advection by westerly winds from the Atlantic, and in agreement with that only relatively small temperature deviations from the climatological values are found north of the Alps, mostly less than 1° C. An exception is areas north of approximately 60°N where the Atlantic is warmer than the land. Thus, the positive biases found here might be explained by the excessive advection from the sea. Elsewhere, over most Europe the temperature biases are negative, at some places they are below - 2°C, especially south of the Alps (-3.0° C in sub-area "S"). Some of the cold areas may be due to the reduction to MSL but in addition there seem to be an overall cold bias which is not easily explained by errors in the dynamical fields and is therefore most likely due to errors in the physical parameterization schemes.

In the ARPEGE T63s autumn simulation the southern maximum in MSLP systematic errors has increased and has moved northward and so has the northern minimum. The too strong westerlies are now north of about 55° N (Fig. 2.8). The cyclone activity compares well with the climatology except in the south where it has decreased slightly. The systematic errors in precipitation agree with this, wet north of 55° N (a bias of 35% in "NE") and dry over southern Europe (-30% bias in "SW") (Fig 4.8). The temperature biases are again generally negative except over northern Scandinavia and Finland where the positive biases may be explained by the excessive advection from the Atlantic. The negative biases over southern Europe has increased (extreme sub-area biases -4.0°C in "S" and -2.6°C in "SE") which may be explained by the advection of cold air from north-east and east around the centre of too low pressure over the Alps. Again the overall cold bias, which has increased compared to the T42 simulation, is hard to explain by errors in the dynamical fields.

2.2.2 The MPI simulations

In the systematic MSLP errors in winter of the ECHAM simulation (Fig. 2.1) the southern maximum is stronger and more northerly than in the ARPEGE simulations. As a consequence southern Europe is too dry (-48% bias in "S"). The flow over north-western Europe is of the correct strength but from a too southerly direction, i. e. south-westerly rather than west-south-westerly in the climatology. Therefore the air advected over north-west Europe must be warmer and more moist than in reality. The cyclone track is twisted too and the cyclone activity is reduced compared to the climatology. Consequently, the advection over north-west Europe gives too high temperatures (the bias in sub-area "W" is 2.8°C) and in spite of the reduced cyclone activity too much precipitation (in "NE" the bias is as high as 101%) (Fig.4.1). In the north-eastern corner of the map the MSLP gradient is reduced compared to the climatology, and therefore the strength of the low level westerly flow is reduced. This might explain why the temperatures simulated there are too low.

The simulation with the corresponding RCM, HIRHAM has systematic errors in the MSLP (Fig. 2.2) which are rather similar to those with ECHAM, but the magnitude of the extremes are slightly reduced. The cyclone activity is increased compared to the ECHAM simulation, but it is still lower than in the climatology. The resulting general pattern of the HIRHAM systematic errors in precipitation and temperature (Fig. 4.2) are very similar to those of ECHAM (Fig. 4.1), but as expected the pattern of the orographic precipitation is improved in the HIRHAM simulation (the precipitation bias in "NE" is reduced to 75%).

The ECHAM simulation in spring has relatively small systematic pressure errors in most of Europe and the cyclone activity is again weaker than in the climatology (Fig. 2.2). Apart from the errors related to the smooth model orography there is a deficit of precipitation and too high temperatures in the Mediterranean countries (Fig 4.2) (biases 1.1°C and -35% in "SW") in agreement with the slightly too high pressure there (Fig. 2.2). The too low temperatures in central and south-eastern Europe may be caused by the reduction to MSL. North of approximately 60° N the simulated weak easterlies instead of the observed west-south-westerlies may explain the low temperatures and too much precipitation (biases of -2.8°C and 81% in "NE"). As for the ARPEGE models the cold temperatures in the north-eastern area might also be due to late snow melt resulting from excessive winter snowfall.

The systematic errors in pressure for the HIRHAM simulation in the spring (Fig. 2.3) are again rather similar to those of the ECHAM simulation (Fig. 2.2). The southern maximum has decreased slightly and the eastern minimum increased a little. Slightly too low pressure dominates now in an east-west belt whereas in the ECHAM simulation it was slightly too high. In agreement with that the cyclone activity is increased with a track east-west over southern Scandinavia and is almost at the level of the climatology. The large scale patterns of precipitation and temperature errors are similar to that of ECHAM but the precipitation error has increased over northern Europe (biases 105% and 110% in sub-areas "NE" and "E", respectively) in agreement with the increased cyclone activity and too low pressure there.

For the summer season the ECHAM MSLP systematic errors are very small and the cyclone activity (rather low at this time of the year) is close to observed though the track is too far to the north. Thus, over northern Europe, north of approximately 55° N, the cyclone activity is increased slightly and consistently the MSLP is a little low and there is slightly too much precipitation (17.2% bias in "NE"). The cloud cover is probably also increased which might explain the low temperatures simulated in this region (a -2.6°C bias in "NE").

South of about 55° N too little precipitation and too high temperatures are simulated (biases in "SW" 3.5°C and -62%). In this case the cause seems to be a drying out of the soil in the model over areas in southern Europe, i. e. water available for evaporation has become insufficient. In summer advection from the Atlantic is small and dry air is supplied from above by subsidence in the more or less prevailing ridge of high pressure that covers the region. The region will loose water by run-off and by a net flux of water vapour in the atmosphere out of the ridge region. Consequently the soil moisture decreases. This drying out process is most likely initiated in the model because of an overestimation of the clear sky solar radiation reaching the ground. Wild et al. (1995a) identified in a stand alone validation of the ECHAM3 radiation scheme such an overestimation of up to 50 W/m^2 for daily maximum values of incoming short wave fluxes un-

der cloud-free summer conditions. This may have caused too high temperatures locally during the spring and early summer causing an excessive evaporation of soil water all of which is not returned to the soil as precipitation (due to run-off and advection out of the region). Eventually, we find that the evaporation decreases, because the soil moisture reaches the minimum level in more and more grid points. Then the cloud cover and the precipitation will decrease further because less water vapour will be available and the temperature will rise further because more solar radiation reaches the surface due to less clouds and because less heat will be used for evaporation.

We see the same drying out symptoms in precipitation and temperature errors over south-eastern Europe in the UKMO and the Météo-France GCM simulations, although less pronounced than in the ECHAM simulation. That the drying out process and its effects on temperature and precipitation become especially pronounced and widespread in the MPI model seems to be a consequence of the excessive short wave radiation and of the facts that it has the weakest mean advection of moisture from the Atlantic in the summer season and that for that model there has been a particular large deficit of precipitation in the preceding seasons over southern Europe, as seen in Figure 5.2.

The HIRHAM systematic MSLP errors for the summer season resembles those of the ECHAM except that here negative errors dominate over the whole verification area, though still with relatively small magnitudes. The cyclone activity is increased compared to the ECHAM simulation and is again similar to that in the climatology with the track too far to north and a corresponding increase in precipitation (55% bias in "NE"). As in the ECHAM simulation it seems likely that also the cloud cover is increased, again explaining the low temperatures (a -2.2°C bias in "NE"). Also too little precipitation and too high temperatures are simulated south of about 55° N (biases in "SW" are 3.5°C and -48%) due to drying out of the soil. The same symptoms, but less pronounced or widespread, are seen in the UKMO and the Météo-France RCM simulations. Generally the errors are larger in the RCMs than in the corresponding GCMs, especially for temperature. In each case this seems to be a consequence of the differences in systematic errors of MSLP and the differences in the model orographies. The HIRHAM, for instance, is wetter in a belt between 50° N and 60° N due to stronger westerlies there and the main deficit in precipitation and the too high temperatures are south and east of the relatively high and sharp Alp-Carpathian mountain chain, which in HIRHAM block advection of moist air from the Atlantic. In the ECHAM the much smoother mountains do not have the same blocking effects and there is even up-slope over the Balkans at about 20° E explaining the relative maximum in precipitation (Fig. 4.5).

In the autumn the systematic MSLP errors in the ECHAM simulation have a maximum over south-west Europe with an associated warming and drying (biases in "SW" are 1.3°C and -54%). The other, relatively modest, systematic errors in temperature and precipitation seem not be related clearly to the dynamical systematic errors. An exception might be the area in north-east with too much precipitation (bias 45% in "NE"), as discussed below for the HIRHAM simulation.

The HIRHAM systematic MSLP errors for autumn resemble those of the ECHAM except that their magnitude is increased, and in agreement the warm and dry south-western Europe biases

increased slightly (in "SW" to 1.4°C and -54%, respectively). Like in the ECHAM simulation an area of too much precipitation is seen in the north-east (bias 64% in "NE"). This might be explained by the fact that the simulated mean low level flow is approximately parallel to the Scandinavian mountain chain whereas the ECMWF climatological flow has a component across, from the west. This should mean that the low level flow in the simulation would transport more moist air to the east side of the mountain chain than in reality where more of this air would have passed the mountain chain. Supporting this explanation is the fact that the simulation has a deficit of precipitation on the west side of the mountain chain (bias -4% in "N"). This explanation might apply to the ECHAM simulation as well.

2.2.3 The UKMO simulations

As previously mentioned, for the winter simulation of the UKMO GCM the systematic MSLP errors (Fig. 2.1) form a saddle pattern with a belt of relatively low pressure between a western and an eastern minimum with associated cyclone activity higher than in the climatology. The precipitation is a little above the observed (e.g. biases 45% in "NE" and 33% in "C") which may be explained by the too high cyclone activity. That the mean temperature at most places is less than observed (extreme biases of -5.2°C and -5.8°C in "N" and "S", respectively) seems not to be explained by the in the dynamical systematic errors and therefore is probably due to errors in the physical processes (e. g. radiation). However, the low temperatures and normal precipitation in the north-eastern corner of the region may be due to the reduction of the MSLP gradient in the north (Fig. 2.1) with its associated reduction in low level westerly flow.

MSLP errors in the UKMO RCM are similar to those in the driving GCM (Figures 2.1 and 2.2). The main difference is that the eastern and western minimum and the belt of relatively low pressure are deepened compared to the GCM field. Consistent with that the excessive cyclone activity over Europe is increased in the RCM simulation, now with a maximum over Denmark. The precipitation is increased substantially practically everywhere compared to the GCM simulation (Figures 4.1 and 4.2). For Europe as a whole the average bias has increased about 20% (the largest bias now being 52% in "NE"). One possible explanation is enhanced orographic uplift of moist air in the RCM. To check this, Jones et al. (1995) re-ran one year of the RCM integration with the RCM orography replaced by the GCM orography (Fig. 1). However, the increase in precipitation was still present. They then showed that it is the dynamical precipitation that is increased in the RCM (convective precipitation is slightly reduced) caused by an increase in vertical motions, - the variance of daily values of vertical motion is much larger than in the GCM. This is in agreement with general experiences from NWP, the higher resolution in the RCM allows it to resolve more of the spectrum of atmospheric motions, hence deeper, more intense low pressure systems with better resolved and therefore steeper / more intense fronts, increased cyclone activity and larger vertical motions. Again in the RCM simulation the temperatures are in general too low which again might be due to systematic errors in the physical tendencies. The negative temperature biases are, however, not nearly as large as in the GCM (the largest sub-area bias in "S" is now only -1.8°C). The decreased westerly flow in the north-eastern corner of the map may explain the extreme too low temperatures there and the slightly too high temperatures form France north of the Alps and into the Balkans may be explained by the increased westerlies there.

The UKMO GCM simulation during spring has systematically too low pressure in a belt from 50° N at 15°W to 40° N at 35°E across the CRU domain and increased cyclone activity compared to the climatology in southern Europe. In agreement with that generally too much precipitation is simulated over southern Europe (bias 44% in "S"). At about 70° N is situated a maximum in the MSLP systematic error which turns the low level flow to south-east in the north-eastern part of the map. This may explain the excessive precipitation over the east slope of the Scandinavian mountain chain (bias 66% in "NE"). As seen in Figure 4.3 the temperatures are again systematically too low all over Europe (extreme biases of -3.8°C in "N" and -4.1°C in "S"), probably due to systematic errors in the physical tendencies.

The RCM systematic errors in spring resembles those in the driving GCM simulation, except that the belt of too low pressure is deeper and in agreement with that a broader belt across the domain has increased cyclone activity. This and the associated increase in vertical motions seem to explain the excessive precipitation simulated all over Europe (the largest sub-area bias is 108% in "NE"). The remarks concerning precipitation at the east slope of the Scandinavian mountain chain and the systematically too low temperatures all over Europe made for the GCM simulation apply equally well for the RCM simulation.

The GCM dynamical systematic errors in the summer season resemble those in the previous seasons with a belt of relatively low pressure and high cyclone activity across Europe. In agreement with that generally too much precipitation is simulated over Europe (extreme biases of 32% in "SW" and 59% in "S"). The temperatures are again systematically too low over most Europe (e.g. biases of -3.7°C and -2.8°C in "N" and "S", respectively). An exception is the area of high temperatures and little precipitation over the eastern European states and Ukraine. As in the ECHAM simulation this is most likely the consequence of a drying out of the soil in the model in an area with very weak advection from the Atlantic. These temperature and precipitation errors are not as excessive and widespread as in the ECHAM simulation.

The RCM systematic MSLP errors in the summer season are very small but as usual the cyclone activity is increased compared to the driving GCM simulation. A larger area at mid-latitudes has dried out in the RCM and the magnitude of errors, low precipitation and high temperatures, are larger (biases in "SE" are 1.8°C and -38%). Similar differences between the HIRHAM and the ECHAM simulations seemed to be a consequence of the differences in MSLP errors and the model orographies. This is the case here too. The advection from the Atlantic to the area in question is weaker in the RCM and furthermore it is blocked by the relatively high and sharp Alp-Carpathian mountain chain in the model. In the GCM the much smoother mountains do not have the same blocking effects on the advection and as mentioned above the area of weak advection is situated differently. At high and low latitudes we see the usual too low temperatures (biases of -2.6°C in "NE" and -1.1°C in "SW") and increased precipitation (extreme biases of 47% in "N" and 49% in "SW") compared to the driving GCM simulation, the latter in agreement with the increased level of cyclone activity.

In the GCM simulation in autumn the belt of low pressure and high cyclonic activity is south of approximately 55°N. In agreement with this we get slightly too much precipitation there (e.g. a bias of 19% in "SE"). Between about 50°N and 60°N the westerlies are reduced which seems to explain too little precipitation in sub-area "W" (bias -36%). As in the ARPEGE T42 and the

ECHAM too little precipitation is simulated in "N" (bias -20%) and too much in "NE" (bias 27%) which is a consequence of the smooth model topography and the low level flow pattern as explained above for the HIRHAM simulation in autumn. As usual generally too low temperatures are simulated (extreme biases of -3.2° C in "N" and -4.7° C in "S").

The dynamical systematic errors in the RCM simulation for the autumn season resembles those for the GCM simulation, except that they are of larger magnitude. Consequently the positive precipitation biases are larger (in "SE" 41%) and the negative smaller in magnitude (-27% in "W"). As usual the negative temperature biases are reduced compared to the GCM simulation (extreme biases of "only" -1.9° in "NE" and "S").

3.0 Discussion and Conclusions

We shall first summarise the main findings in the above validation of the different model simulations and discuss associated points of interest. Finally we shall present our conclusions.

We have seen that the UKMO GCM for Europe simulates too much precipitation except autumn when the bias is close to zero (Table 1.1). We think this is due to too much cyclone activity. We have estimated the systematic error in cyclone activity from the standard deviation of the band-pass filtered 500 hPa height field (SBPF) relative to that of the 14 year ECMWF climatology. It turns out, however, that climatological values of the SBPFs over Europe determined from UKMO analysis are significantly higher than the ECMWF values we have used as a basis. This can be seen by comparing Figure 6 of Jones et al. (1995) with Figures 2.1 and 2.5 in the present report. The basis for comparison when verifying the cyclone activity may therefore be questioned. However, the values of SBPF are substantially higher in the UKMO model simulations than in those of the Météo-France and MPI models. Therefore, it seems likely that also the UKMO analyses have a relative high level of cyclone activity since the UKMO UM, or its predecessor, has been used in the data assimilation in which the UKMO analyses were produced. As a consequence we find that the ECMWF climatology at least is a more neutral basis for our validation than the UKMO one would have been.

We found (Table 1.2) that for Europe as a whole the UKMO simulation is systematically too cold. As seen in Figure 3.2 the negative bias in the GCM simulation (relative to the ECMWF climatology) is found through out the troposphere and is increasing with height. We have suggested that errors in the physical tendencies could be the reason for this cold bias. As the bias is increasing with height the model atmosphere is more unstable than the ECMWF climatology, which could be the reason for the high level of cyclone activity in the model. The cyclone activity and vertical velocities increase with increasing resolution and in agreement with that the total precipitation in Europe is generally 10-20% higher in the RCM than in the GCM, except in the summer season when the drying out of the soil in central and eastern Europe is more widespread in the RCM. The higher temperatures in the RCM, which as seen in Figure 6.3 are found through out the troposphere, might perhaps be explained by the release of latent heat due to the increased precipitation. Sub-area biases in the GCM simulation are found to be in the intervals -5.8°C to 0.5°C and -36% to 66%. For the RCM they are -2.6°C to 1.8°C and -38% to 108%.

The main reason for the temperature and precipitation biases in both ARPEGE simulations

seems to be the too strong low level westerlies which were found throughout the year. These imply in general too much precipitation, too high temperatures in the winter and too low temperatures in the summer. In summer and autumn, in the stretched T63 simulation especially, too high pressure over southern Europe explains too little precipitation there. In the stretched T63 simulation, in autumn, advection of cold air from north-east and east around the centre of too high pressure seems to explain relatively large negative temperature biases over southern Europe. In both simulations the validation shows in autumn an overall negative temperature bias, probably caused by deficiencies in the physical parameterization. The T42 simulation had sub-area biases between -3.7°C and 4.6°C and -19% and 111%. For the T63 simulation the biases were in the intervals -4.0°C to 4.0°C and - 41% to 114%.

The MPI simulations evaluated here are for a relatively short period, 46 months, compared to the 10 year simulations from the other two institutions. (The HIRHAM integrations are relatively expensive in computer time due to the large integration area used and the simulation had to be stopped due to a change of computer). We have compared the simulated mean seasonal surface air temperatures and precipitation in the 46 months ECHAM simulation with those in the same integration extended to 10 years. We find that the deviations between the 46 month fields and the 10 year fields are small compared to the biases of the 46 month simulation. Thus, the 46 month ECHAM simulation seems to be representative of the 10 year simulation. We expect that the same is the case for the HIRHAM integration.

In the MPI simulations the main systematic dynamical error was too high pressure over southern Europe in winter and the adjacent seasons giving reduced precipitation. Over northern Europe too much precipitation was related to various errors in the low level flow and in local increases of cyclone activity. The largest (positive) biases in temperature and deficits in precipitation seem to be caused by a spurious drying out of the model soil in the summer season. For the ECHAM simulation the sub-area biases are between -2.8°C and 3.5°C and between -62% and 101%. The HIRHAM simulation has biases in the intervals -2.1°C to 4.6°C and - 54% to 105%.

Figures 3.4 and 3.5 show that the temperature biases of the MPI models averaged over the whole CRU domain are increasing with height in the troposphere. That is, the simulations are too stable which is in agreement with the relatively low level of cyclone activity and too high pressure over southern Europe. It is seen that the troposphere is slightly too moist in winter and too dry in summer. Note, in particular the relatively large negative biases in relative humidity in summer at the lowest levels, another indication of the drying out of the soil in southern Europe. In summer and adjacent seasons the troposphere is warmer and dryer in the HIRHAM than in the ECHAM (Figure 3.7) simulation which should be expected due to more precipitation in the HIRHAM simulation.

In the present validation we have used the climatological data we think are the best available though the two data sets cover different periods. The CRU surface air temperature and precipitation data are based on 30 years of observations (1961-1990) whereas the ECMWF upper air data are from 14 more recent years (1979,1981-1993). We know that some variations have taken place in Europe since 1960, in particular a general heating over land. Thus Hurrell (1995) show that the December to March 1981-1993 mean temperatures are between approximately

0°C and 1.5°C higher over land in the CRU domain than in a 1951-1980 climatology. This indicates some differences in the mean climate for the two different periods and thus that the systematic error patterns of the dynamical fields (e.g. MSLP) computed with the ECMWF data as reference may differ from similar fields computed for the 30-year period. The dynamical error patterns with the 14-year reference were, however, only used to explain the temperature and the precipitation biases. As this was quite successful the 14-years statistics we used seems to be sufficiently representative of the 30-year period -at least for this application.

Another more difficult question is to what extent the biases in temperature and precipitation with respect to the 30-year CRU climatology which we have computed from our multi-year integrations are really long-term systematic errors or just manifestations of some large amplitude decadal variability over Europe. Here, by long-term systematic errors we mean biases which are relatively independent of which decadal simulation is considered, or in other words which are large compared to the observed or modelled decadal variability. We shall present evidence which shows that for the ECHAM simulation at least the larger temperature and precipitation biases found are indeed long-term systematic errors of the model.

Figure 6.1 and 6.2 show for each season and each of the sub-areas (except for the Alp Region) the biases of the 46 month ECHAM3 simulation together with some estimates of the observed and the modelled variability of 10-year averages.

In order to get an estimate of the observed decadal variability we have used the 30-years time series of monthly fields of deviations from the 1961-1990 CRU climatology which were supplied to us by CRU together with the climatology. From these time series we have for each sub-area and for each season constructed 21 running 10-year averages of the anomalies of the mean temperature and the mean precipitation. Again for each sub-area and each season we define as a measure of the observed decadal variability the difference between the maximum and the minimum anomaly among these 21 estimates.

In order to estimate the model variability we use five different 10-year AMIP runs performed with the ECHAM3 model. For each of the AMIP runs, which have different initial conditions, we determine the seasonal sub-area biases of the mean temperature and the mean precipitation. We then define for each sub-area and each season as a measure of the decadal model variability the difference between the minimum bias and maximum bias among the five model estimates.

In each diagram in Figure 6.1 and 6.2 the bar in the middle shows the bias of the 46-month simulation, the right hand bars show the minimum and maximum of the biases obtained in the five different 10-year AMIP runs and the left hand bars show the minimum and the maximum of the 21 observed 10-year averages. Each decadal variability as defined above are indicated by shading.

From the Figures it is seen firstly, that in most cases the biases of the 46 months run are within or very close to the interval of model variability. There are only few exceptions and in all cases the deviations are less than about 1°C and 0.5 mm/day. This illustrates that the 46 months ECHAM simulation is representative of a 10-year simulation as previously argued. Secondly, we note that in all cases of larger biases the interval of model variability is clearly separated from the interval of observed variability. This means that any of the five AMIP 10-year

ECHAM3 simulations would show relatively large biases similar to those found in the 46 months simulation and that these biases would fall outside the intervals of observed variability. On this basis we conclude that the larger biases of the 46 months simulation may be characterized as long-term systematic errors. Thirdly, a comparison of the magnitudes of the observed and modelled variabilities do not show a systematic difference which indicates that our estimate of the model variabilities is realistic.

We have not carried out similar investigations of the variabilities of the other model simulations. Concerning the HIRHAM simulations which is driven by boundary conditions from the ECHAM3 simulation we have seen that the larger biases are similar to those of ECHAM3 and seems to be caused by similar large-scale errors in the dynamic fields or similar errors in the physical parameterization schemes. It seems therefore likely that the results obtained from the ECHAM3, namely that the larger biases are long-term systematic model errors, apply also for the HIRHAM simulation. We can see no reason why this should not be the case also for the UKMO and the Météo-France models. In all of these 10-year integrations we have found large biases which fall well outside the intervals of the observed decadal variabilities shown in Figure 6.1 and 6.2. This means that if the decadal variabilities of the models have realistic (or even smaller) decadal variabilities than the observed ones we can conclude also for these models that the larger biases reveals long-term systematic model errors. We think that this is indeed the case.

In the present assessment the main emphasis was put on the validation of precipitation and surface air temperature simulations. The relatively large biases or systematic errors in these parameters in both the GCM and RCM simulations seem in most cases to be explained as the effects of systematic errors in the surface pressure or the low level flow and in the cyclone activity. We have not proven that quantitatively by a direct evaluation of these effects. We have, however, shown that at least the main temperature and precipitation biases are in qualitative agreement with these dynamical systematic errors. In most remaining cases when systematic errors in the dynamical fields seem not to explain the temperature and precipitation errors they seem to be due to defects in specific physical parameterization schemes.

As expected increased resolution gives generally improved orographic precipitation. Also synoptic systems seem more realistic in the high resolution simulations with sharper fronts and often deeper lows. As evidenced from maps of standard deviations of band-pass filtered 500 hPa heights the cyclone activity increases with resolution. This is generally an improvement. The validation has shown, however, that a regional increase of resolution alone does not solve all problems. The biases are also in the RCM simulations of the same order of or larger than the changes expected due to increase in greenhouse gas concentrations (at least to the 2xCO2 level). Therefore, at the present state of development it seems that the high resolution climate change scenarios that can be produced by the dynamical regionalization techniques tested here are not yet accurate enough to be used for impact studies.

Before useful local and regional simulations can be produced certain parameterization schemes involved must be improved. Equally important is that the systematic dynamical errors are reduced. The large integration area chosen for the HIRHAM simulations was chosen in order to be able to reduce the systematic errors, if possible. Only in the winter season we find slight im-

provements in the pressure pattern with increasing resolution, while the changes were insignificant or even small deteriorations in the other seasons. Similar results were found for the ARPEGE simulations. The too low pressure in the UKMO simulations was found to decrease further with resolution consistent with the increase in cyclone activity. The increase of cyclone activity with increasing resolution was a deterioration for the UKMO simulations as the level of cyclone activity was already too high in the GCM simulation, whereas for the MPI and partly also the Météo-France simulations it was an improvement. Thus, an increased cyclone activity can be achieved by increasing the resolution regionally, i.e. over and in the neighbourhood of Europe, whereas the large scale error patterns in Europe cannot be influenced significantly in that way. The cause(s) of the large scale dynamical systematic errors over Europe are most likely due to model defects elsewhere on the globe, probably in the physical parameterization schemes. The present validation strongly suggest that these defects in the GCMs must be localized, and they must, if possible, be corrected or at least reduced before we will be able to produce significantly more accurate local and regional climate simulations by the dynamical regionalization approaches.

As mentioned above, Section 1, during the remaining RACCS project period experimental high resolution climate change scenarios, i.e. control runs and 2xCO2 runs, are being produced. When they are ready a careful validation against climatological data will be performed for the control simulations and the resulting biases will be compared with the climate changes obtained. These simulations will be performed among others with the same atmospheric models as above except that it will be newer improved versions and that coupled atmosphere-ocean GCMs will be used. As the SST and sea-ice fields produced by the coupled GCMs are expected to be realistic we expect reductions in the biases as a result of the model improvements. For the MPI models for instance a new physical parameterization package, the ECHAM4 package, has been introduced and a preliminary validation of a 10 year time-slice of the control run with the coupled ECHAM4/OPYC model do show such improvements. In particular, in this simulation there are no large surface air temperature biases due to a spurious drying out of the soil in the summer season as those we found in the ECHAM3 AMIP simulation presented here, where as mentioned above it gave rise to the largest temperature biases. We expect that these large errors will be absent also in the HIRHAM control simulation. The results of the new validation will show to what extent the model changes which have been made have lead to increased accuracy of the high resolution simulations and weather this is sufficient to make climate change simulations with the dynamical techniques tested here sufficiently reliable over Europe.

Acknowledgements

This study was supported by the European Commission under the contracts EV5V-CT92-0126 and EV5V-CT94-O5O5. The authors would like to thank the partners in these contracts and the colleagues at there home institutions for there support and helpful discussions.

References

Blackmon M.L.,1976: A climatological spectral study of the 500 mb geopotential height of the northern hemisphere. J Atmos Sci 33, 1607-1623.

Barrow, E., M. Hulme and T Jiang, 1993: A 1960-90 Baseline Climatology and Future Climate Change Scenarios for Great Britain and Europe. Part I: 1960-90 Great Britain Baseline Climatology. Climate Research Unit Report, University of East Anglia, Norwich, U.K., 50 pp.

Christensen, J. H. and E. van Meijgaard, 1992: On the construction of a regional atmospheric climate model. DMI Technical Report 92-14. (Available from DMI, Lyngbyvej 100, DK-2100 Copenhagen Ø, Denmark).

Christensen, J.H., C. Cacciamani, M. Castro, C. Schär, G. Visconti and B. Machenhauer, 1996: Validation of present-day regional climate simulations over Europe: LAM simulations with observed boundary conditions. Danish Meteorological Institute Scientific Report. Under preparation.

Dickinson, R.E., R.M. Errico, F. Giorgi and G. T. Bates, 1989: A regional climate model for the western United States. Climatic Change, 15, 383-422.

Déqué M., C. Dreveton, A. Braun, D. Cariolle, 1994: The Arpege-IFS atmosphere model: a contribution to the French community climate modelling. Climate Dynamics,10, 249-266.

Déqué M. and Piedelievre J.P., 1995: High resolution climate simulation over Europe. Clim. Dyn., 11, 321-339.

DKRZ modelling Group, 1992: The ECHAM3 atmospheric general circulation model. DKRZ Technical Report No. 6 Hamburg, October 1992, 184 pp.

Gates, L. W., 1992: AMIP: The Atmospheric Model Intercomparison Project. Bull. Am. Meteorol. Soc., 73, 1962-1970.

Giorgi, F., M.R. Marinucci and G. Visconti, 1992: A 2xCO2 climate change scenario over Europe generated using a Limited Area Model nested in a General Circulation Model. II: Climate change scenario. J. Geophys. Res., 97, 10011-10028.

Hulme, M.,1994: Global changes in precipitation in the instrumental period. In: *Global Precipitations and Climate Change* (Ed. M. Desbois and F. Desalmand), NATO ASI Series, Springer Verlag, Berlin, pp. 387-405.

Hulme, M., D. Conway, P.D. Jones, T. Jiang, E.M. Barrow and C. Turney, 1995: Construction of a 1961-1990 European climatology for climate change modelling and impact applications. Int. J. Climatol., 15, 1333-1363.

Hurrell, J.W.,1995: Decadal trends in the North Atlantic Oscillation and Regional Temperature and Precipitation. Accepted for publication in Science.

Hutchinson, M.F.,1991: The application of thin plate smoothing splines to continent-wide data-assimilation. In Data Assimilation Systems (Ed. J.D. Jasper), BMRC Research Report No. 27, Bureau of Meteorology, Melbourne, Australia, 104-113.

Jones, P. D., 1994: Hemispheric surface air temperature data sets: an improvement and an update to 1993. J. Climate.

Jones, R. G., J. M. Murphy and M. Noguer.,1995: Simulation of climate change over Europe using a nested regional climate model. Part I. Assessment of control climate including sensitivity to location of lateral boundaries. Quart. J. Roy. Met. Soc. (1995), 121, 1413-1449.

Kållberg, P., 1990: HIRLAM Forecast Model Level 1. Documentation Manual. Available from SMHI, S-60176 Norrkoeping, Sweden. 77 pp.

Legates, D.R. and C.J. Willmott, 1990: Mean seasonal and spatial variability in gage-corrected, global precipitation. Int. J. Climatol., 10, 111-127.

Machenhauer, B., 1988: The HIRLAM Final Report. HIRLAM Tech. Report No. 5, Available from DMI, Lyngbyvej 100, DK-2100 Copenhagen Ø, Denmark. 116 pp.

Marinucci, M. R. and F. Giorgi, 1992: A 2xCO2 climate change scenario over Europe generated using a Limited Area Model nested in a General Circulation Model. I: Present day simulation. J. Geophys. Res., 97, 9989-10009.

Marinucci, M. R., F. Giorgi, M. Beniston, M. Wild, P. Tschuck, A. Ohmura, and A. Bernasconi, 1994: High resolution simulations of January and July climate over the western Alpine region with a nested regional model system. Theor. Appl. Climatol., 51, 119-138.

Roeckner, E., K. Arpe, L. Bengtsson, S. Brinkop, L. Dümenil, M. Esch, E. Kirk, F. Lunkeit, M. Ponater, B. Rockel, R. Sousen, U. Schlese, S. Schubert and M. Windelband, 1992: Simulation of the present-day climate with the ECHAM model: Impact of model physics and resolution. MPI for Meteorology Report No. 97, Hamburg, December 1992.

Simmons, A.J. and D.M. Burridge, 1981: An energy and angular-momentum conserving finite-difference scheme in hybrid coordinates. Mon. Wea. Rev., 109, 758-766.

Wild, M., A. Ohmura, H. Gilgen and E. Roeckner, 1995a: Validation of general circulation model simulated radiative fluxes using surface observations. J. Climate, 8, 1309-1324.

Wild, M., A. Ohmura, H. Gilgen and E. Roeckner, 1995b: Regional climate siumulation with a high resolution GCM: surfasce radiative fluxes. Clim. Dyn., 11, 469-486.

Precipitation	**DJF**	N	NE	W	C	E	Alps	SW	S	SE	Total
CRU	$[\frac{mm}{day}]$	3.83	1.21	3.65	1.72	1.32	3.04	2.61	3.24	1.76	2.10
UKMO GCM	[Δ%]	-16.9	45.0	-31.3	33.3	31.2	8.6	-9.4	-23.7	20.3	3.9
UKMO RCM	[Δ%]	23.5	51.9	-7.0	48.6	51.7	31.4	28.1	15.8	27.1	24.6
ARPEGE T42	[Δ%]	-17.7	88.8	9.9	101.7	89.4	38.4	46.3	6.0	16.8	38.6
ARPEGE T63s	[Δ%]	9.2	72.1	35.8	89.3	67.5	33.4	16.3	-3.1	-11.7	30.6
ECHAM	[Δ%]	-6.4	101.2	-13.2	29.7	49.6	-27.9	-16.2	-48.0	-23.0	5.6
HIRHAM	[Δ%]	5.3	74.8	-16.8	24.3	56.0	-22.8	-13.9	-43.0	-30.5	2.6

Precipitation	**MAM**	N	NE	W	C	E	Alps	SW	S	SE	Total
CRU	$[\frac{mm}{day}]$	2.48	1.10	2.61	1.74	1.39	3.58	2.11	2.29	1.78	1.83
UKMO GCM	[Δ%]	11.1	66.1	-5.6	26.2	26.7	4.8	14.0	44.4	38.2	23.9
UKMO RCM	[Δ%]	38.4	107.7	14.0	34.6	52.0	31.7	37.5	66.7	46.8	44.8
ARPEGE T42	[Δ%]	16.2	102.6	25.1	99.7	111.2	36.8	1.3	33.2	56.0	57.8
ARPEGE T63s	[Δ%]	91.4	114.0	54.1	89.2	108.3	10.7	-13.6	-21.0	4.9	52.2
ECHAM	[Δ%]	10.7	81.2	-13.4	19.5	45.2	-19.8	-35.6	-10.7	5.2	11.4
HIRHAM	[Δ%]	42.9	104.8	-3.0	38.2	100.0	5.9	-28.2	-22.3	7.6	31.0

Precipitation	**JJA**	N	NE	W	C	E	Alps	SW	S	SE	Total
CRU	$[\frac{mm}{day}]$	2.91	2.17	2.45	2.25	2.49	4.06	1.06	1.35	2.15	2.23
UKMO GCM	[Δ%]	24.9	9.4	9.7	21.4	-15.6	-0.4	31.7	59.2	1.8	8.7
UKMO RCM	[Δ%]	46.9	30.6	1.2	-12.7	-21.0	-16.4	48.9	14.4	-38.4	-0.8
ARPEGE T42	[Δ%]	39.7	62.9	27.1	64.3	36.9	15.7	90.3	89.7	13.1	45.5
ARPEGE T63s	[Δ%]	110.1	73.9	12.9	29.5	26.2	-8.2	-6.3	-23.2	-40.8	28.0
ECHAM	[Δ%]	1.0	17.2	-38.7	-27.5	-25.5	-44.5	-61.9	-1.6	-26.8	-18.0
HIRHAM	[Δ%]	46.8	54.6	-44.1	-14.4	11.6	-16.5	-48.4	-31.9	-36.5	2.9

Precipitation	**SON**	N	NE	W	C	E	Alps	SW	S	SE	Total
CRU	$[\frac{mm}{day}]$	4.54	1.86	3.77	2.10	1.82	3.55	2.29	3.23	1.69	2.41
UKMO GCM	[Δ%]	-20.4	27.3	-36.2	7.8	2.5	13.2	-8.9	14.6	19.4	-1.1
UKMO RCM	[Δ%]	8.1	36.1	-27.2	6.7	24.4	33.0	45.3	43.8	40.6	16.6
ARPEGE T42	[Δ%]	-12.7	49.1	-10.7	36.6	36.6	-2.5	-19.2	-10.5	5.6	8.2
ARPEGE T63s	[Δ%]	33.9	34.9	-17.6	-6.5	2.6	-32.7	-30.1	-24.5	-28.2	-6.8
ECHAM	[Δ%]	-16.7	44.7	-36.0	-15.0	-3.3	-42.2	-54.4	-44.3	-23.1	-17.0
HIRHAM	[Δ%]	-4.3	63.7	-41.8	-15.3	14.5	-37.3	-53.8	-57.3	-27.6	-11.7

Table 1.1: Sub–area means of multi–year averaged seasonal precipitation for land points for climatological data (CRU) [mm/day] and relative difference between model results and climatological values [%]. Last column shows the mean and the relative differences of all landpoints of the 9 areas.

T2m (MSL)	**DJF**	N	NE	W	C	E	Alps	SW	S	SE	Total
CRU	[°C]	-4.45	-9.42	5.14	1.58	-4.34	4.92	10.44	9.05	2.04	-0.15
UKMO GCM	[Δ°C]	-5.19	-3.92	-0.72	-0.16	-2.77	-2.40	-1.88	-5.77	-1.83	-2.73
UKMO RCM	[Δ°C]	-0.68	-1.30	-0.36	0.29	-1.35	0.19	-0.68	-1.81	-0.07	-1.03
ARPEGE T42	[Δ°C]	3.12	3.72	1.72	3.81	4.58	3.34	0.42	0.88	4.28	2.98
ARPEGE T63s	[Δ°C]	2.90	4.62	0.45	2.63	4.03	1.20	-1.33	-1.83	1.90	2.00
ECHAM	[Δ°C]	2.76	-0.58	1.83	1.54	-0.27	1.20	0.70	-0.12	1.33	0.16
HIRHAM	[Δ°C]	0.99	-0.81	1.36	2.06	1.10	2.05	0.60	0.03	1.62	0.49

T2m (MSL)	**MAM**	N	NE	W	C	E	Alps	SW	S	SE	Total
CRU	[°C]	2.37	1.11	8.46	8.57	6.85	12.58	15.21	14.43	11.87	7.97
UKMO GCM	[Δ°C]	-3.82	-2.77	-0.76	-1.33	-2.44	-3.45	-2.45	-4.11	-2.72	-2.50
UKMO RCM	[Δ°C]	-1.20	-1.30	-0.54	-0.79	-0.99	-2.01	-1.85	-2.03	-1.60	-1.34
ARPEGE T42	[Δ°C]	0.62	-1.01	0.94	0.21	-0.27	-1.38	-0.04	-1.23	-0.30	-0.37
ARPEGE T63s	[Δ°C]	-0.46	-0.84	0.26	0.31	-0.63	-0.87	0.14	-1.27	-0.19	-0.53
ECHAM	[Δ°C]	-0.02	-2.79	0.47	-0.31	-1.72	-1.34	1.10	-0.47	-0.36	-1.16
HIRHAM	[Δ°C]	-0.02	-1.79	0.95	0.95	0.04	0.35	1.41	0.80	1.36	0.10

T2m (MSL)	**JJA**	N	NE	W	C	E	Alps	SW	S	SE	Total
CRU	[°C]	13.02	14.02	14.85	17.53	17.68	21.50	24.14	23.77	21.70	18.02
UKMO GCM	[Δ°C]	-3.65	-3.00	-0.63	-0.82	0.50	-2.75	-2.06	-2.75	-0.03	-1.32
UKMO RCM	[Δ°C]	-2.45	-2.62	0.20	0.83	0.19	0.12	-1.12	0.17	1.77	-0.24
ARPEGE T42	[Δ°C]	-1.22	-2.15	-0.26	-2.18	-2.30	-3.70	-1.13	-2.31	-0.99	-1.76
ARPEGE T63s	[Δ°C]	-3.26	-3.33	-0.36	-1.72	-2.25	-2.05	0.01	-0.88	-0.01	-1.76
ECHAM	[Δ°C]	-1.93	-2.61	0.83	0.18	-0.19	-0.95	3.47	0.53	1.77	-0.13
HIRHAM	[Δ°C]	-1.60	-2.20	1.36	1.32	0.56	1.56	3.45	3.20	4.58	1.06

T2m (MSL)	**SON**	N	NE	W	C	E	Alps	SW	S	SE	Total
CRU	[°C]	4.53	2.90	10.63	10.29	7.54	14.18	18.02	17.51	13.02	9.72
UKMO GCM	[Δ°C]	-3.29	-2.41	-1.00	-0.78	-0.89	-3.04	-2.39	-4.65	-1.12	-1.87
UKMO RCM	[Δ°C]	-1.50	-1.89	-0.70	-0.85	-1.37	-1.25	-1.36	-1.87	-0.96	-1.46
ARPEGE T42	[Δ°C]	0.40	-0.13	0.09	-0.66	-0.73	-2.13	-2.02	-3.05	-1.35	-1.01
ARPEGE T63s	[Δ°C]	-0.40	-0.44	-0.54	-0.75	-1.00	-2.25	-2.01	-3.99	-2.57	-1.52
ECHAM	[Δ°C]	1.39	0.34	0.72	0.57	0.28	-0.43	1.26	-0.01	1.30	0.33
HIRHAM	[Δ°C]	0.38	0.05	0.64	0.94	0.98	0.30	1.39	0.41	1.41	0.57

Table 1.2: Sub–area means of multi–year averaged seasonal surface air temperature reduced to mean sea level for land points for climatological data (CRU) [°C] and difference between model results and climatological values [°C]. Last column shows the mean and the differences of all landpoints of the 9 areas.

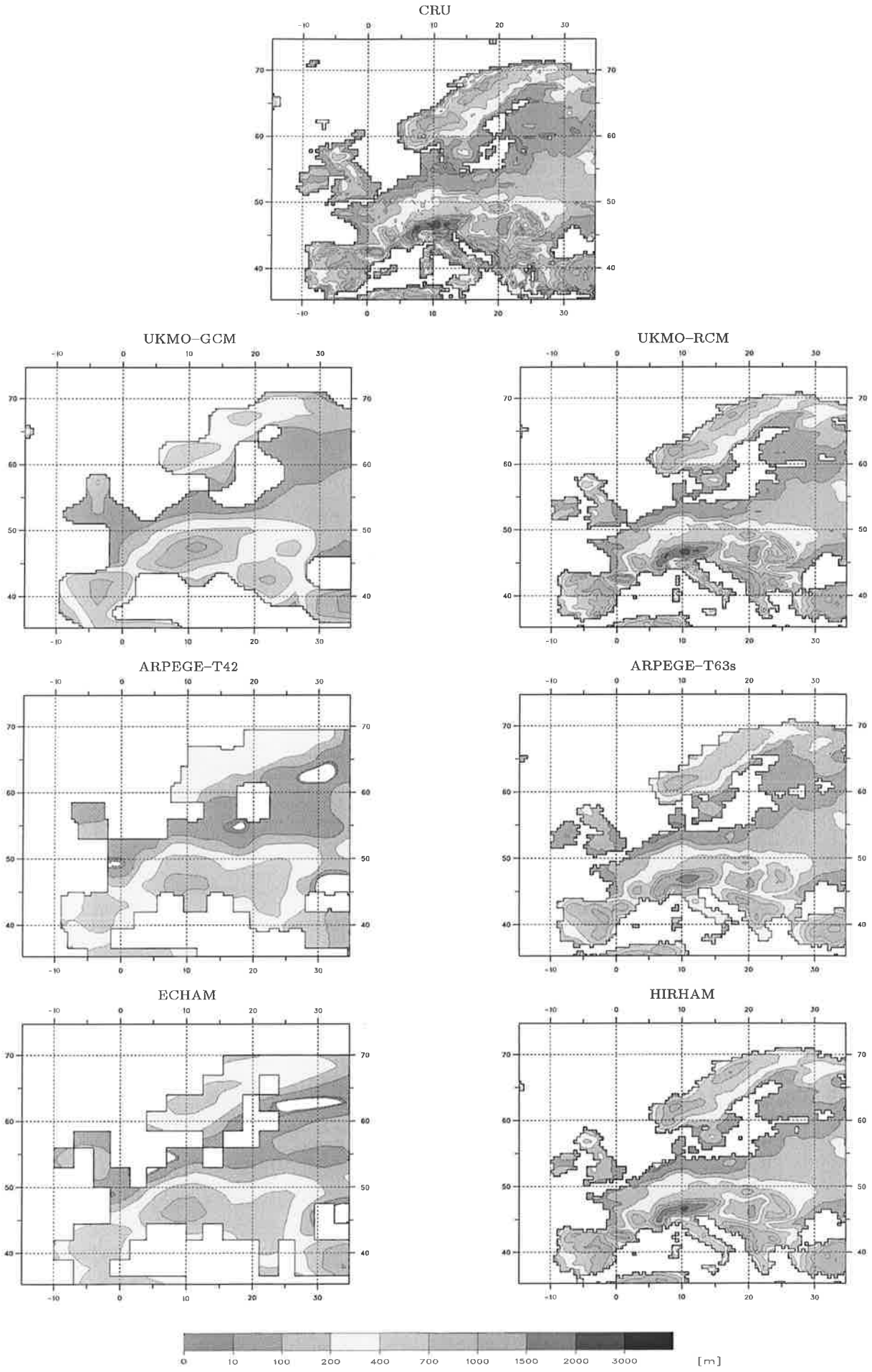

Figure1.1: Orographies of CRU climate data set and those used in GCM's (left) and RCM's (right).

UKMO–RCM

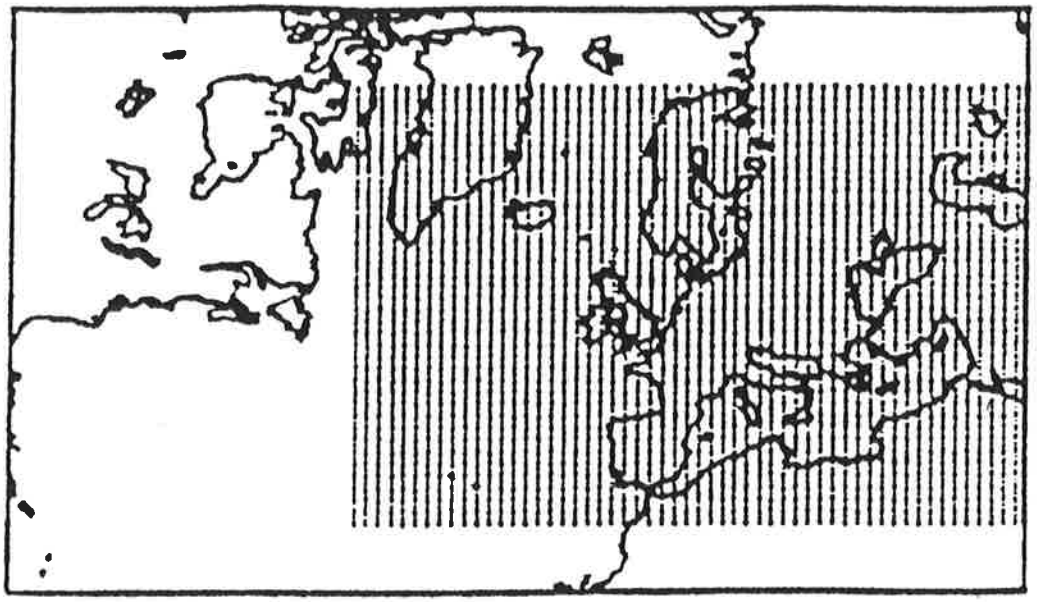

ARPEGE T63s

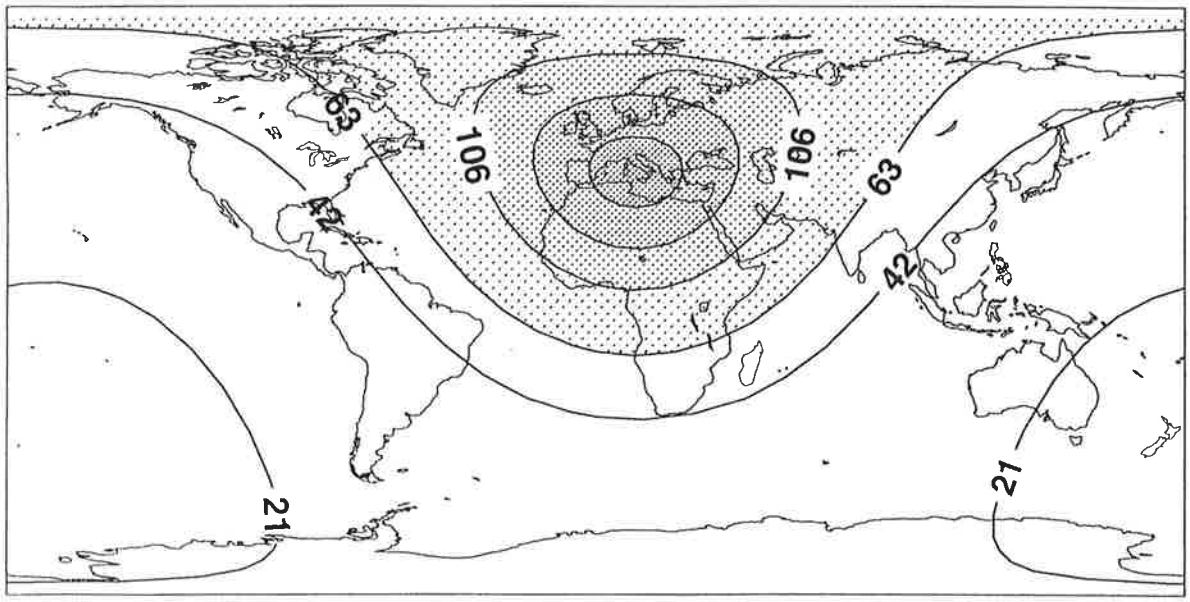

HIRHAM

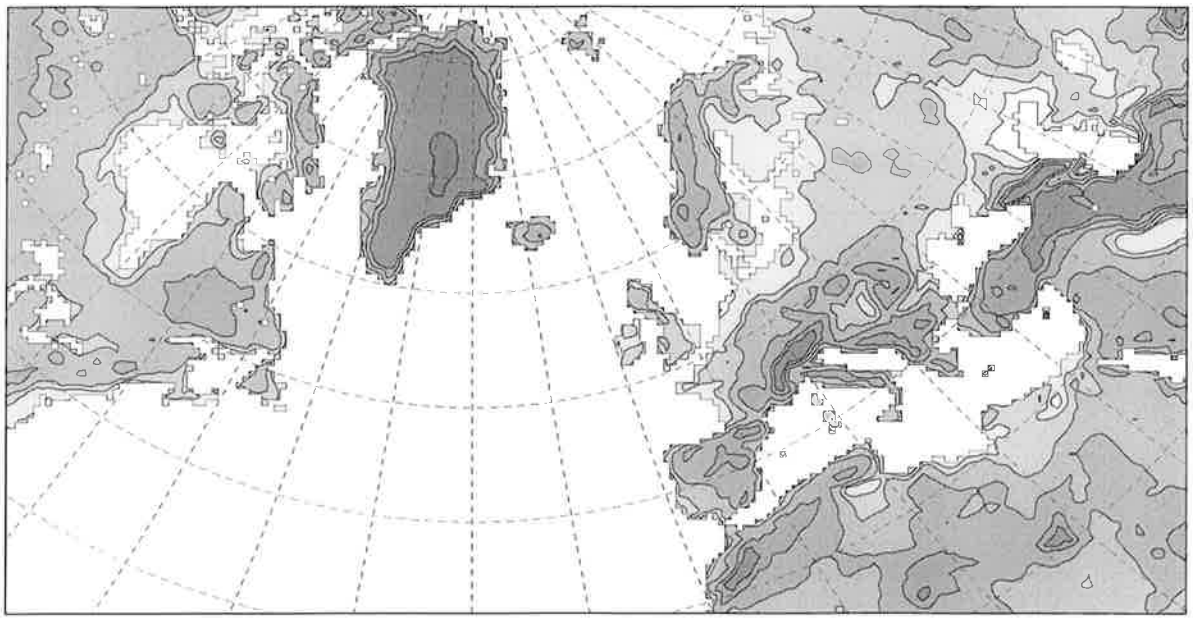

Figure1.2: Integration area of the used RCM's.

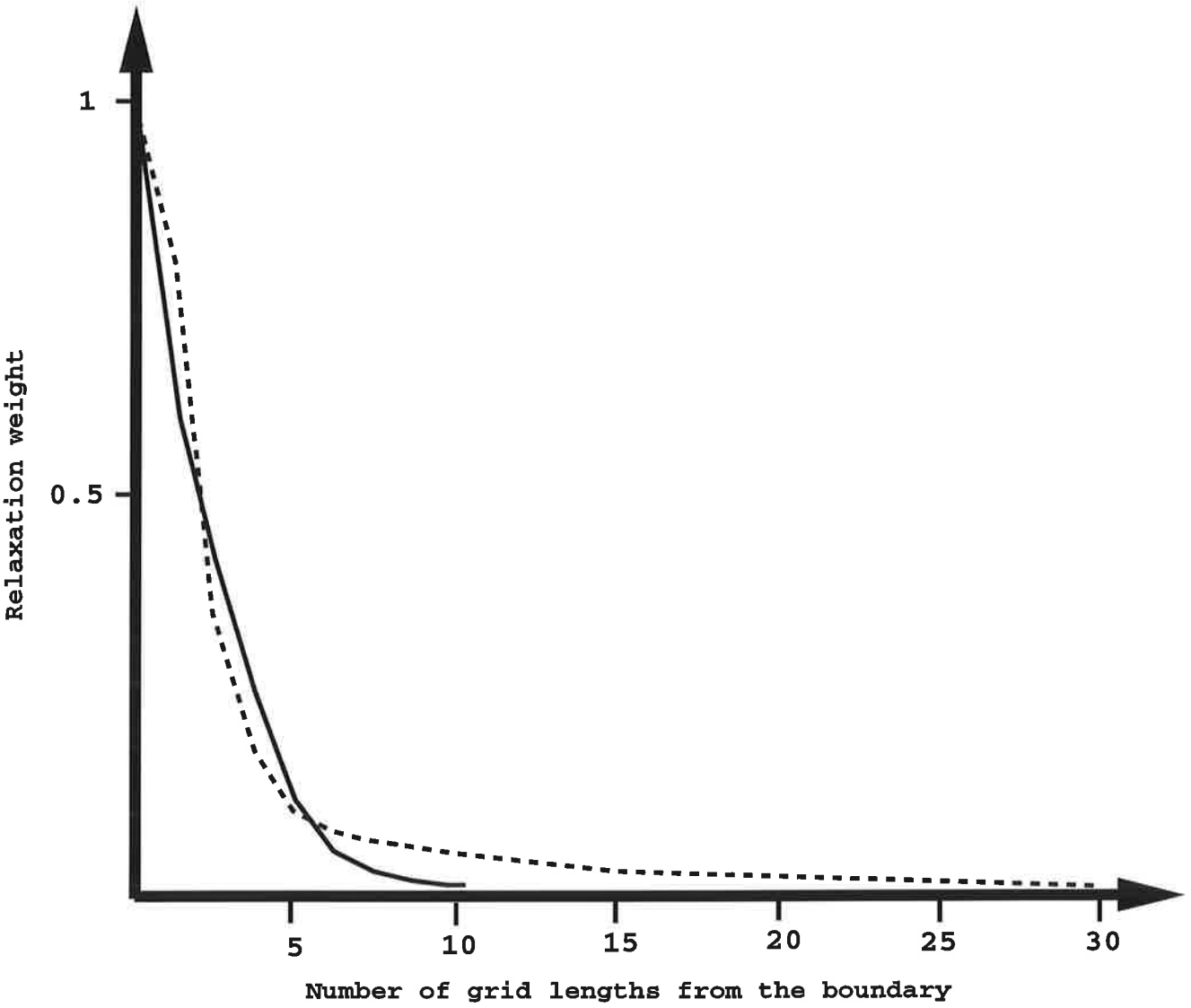

Fig 1.3: Fractional weights given to the ECHAM fields in the boundary zone for the standard 10 point zone (full line) and for the 30 point zone (stipled line).

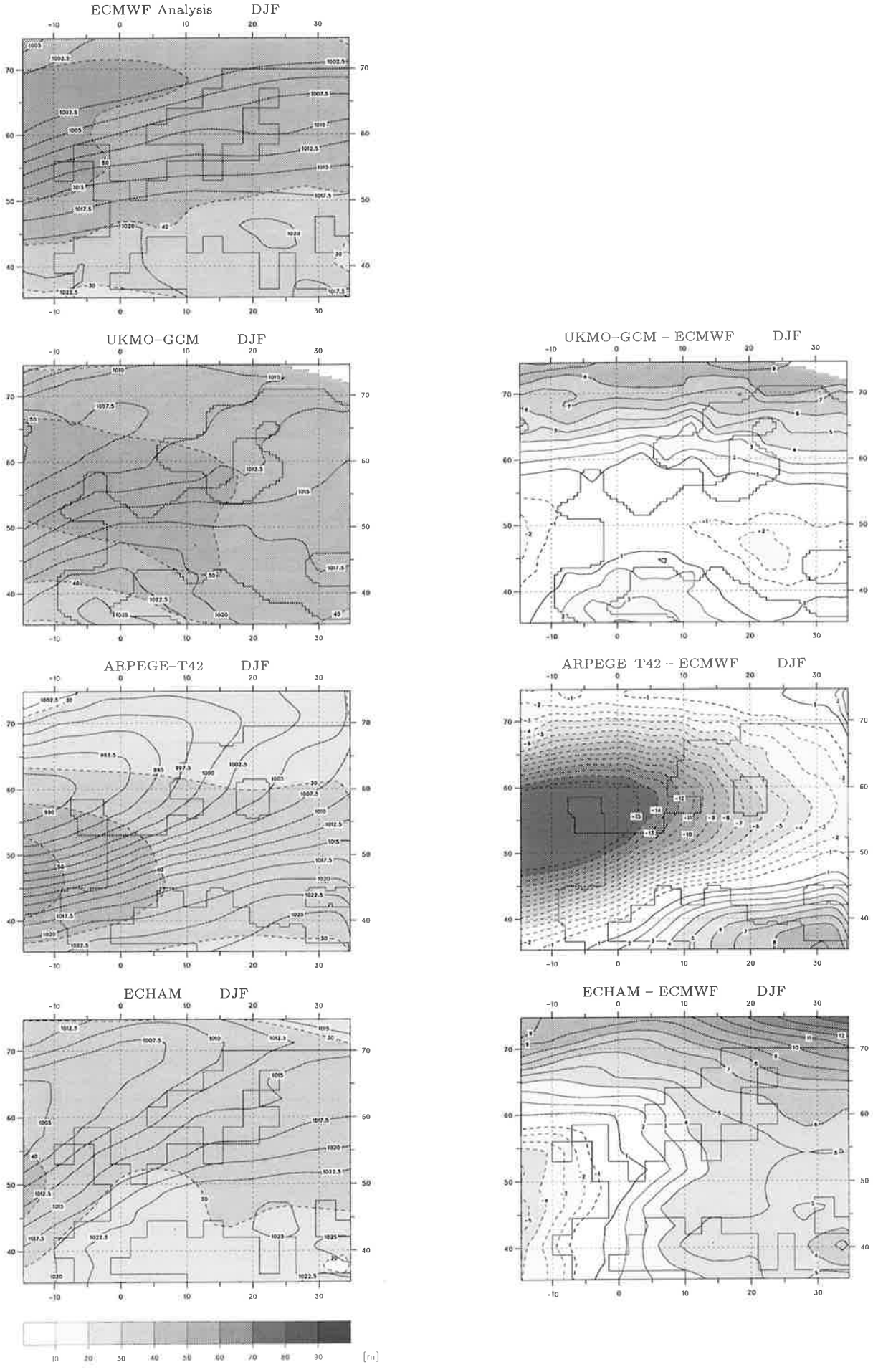

Figure 2.1: **Left column:** MSLP [hPa] for ECMWF Analysis and GCM's for DJF (solid lines) and standard deviation of band pass filtered 500 hPa height [m] (shaded). **Right column:** Systematic error of MSLP [hPa].

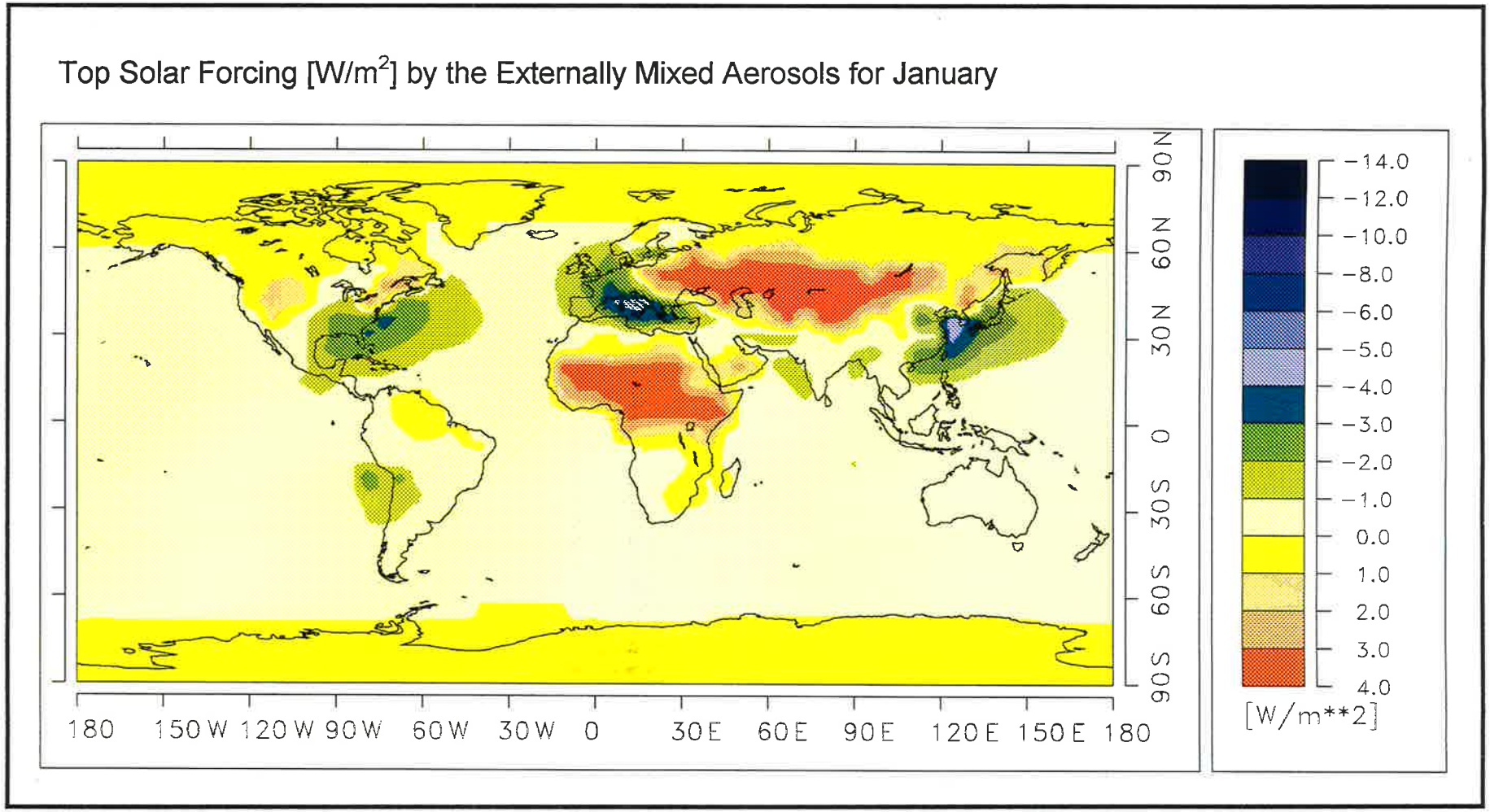

Figure 11a: Top solar radiative forcing of externally mixed aerosols consisting of black carbon and sulfate for January.

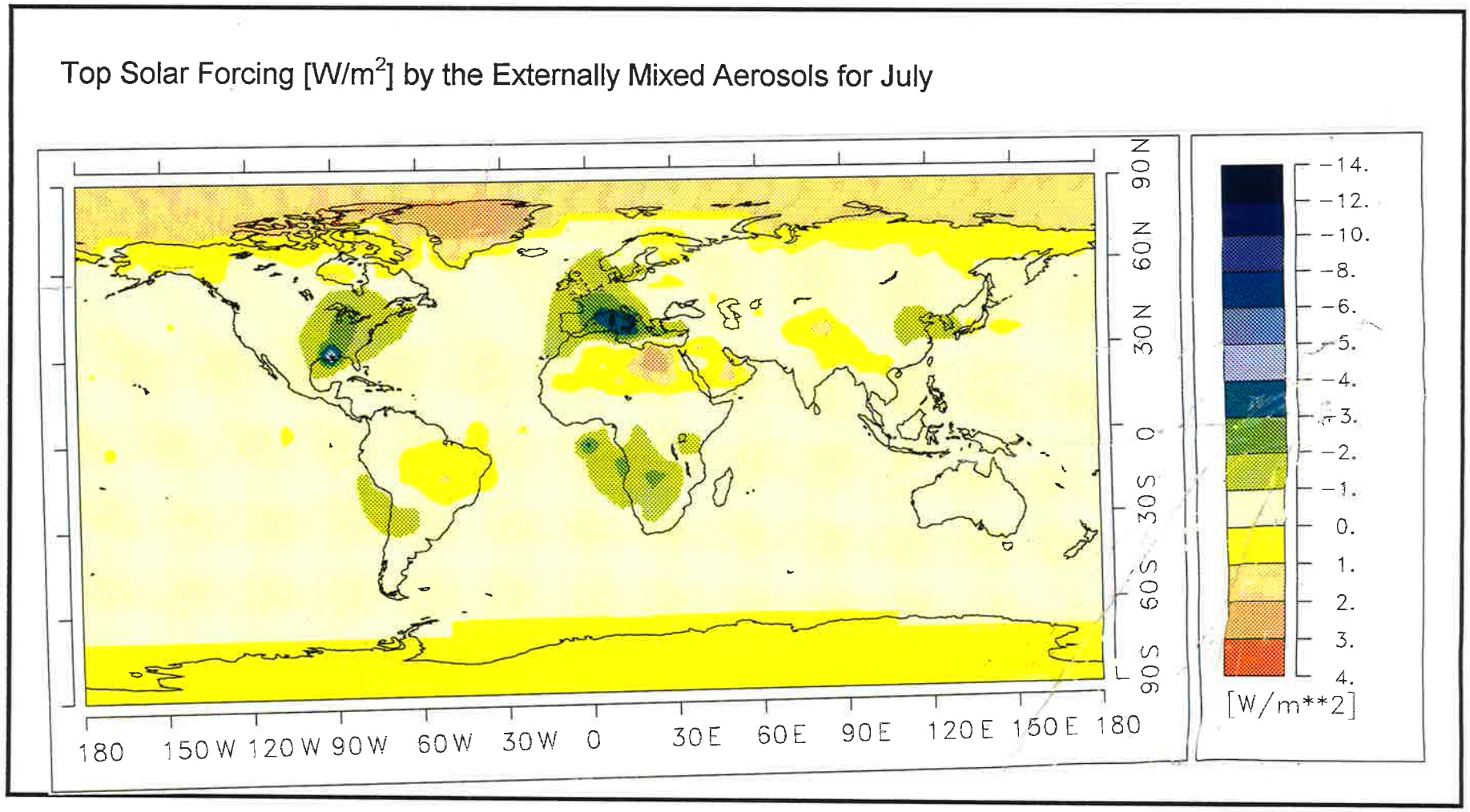

Figure 11b: Top solar radiative forcing of externally mixed aerosols consisting of black carbon and sulfate for July.

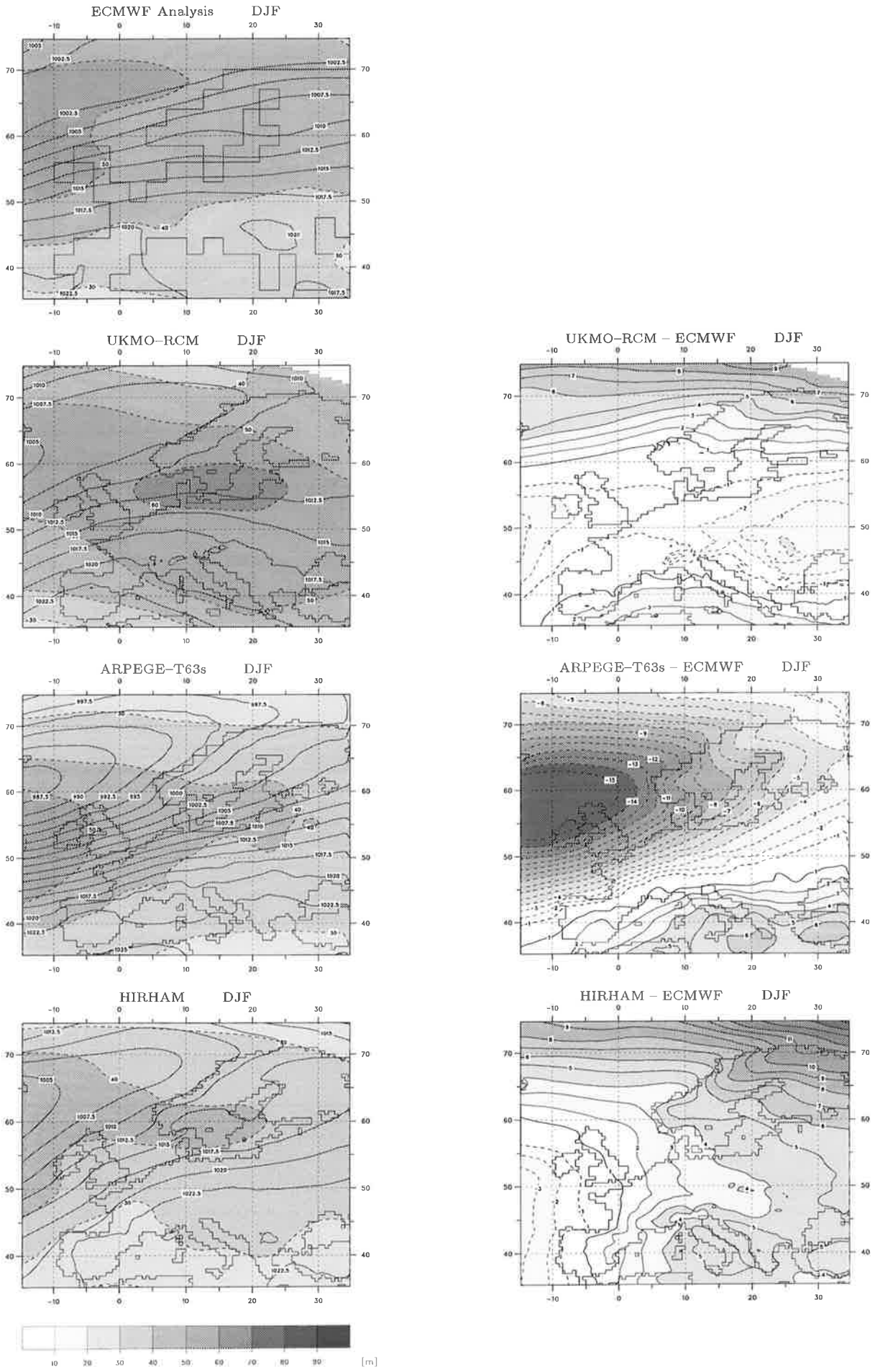

Figure 2.2: **Left column:** MSLP [hPa] for ECMWF Analysis and RCM's for DJF (solid lines) and standard deviation of band pass filtered 500 hPa height [m] (shaded). **Right column:** Systematic error of MSLP [hPa].

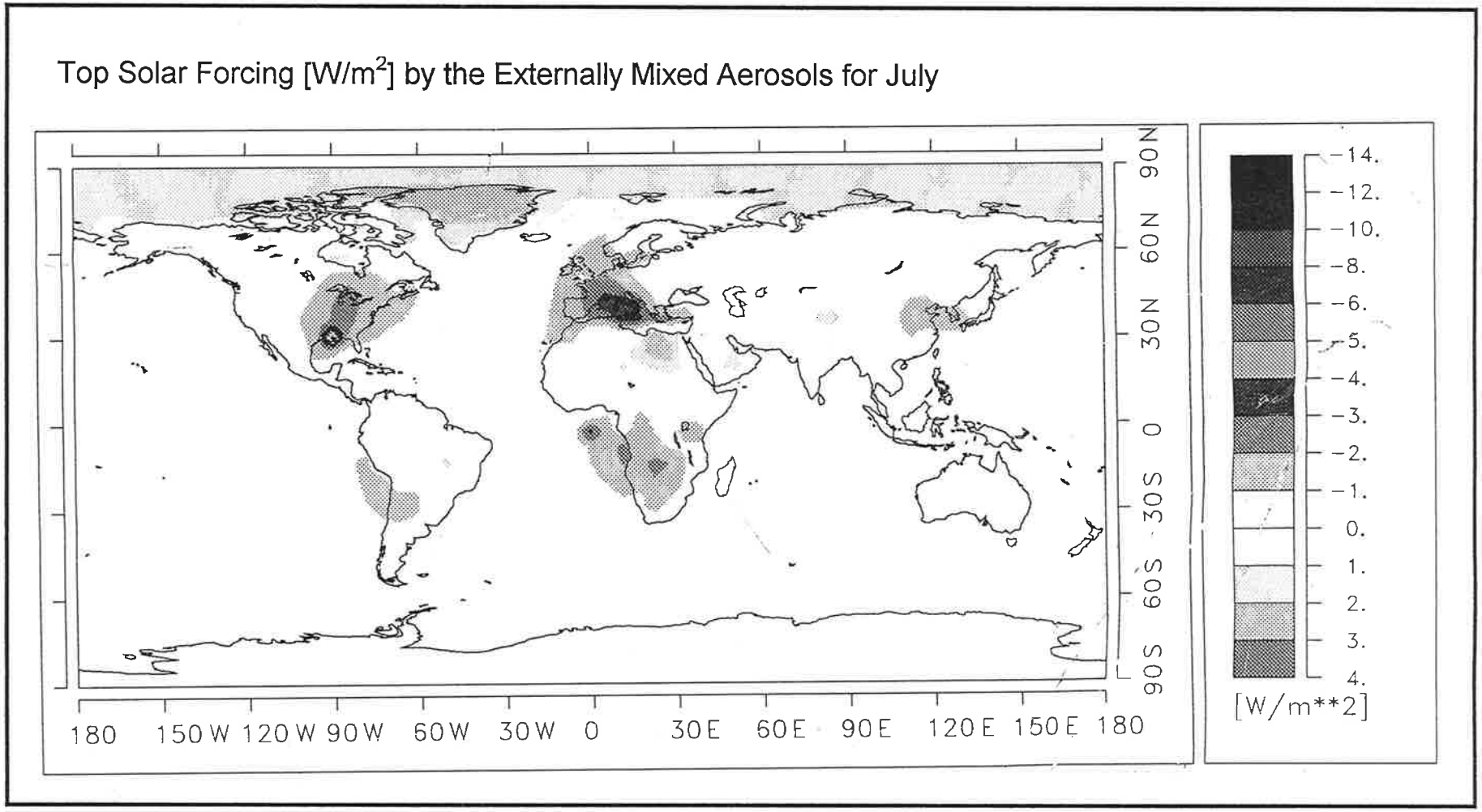

Figure 11b: Top solar radiative forcing of externally mixed aerosols consisting of black carbon and sulfate for July.

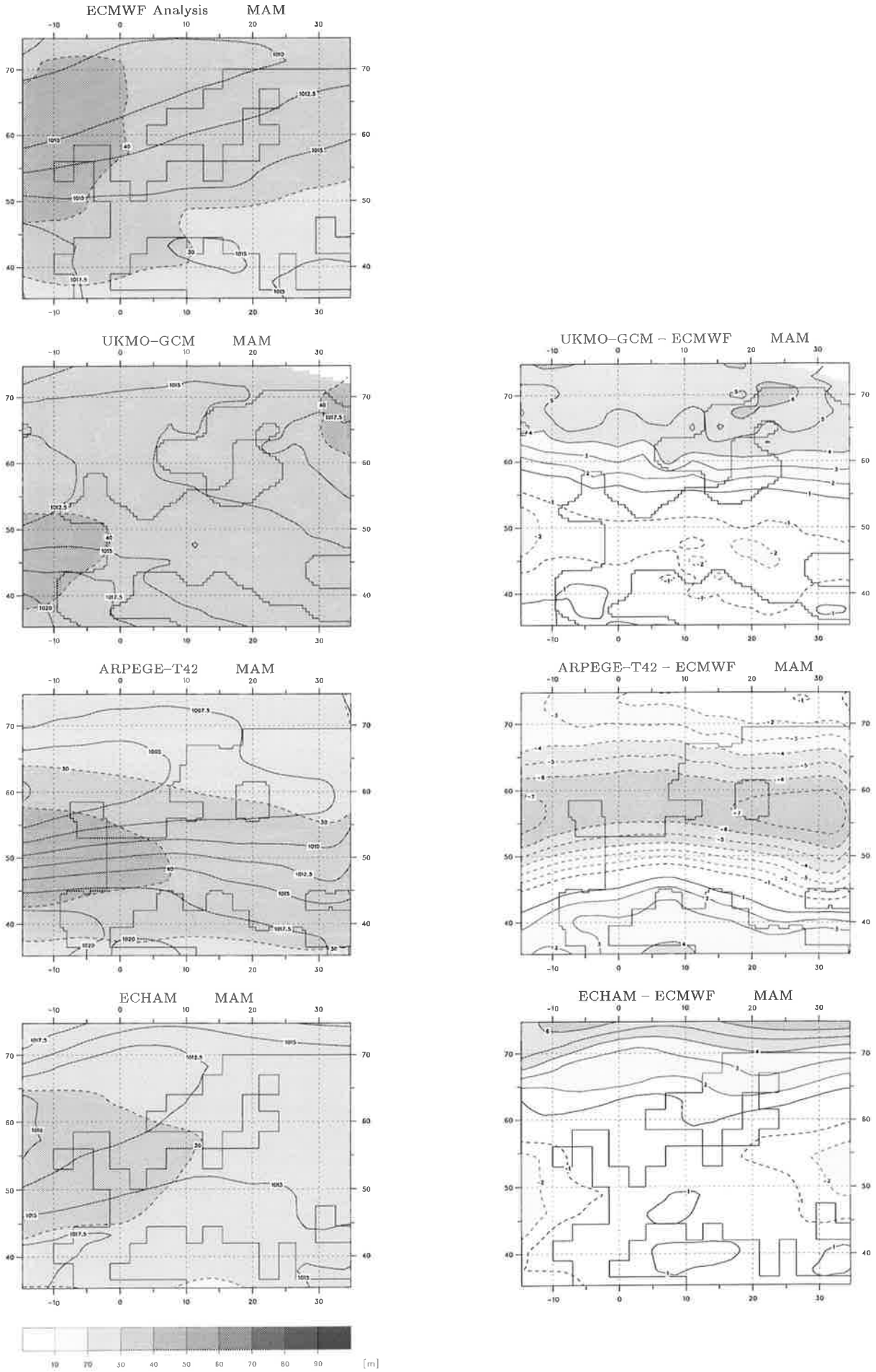

Figure 2.3: **Left column:** MSLP [hPa] for ECMWF Analysis and GCM's for MAM (solid lines) and standard deviation of band pass filtered 500 hPa height [m] (shaded). **Right column:** Systematic error of MSLP [hPa].

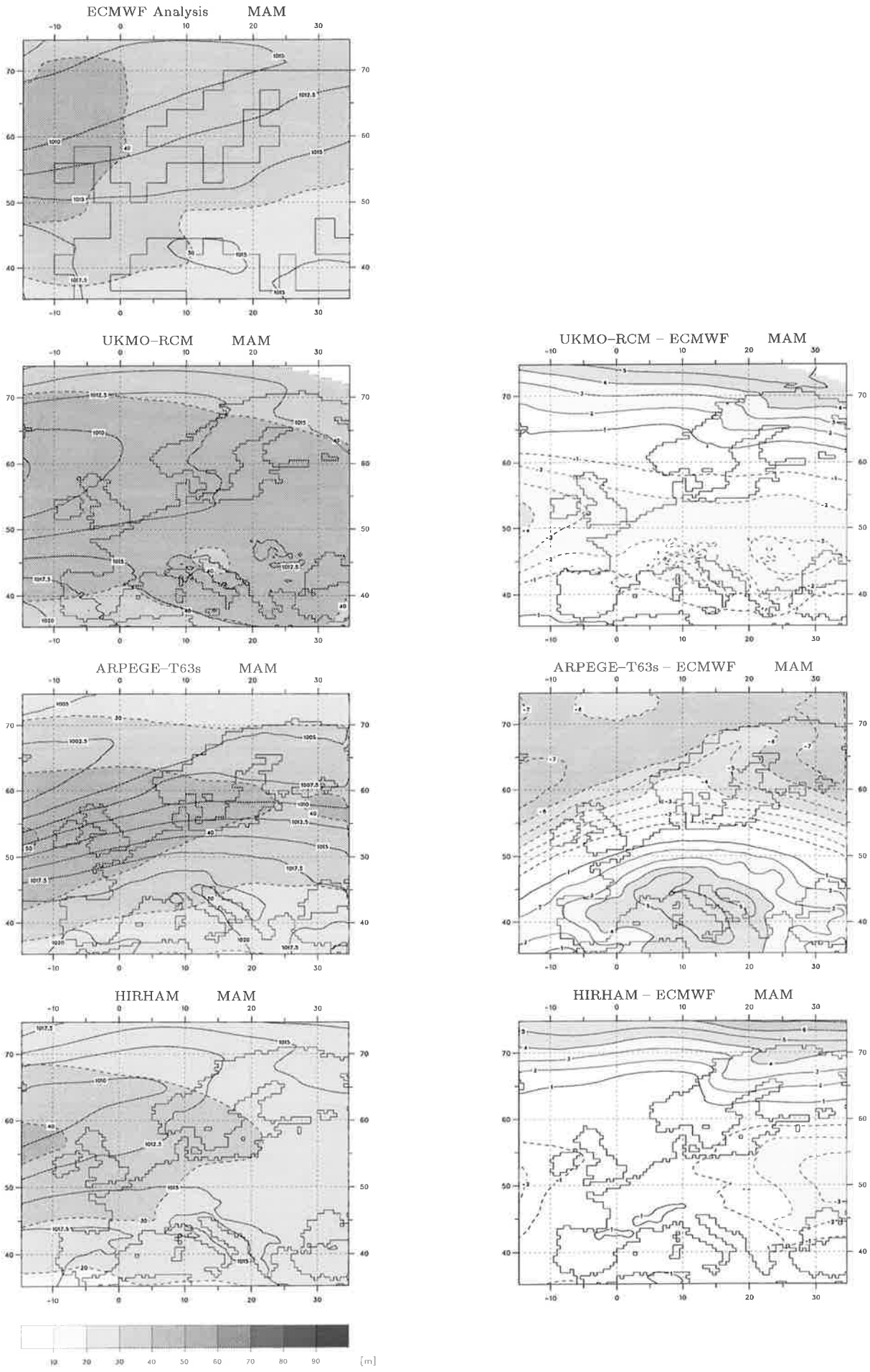

Figure 2.4: **Left column:** MSLP [hPa] for ECMWF Analysis and RCM's for MAM (solid lines) and standard deviation of band pass filtered 500 hPa height [m] (shaded). **Right column:** Systematic error of MSLP [hPa].

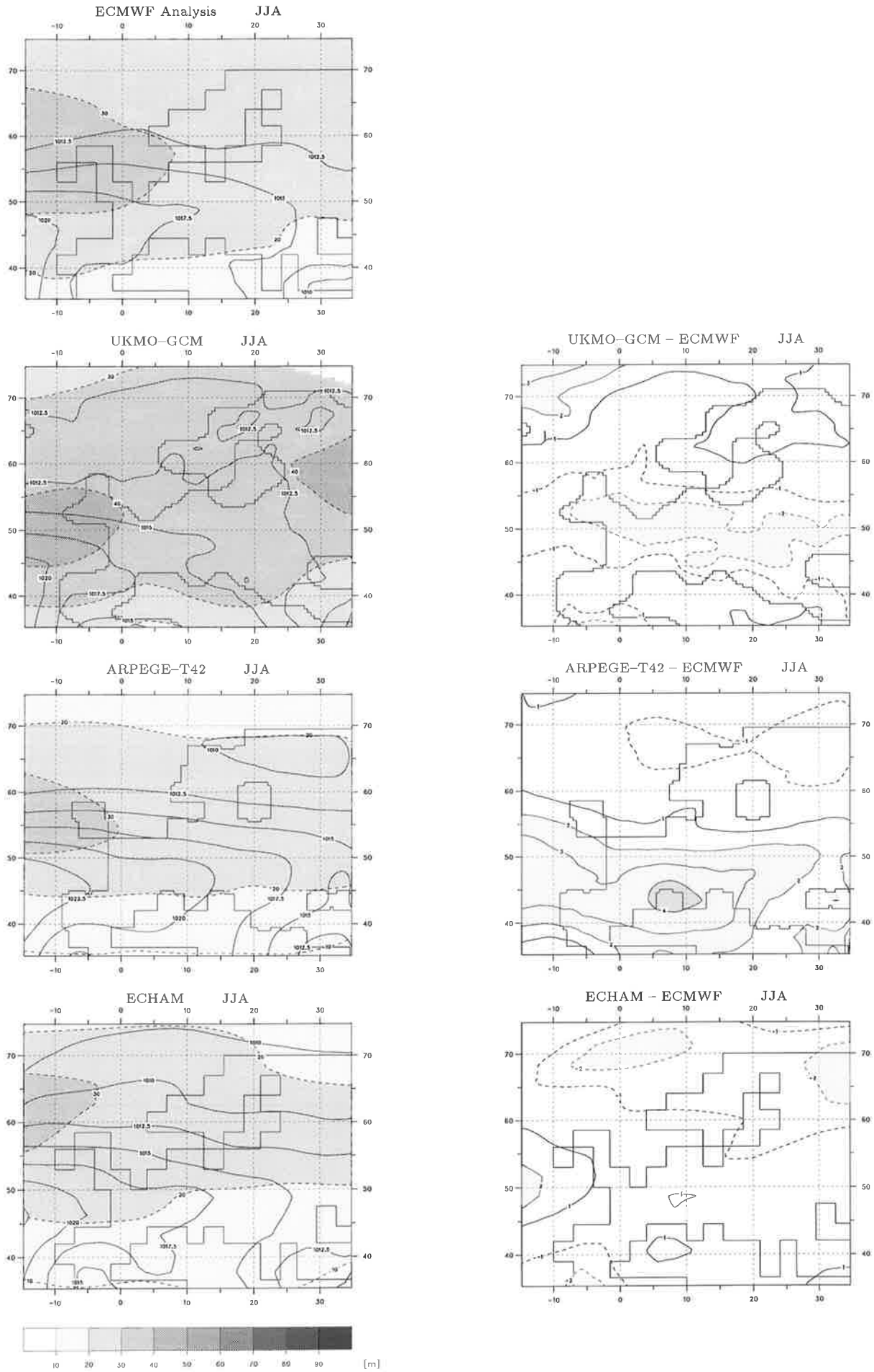

Figure 2.5: **Left column:** MSLP [hPa] for ECMWF Analysis and GCM's for **JJA** (solid lines) and standard deviation of band pass filtered 500 hPa height [m] (shaded). **Right column:** Systematic error of MSLP [hPa].

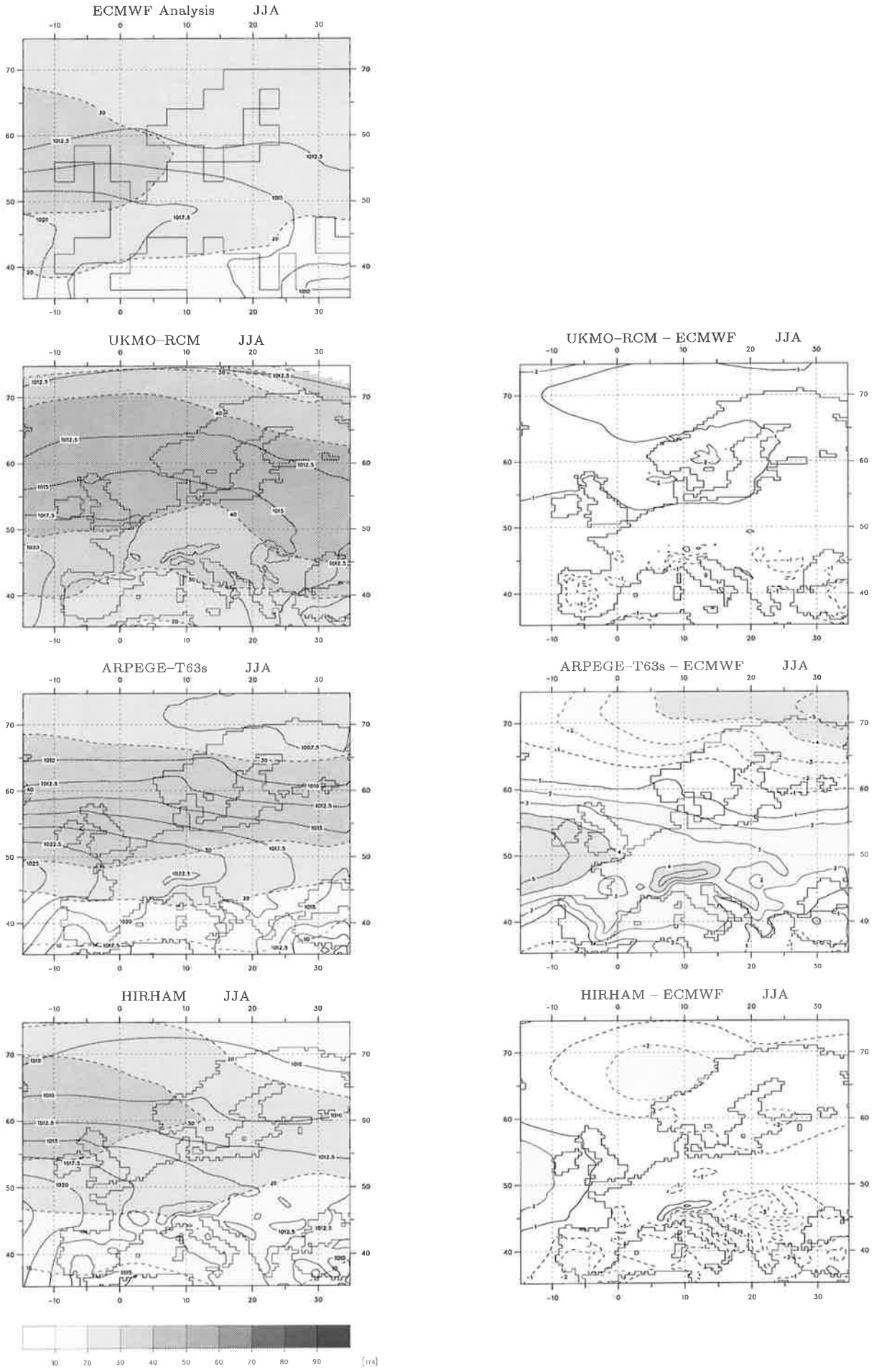

Figure 2.6: **Left column:** MSLP [hPa] for ECMWF Analysis and RCM's for **JJA** (solid lines) and standard deviation of band pass filtered 500 hPa height [m] (shaded). **Right column:** Systematic error of MSLP [hPa].

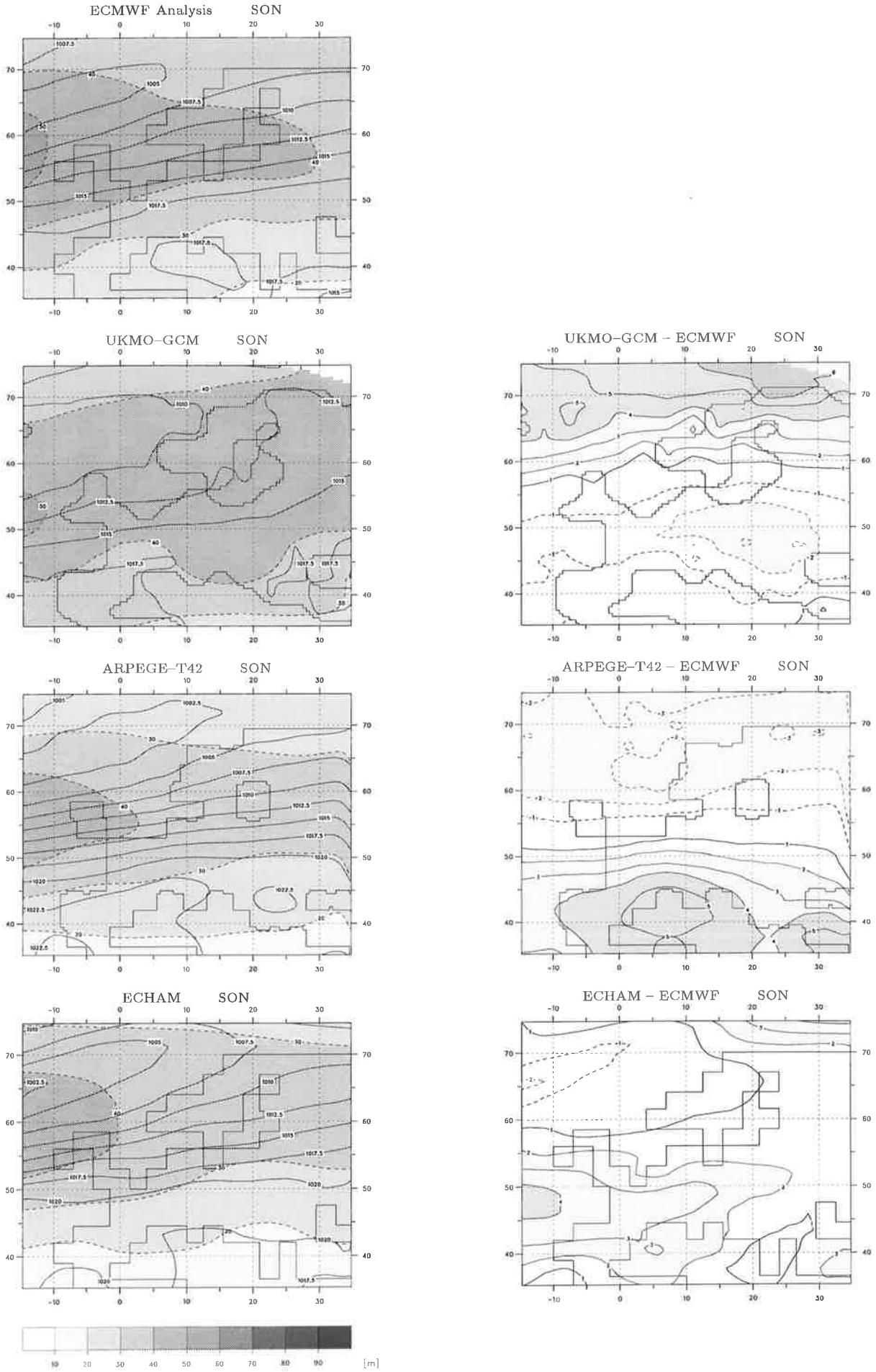

Figure 2.7: **Left column:** MSLP [hPa] for ECMWF Analysis and GCM's for SON (solid lines) and standard deviation of band pass filtered 500 hPa height [m] (shaded). **Right column:** Systematic error of MSLP [hPa].

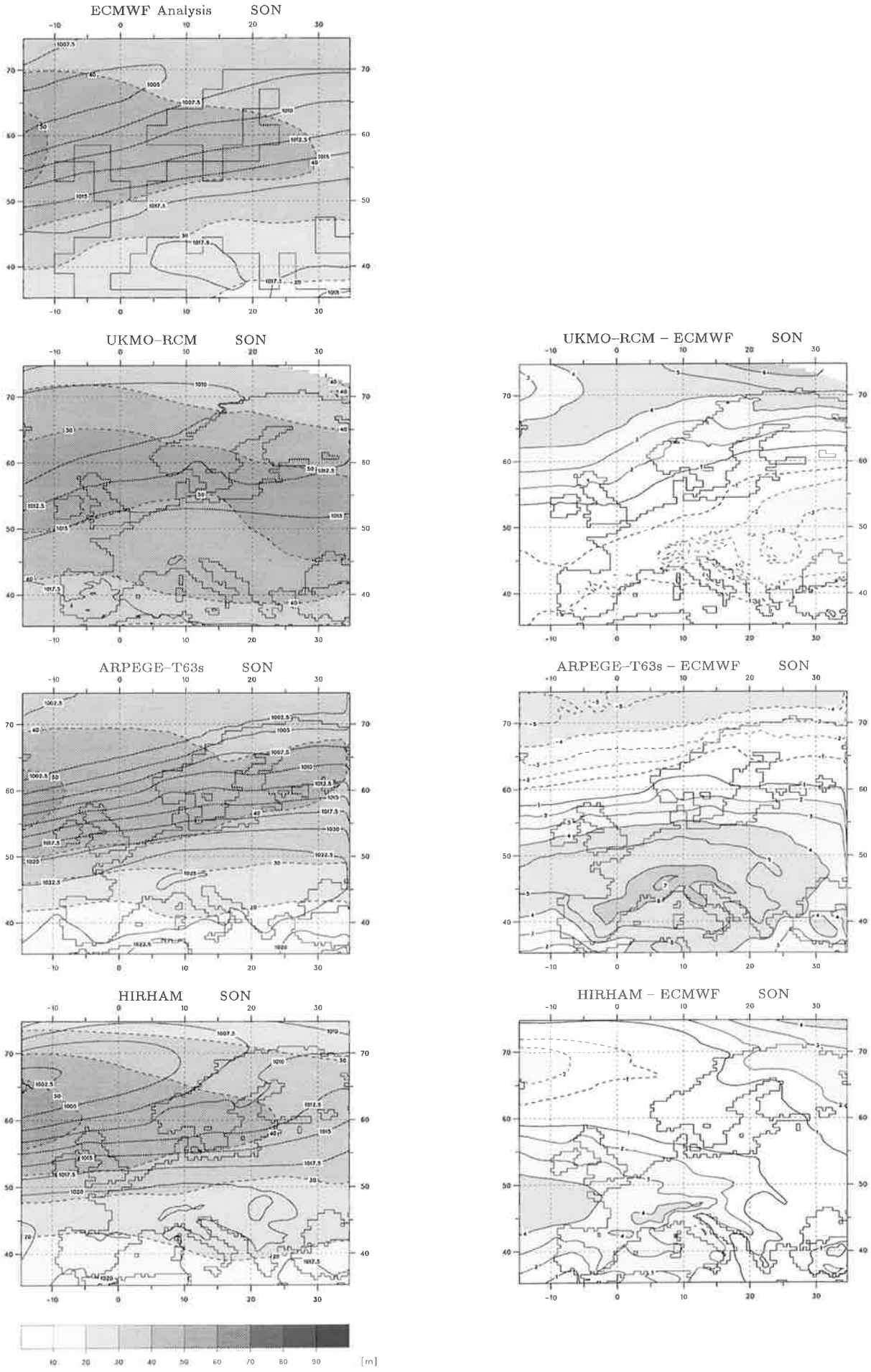

Figure 2.8: **Left column:** MSLP [hPa] for ECMWF Analysis and RCM's for SON (solid lines) and standard deviation of band pass filtered 500 hPa height [m] (shaded). **Right column:** Systematic error of MSLP [hPa].

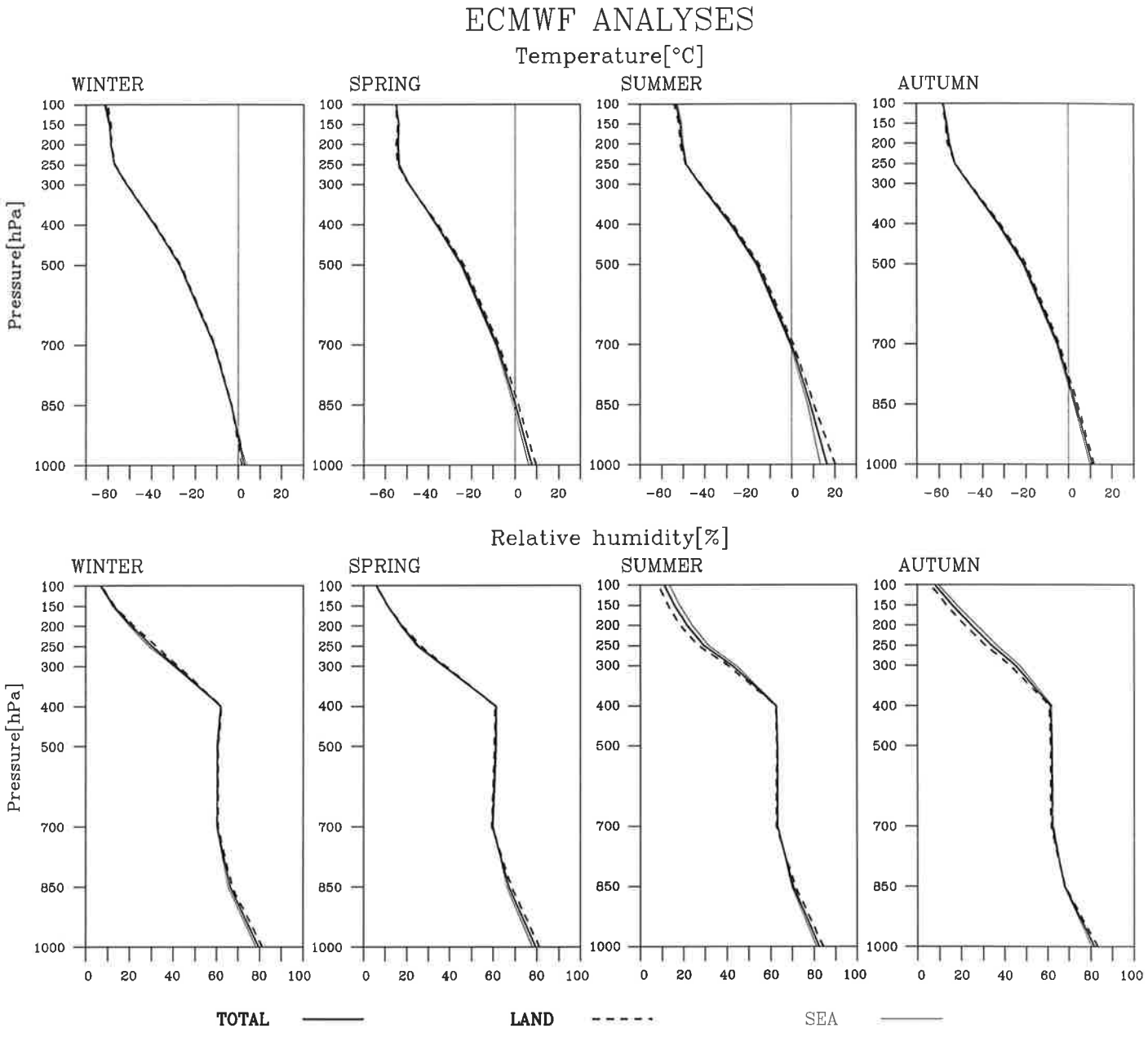

Figure 3.1 Observed profiles avaraged over the CRU domain and the seasons, derived from ECMWF analyses. For temperature 14 years (1979, 1981–1993) and for relative humidity 6 years (1981–1986) of data used.

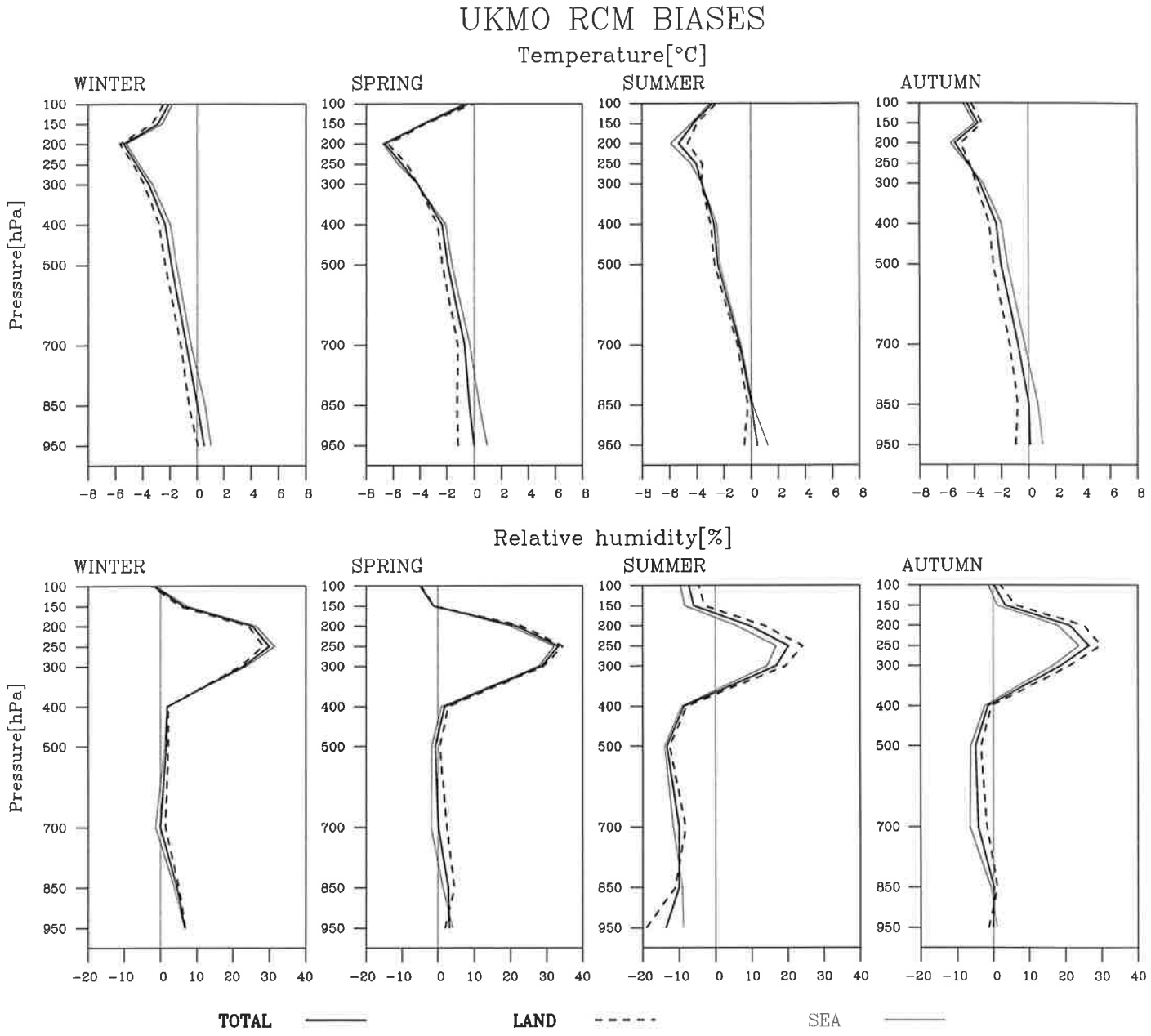

Figure 3.3 As Fig. 3.2 but for UKMO RCM.

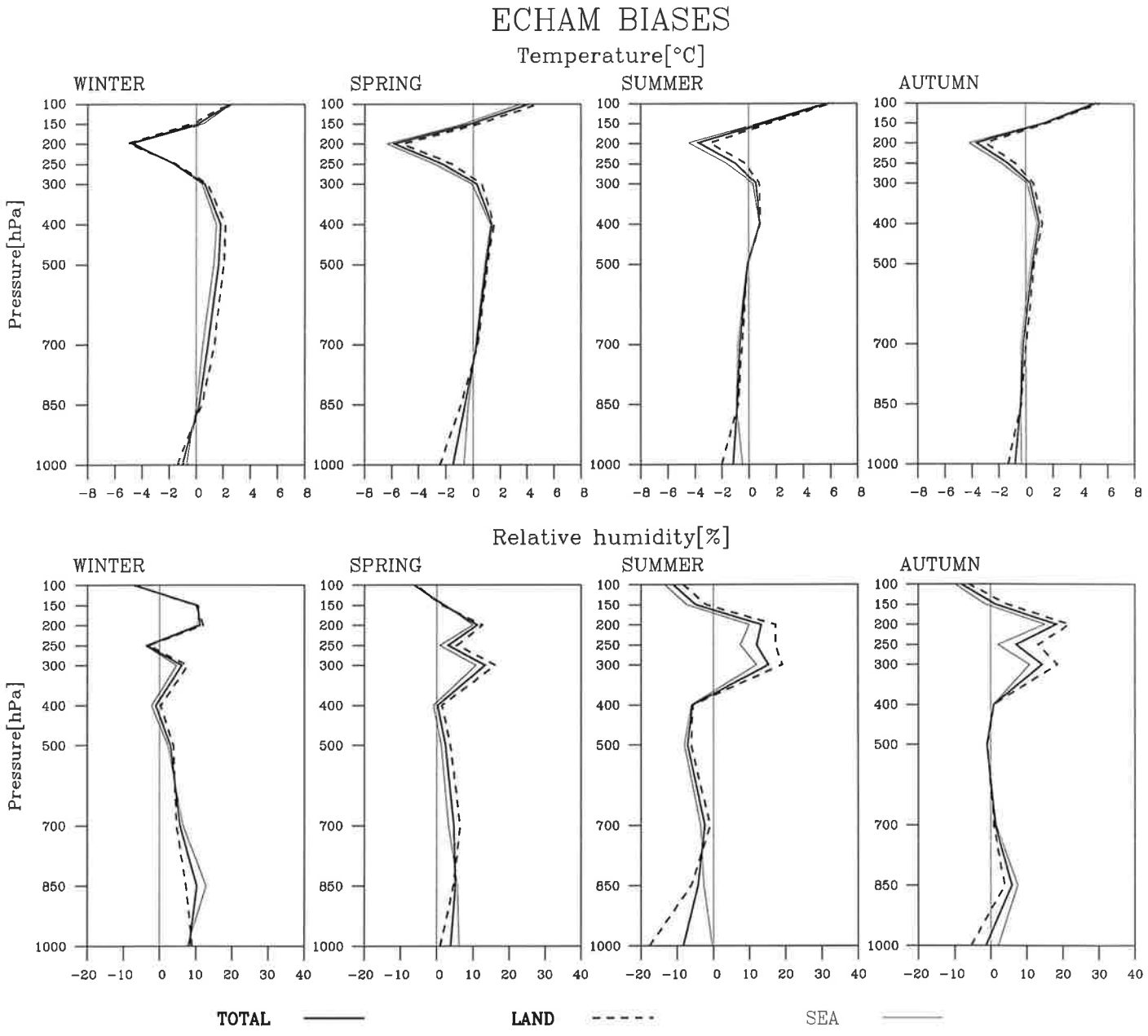

Figure 3.4 As Fig. 3.2 but for ECHAM.

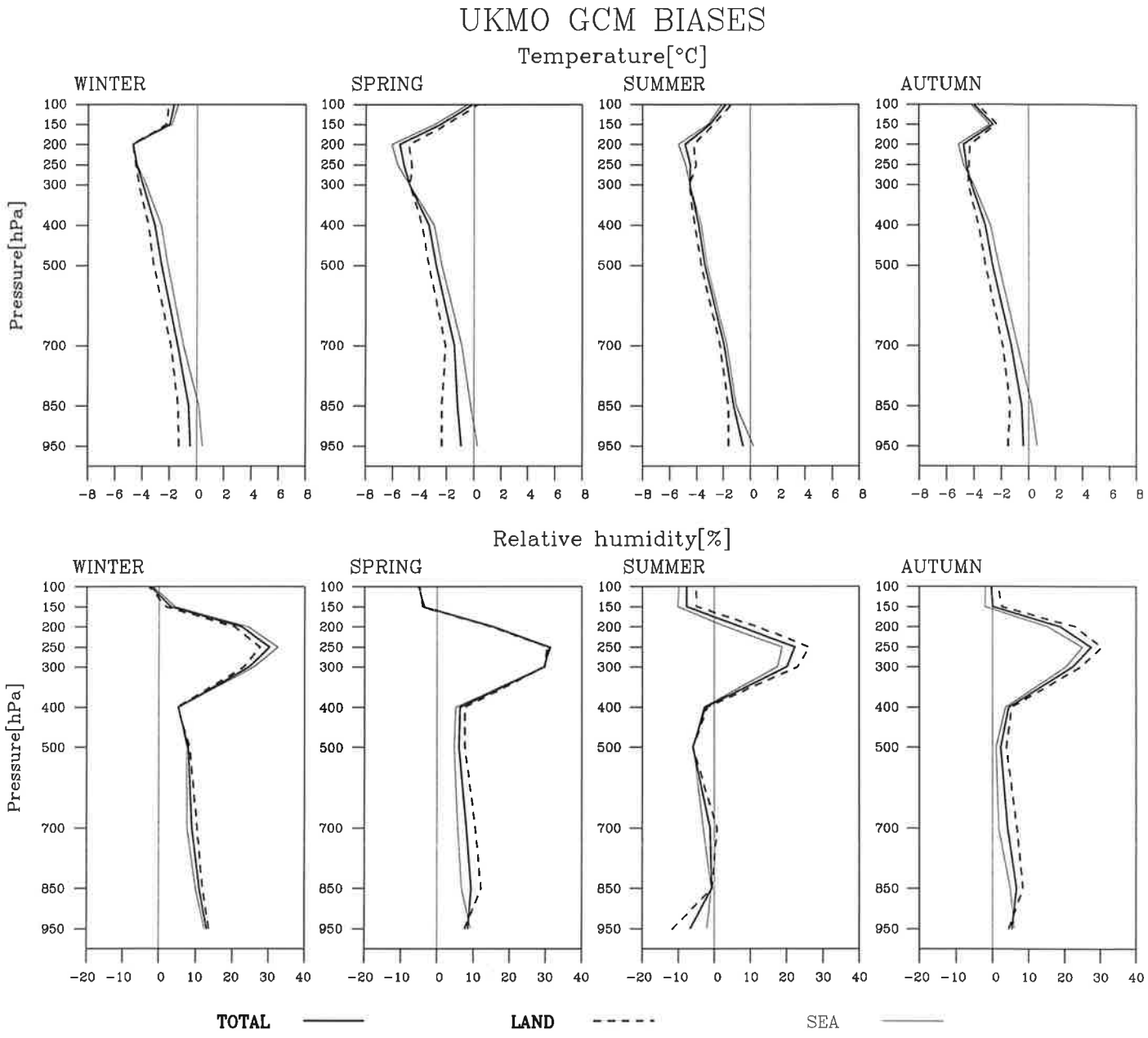

Figure 3.2 Deviations from the observed profiles in Fig. 3.1 (biases) of the UKMO GCM simulation.

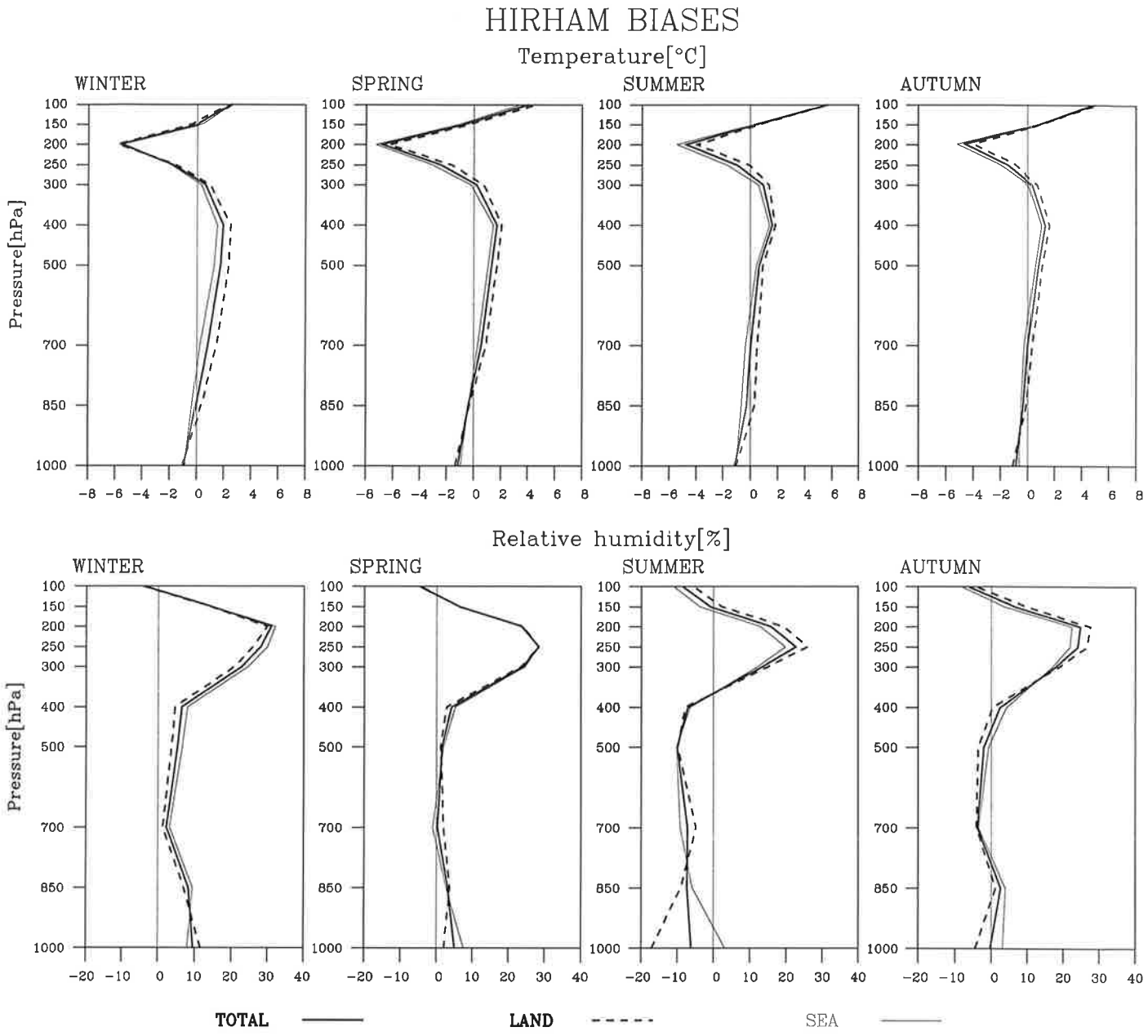

Figure 3.5 As Fig. 3.2 but for HIRHAM.

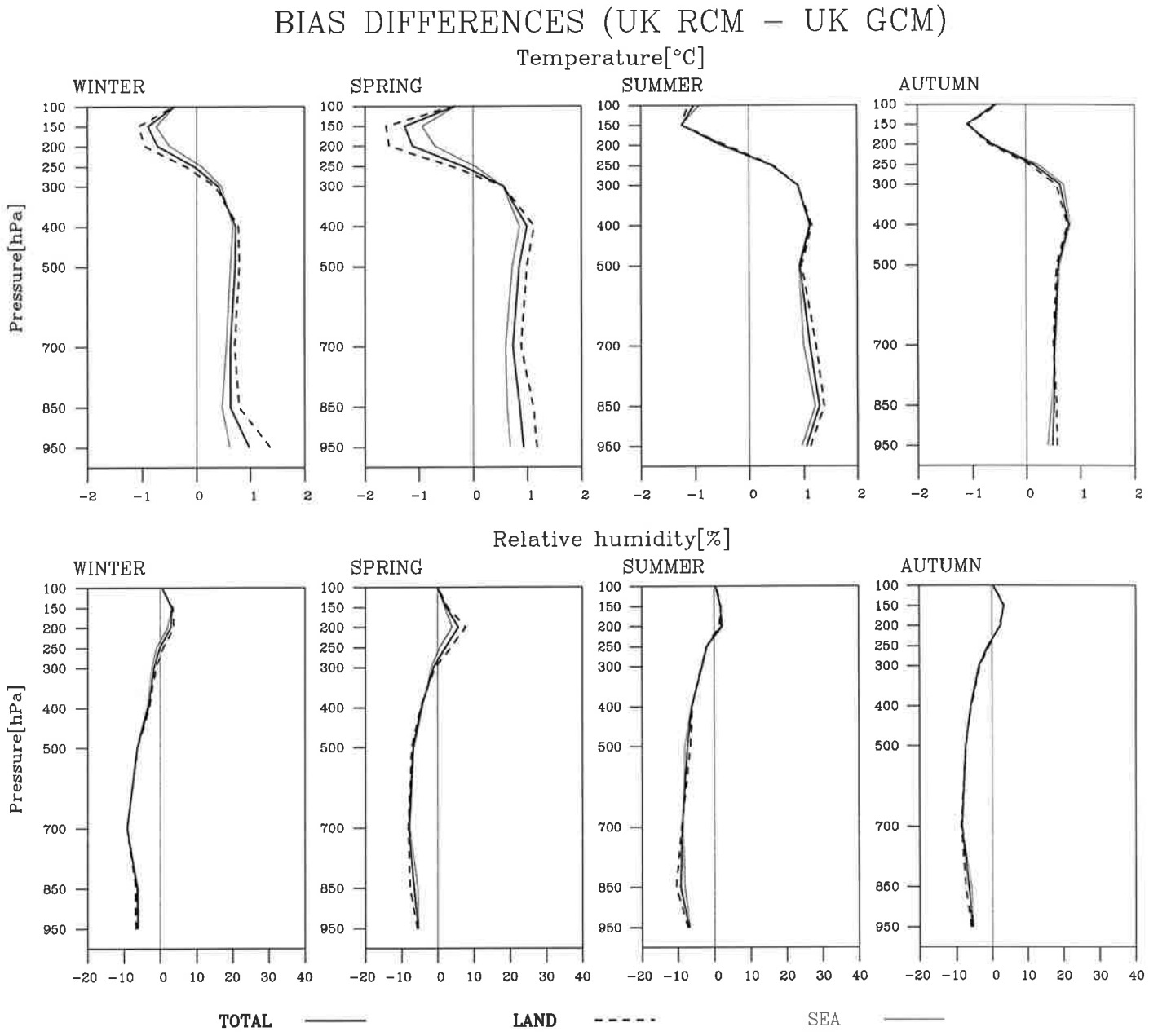

Figure 3.6 Profiles of differences between the biases of the UKMO RCM (Fig. 3.2) and the GCM (Fig. 3.1) simulations.

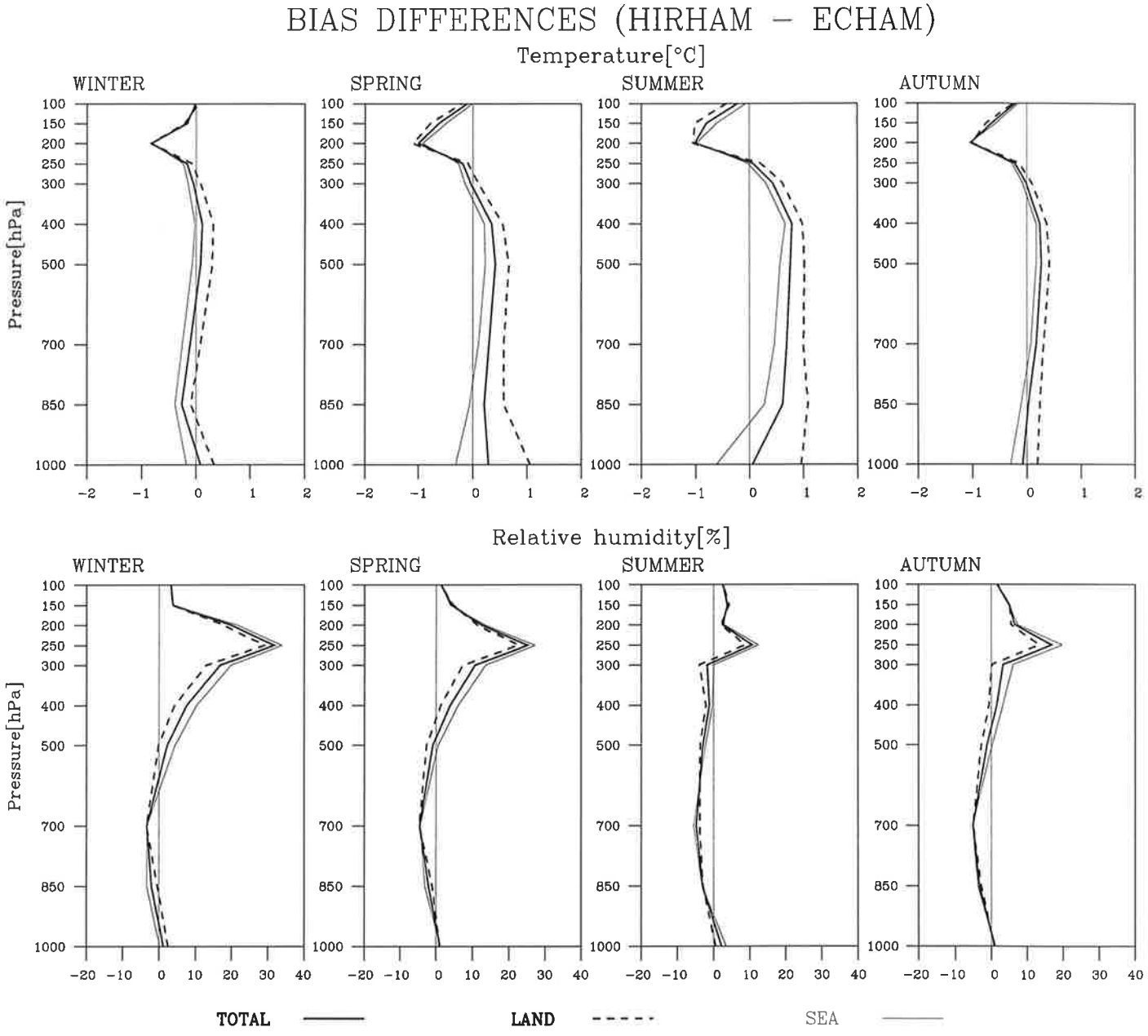

Figure 3.7 Profiles of differences between the biases of the HIRHAM and the ECHAM simulations.

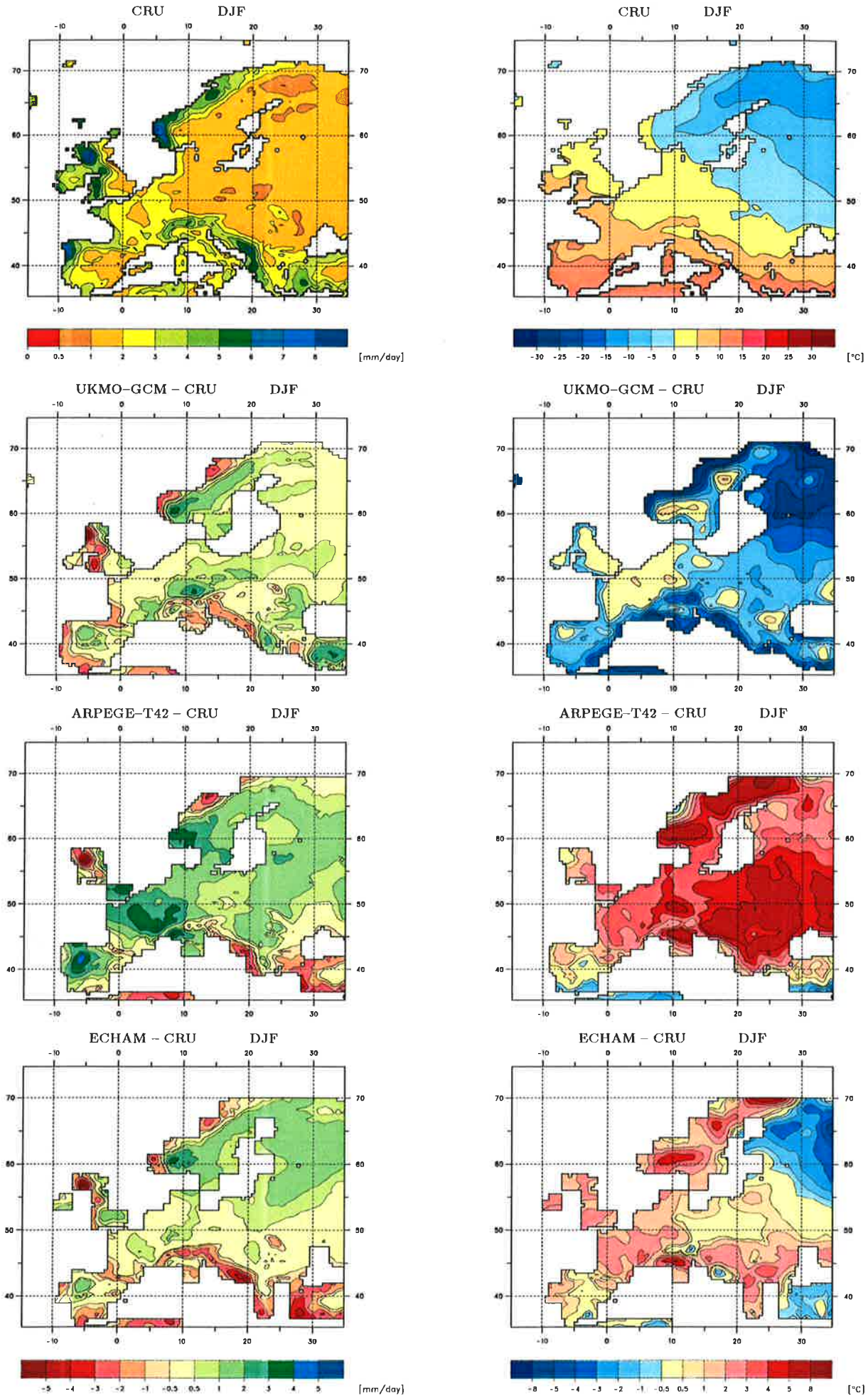

Figure4.1: **Left column:** Precipitation [mm/day] for DJF, upper panel climatology, lower panels difference between GCM's and climatology. **Right column:** Surface air temperature reduced to mean sea level [°C] for DJF, upper panel climatology, lower panels difference between GCM's and climatology.

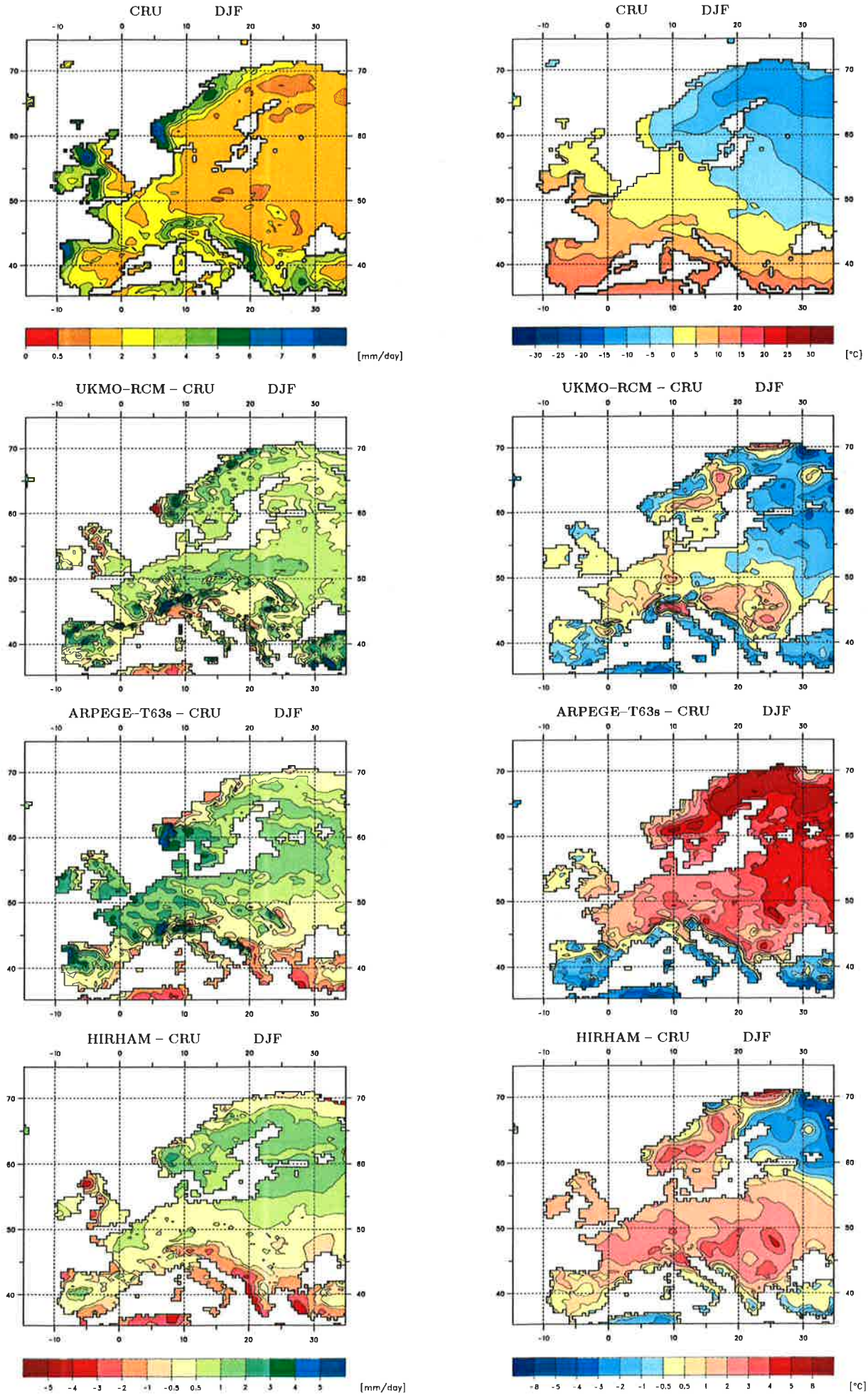

Figure4.2: **Left column:** Precipitation [mm/day] for DJF, upper panel climatology, lower panels difference between RCM's and climatology. **Right column:** Surface air temperature reduced to mean sea level [°C] for DJF, upper panel climatology, lower panels difference between RCM's and climatology.

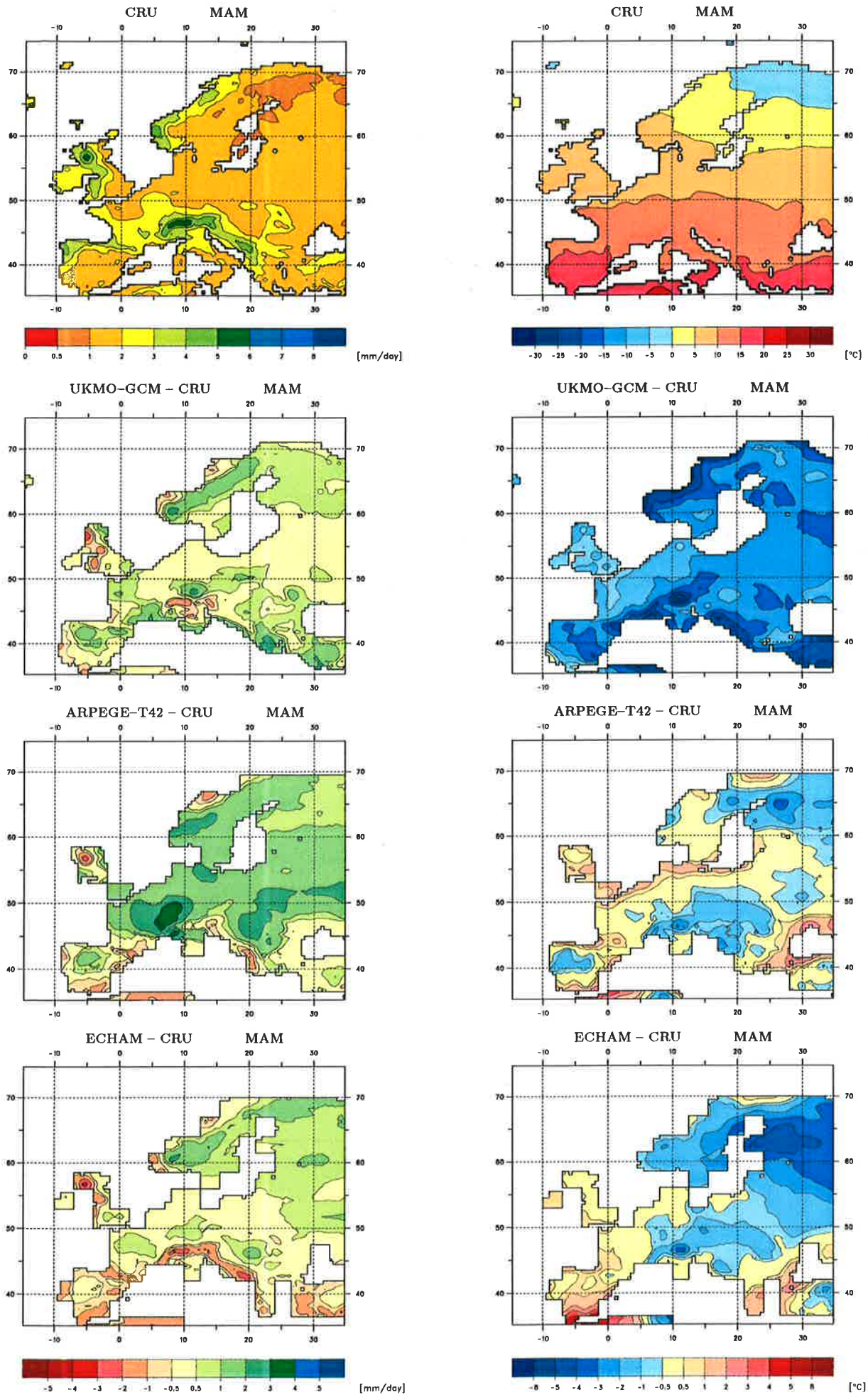

Figure4.3: **Left column:** Precipitation [mm/day] for MAM, upper panel climatology, lower panels difference between GCM's and climatology. **Right column:** Surface air temperature reduced to mean sea level [°C] for MAM, upper panel climatology, lower panels difference between GCM's and climatology.

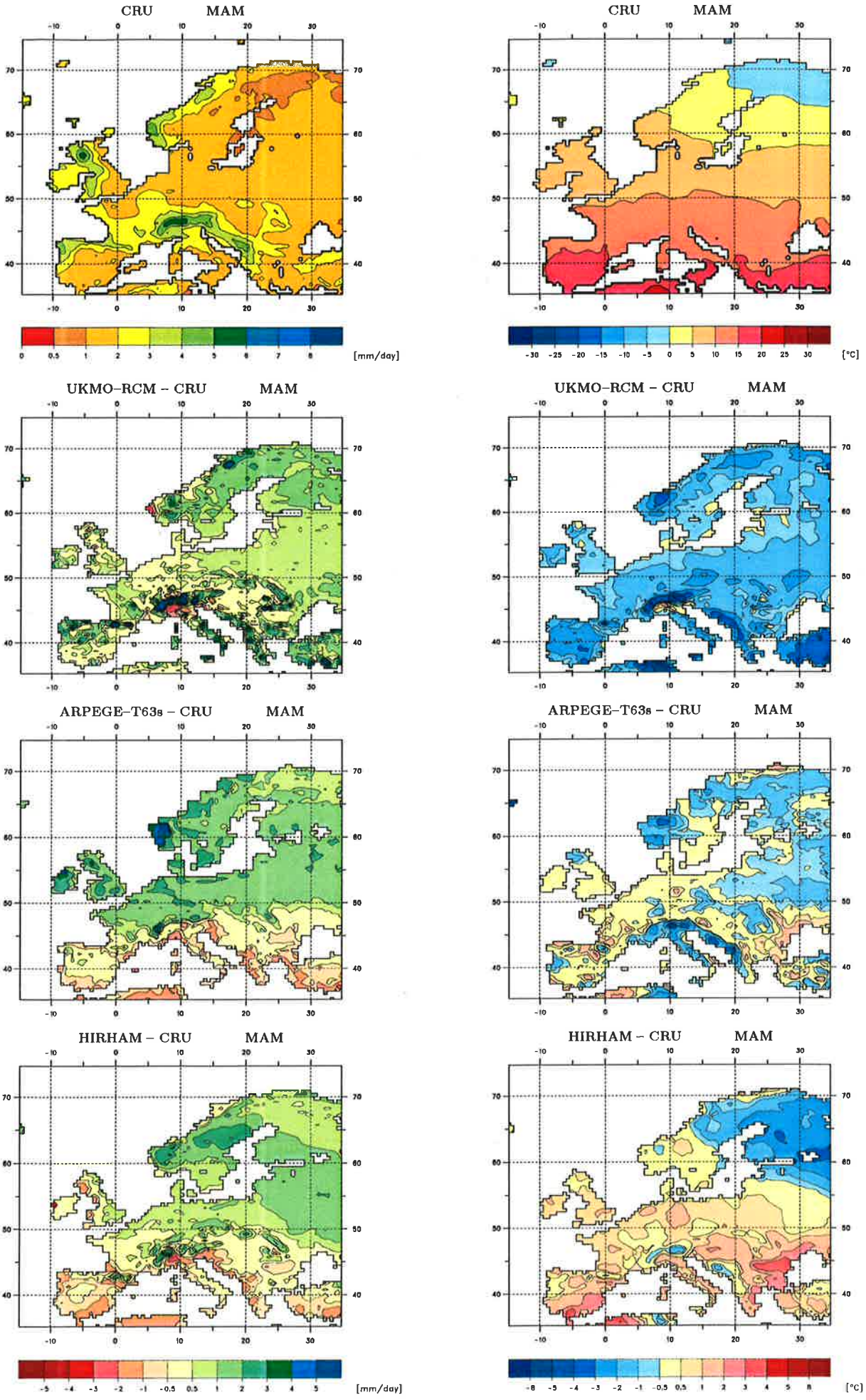

Figure4.4: **Left column:** Precipitation [mm/day] for MAM, upper panel climatology, lower panels difference between RCM's and climatology. **Right column:** Surface air temperature reduced to mean sea level [°C] for MAM, upper panel climatology, lower panels difference between RCM's and climatology.

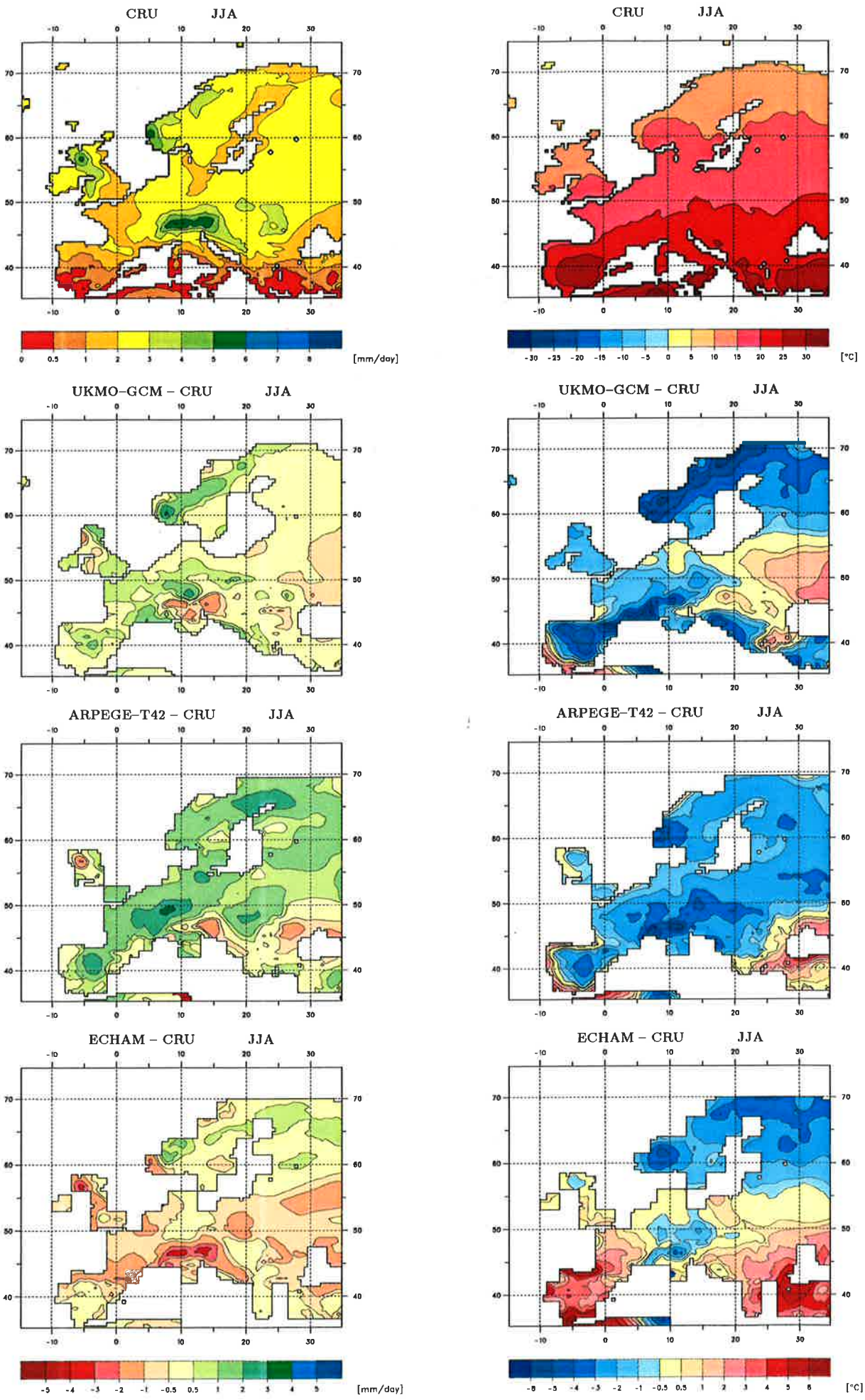

Figure4.5: **Left column:** Precipitation [mm/day] for JJA, upper panel climatology, lower panels difference between GCM's and climatology. **Right column:** Surface air temperature reduced to mean sea level [°C] for JJA, upper panel climatology, lower panels difference between GCM's and climatology.

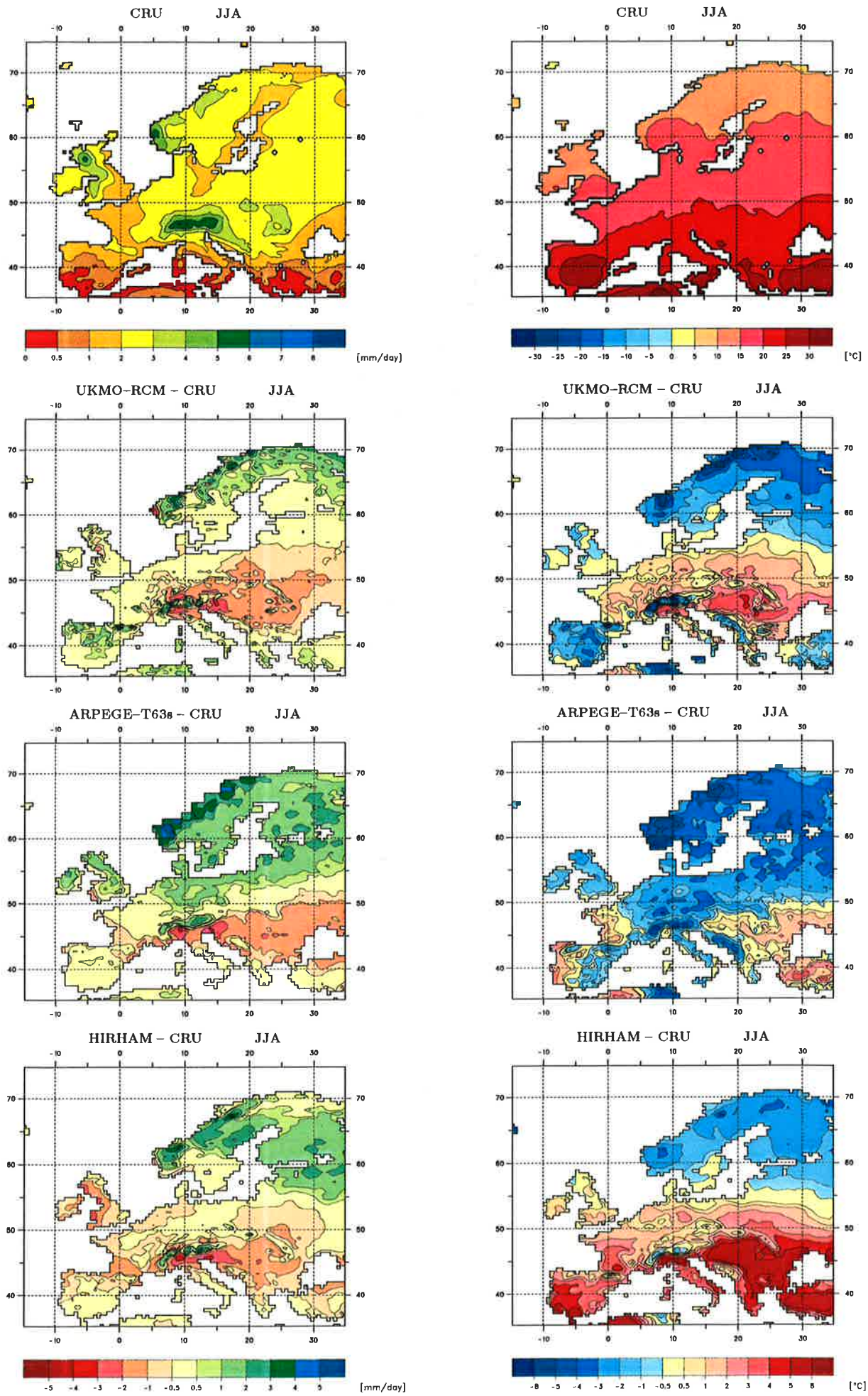

Figure4.6: **Left column:** Precipitation [mm/day] for **JJA**, upper panel climatology, lower panels difference between RCM's and climatology. **Right column:** Surface air temperature reduced to mean sea level [°C] for **JJA**, upper panel climatology, lower panels difference between RCM's and climatology.

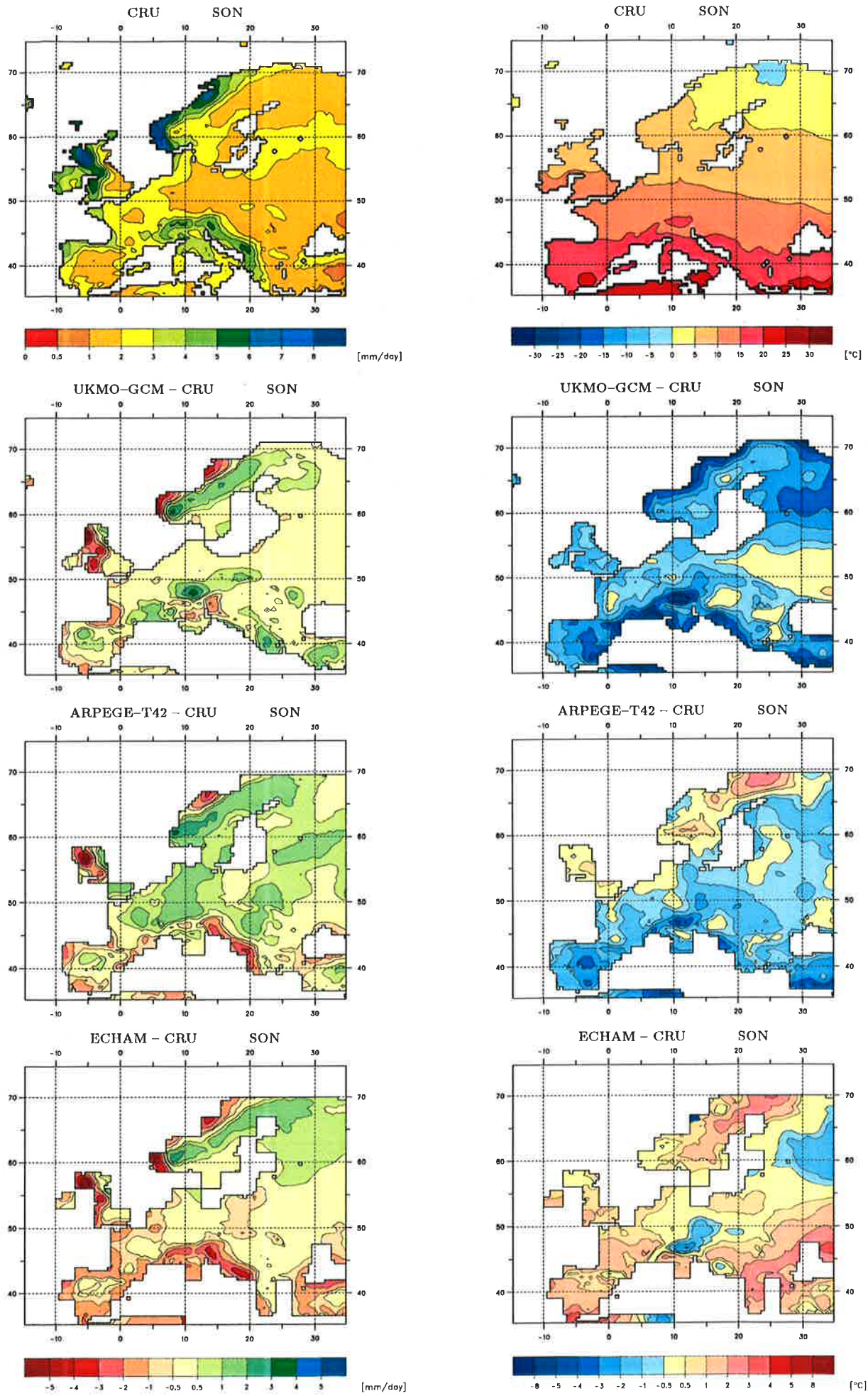

Figure4.7: **Left column:** Precipitation [mm/day] for SON, upper panel climatology, lower panels difference between GCM's and climatology. **Right column:** Surface air temperature reduced to mean sea level [°C] for SON, upper panel climatology, lower panels difference between GCM's and climatology.

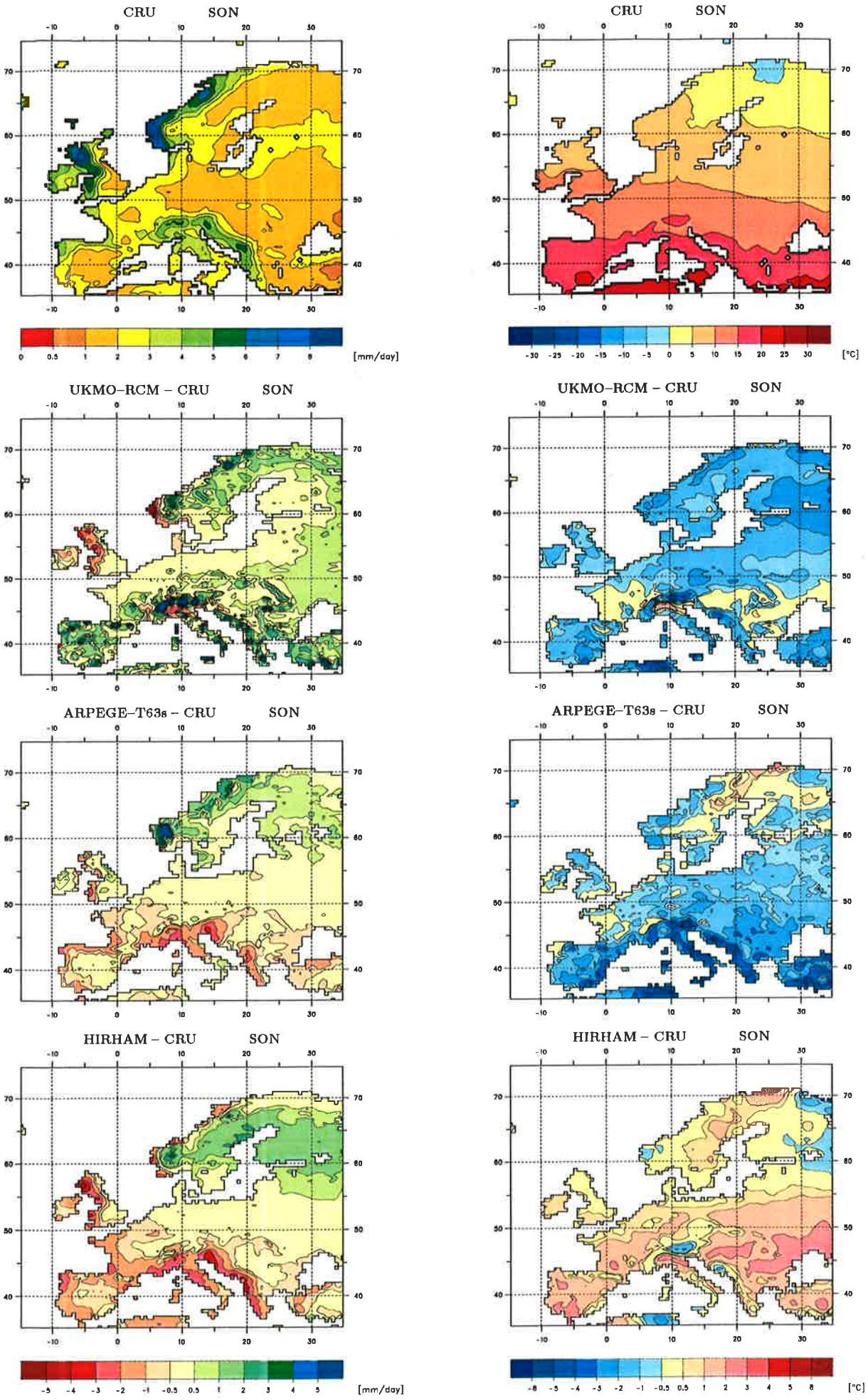

Figure4.8: **Left column:** Precipitation [mm/day] for SON, upper panel climatology, lower panels difference between RCM's and climatology. **Right column:** Surface air temperature reduced to mean sea level [°C] for SON, upper panel climatology, lower panels difference between RCM's and climatology.

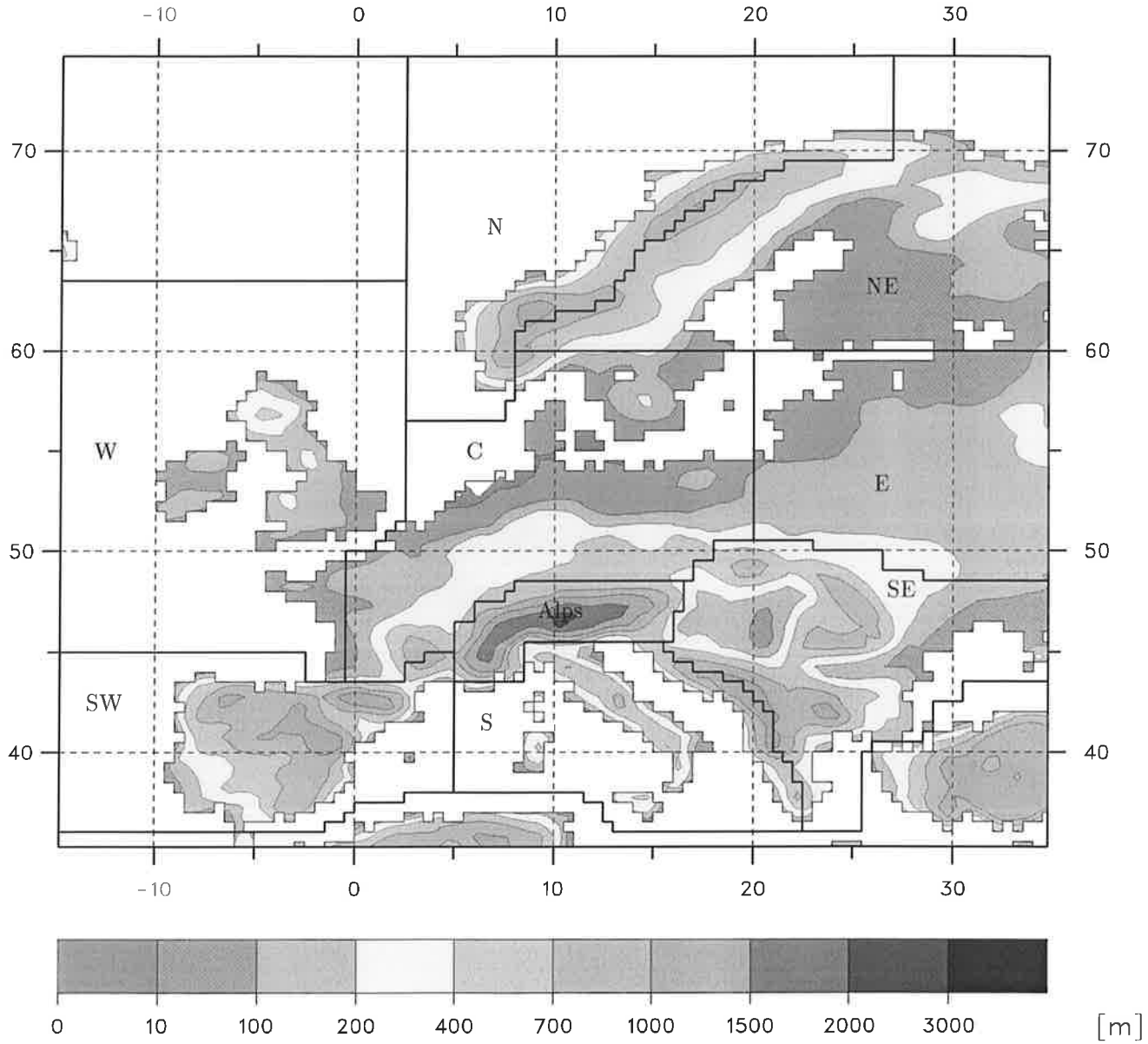

Figure5.1: Sub–areas for Europe shown on HIRHAM orography.

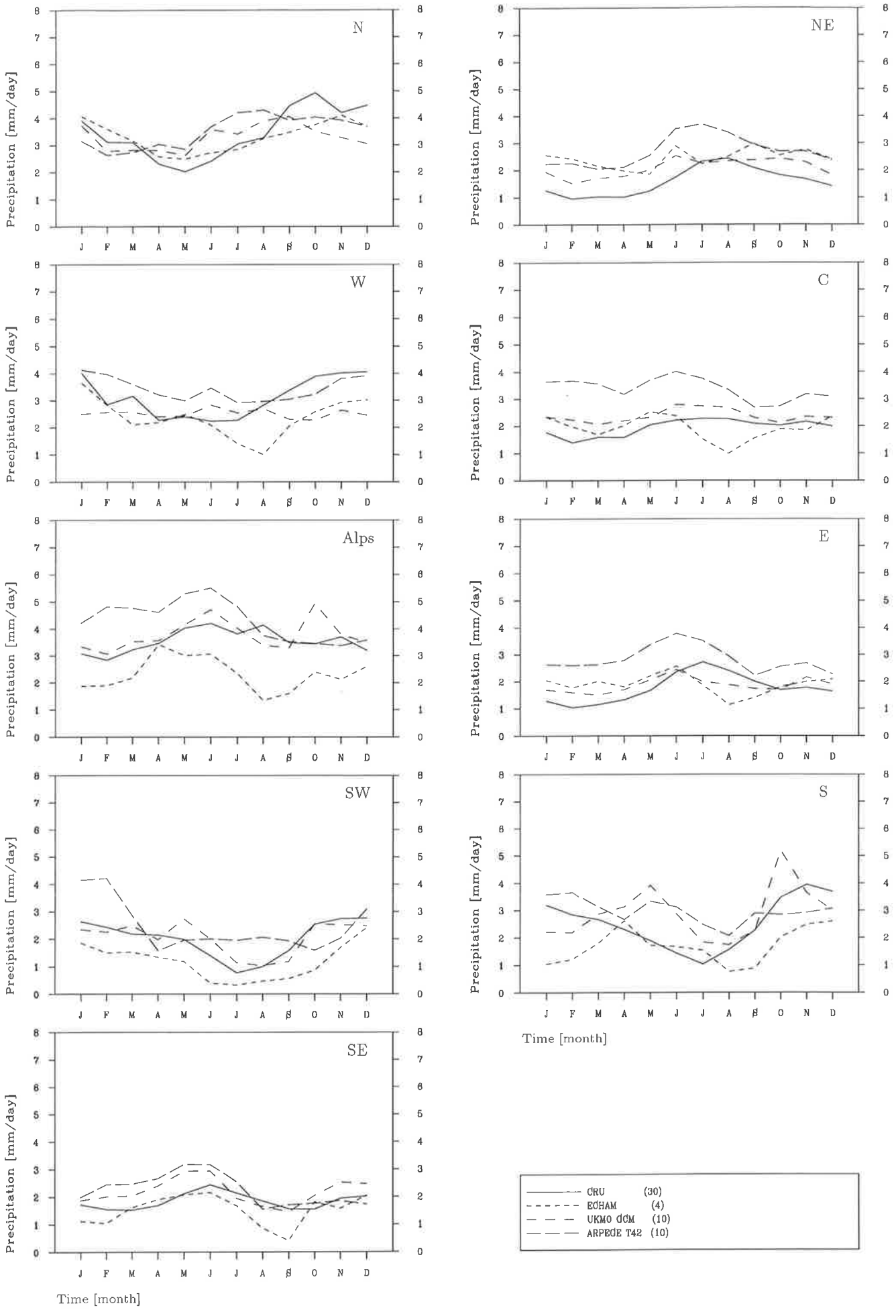

Figure5.2: Sub-area means of multi-year averaged monthly precipitation [mm/day] for land points for CRU and GCM's.

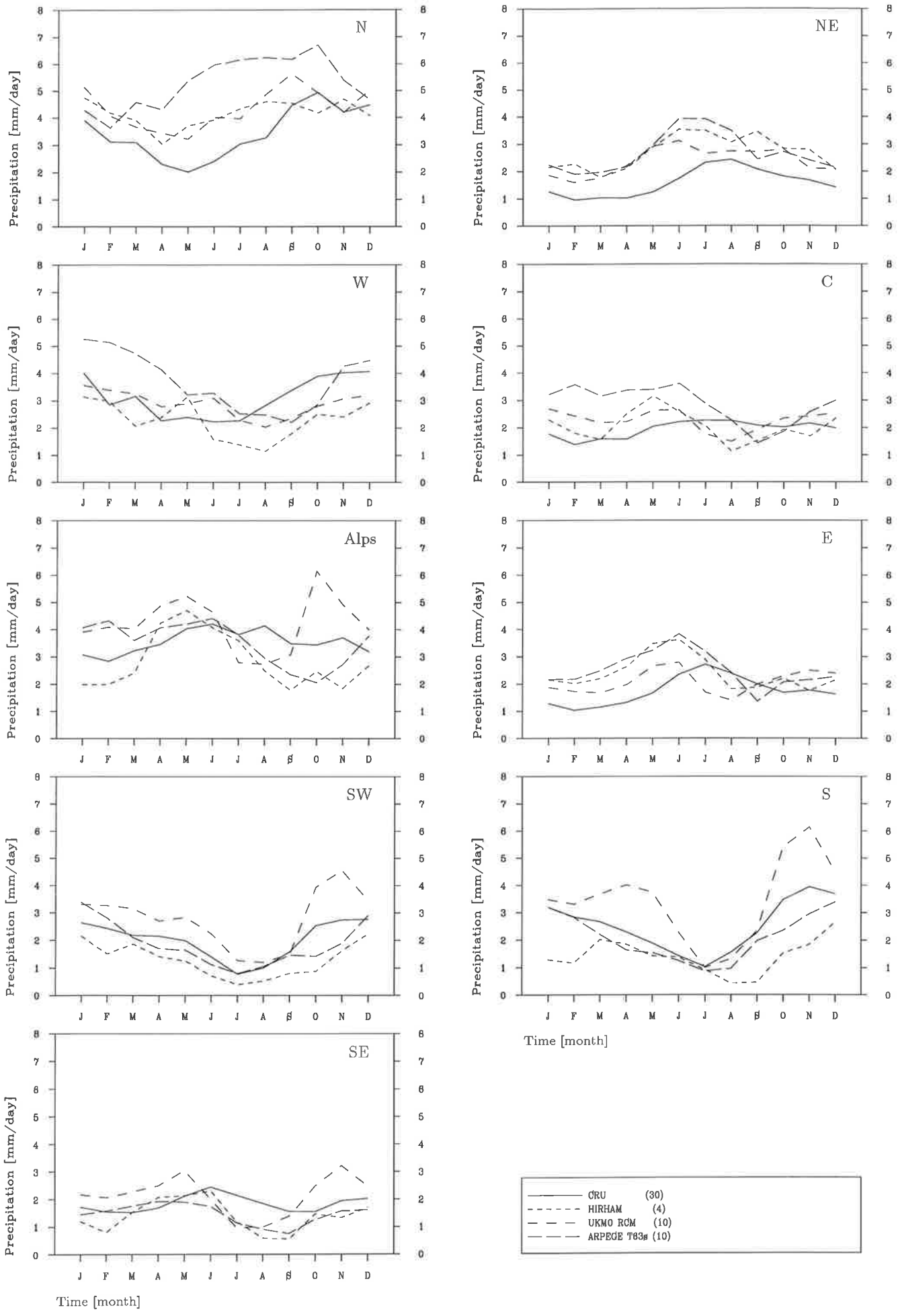

Figure5.3: Sub–area means of multi–year averaged monthly precipitation [mm/day] for land points for CRU and RCM's.

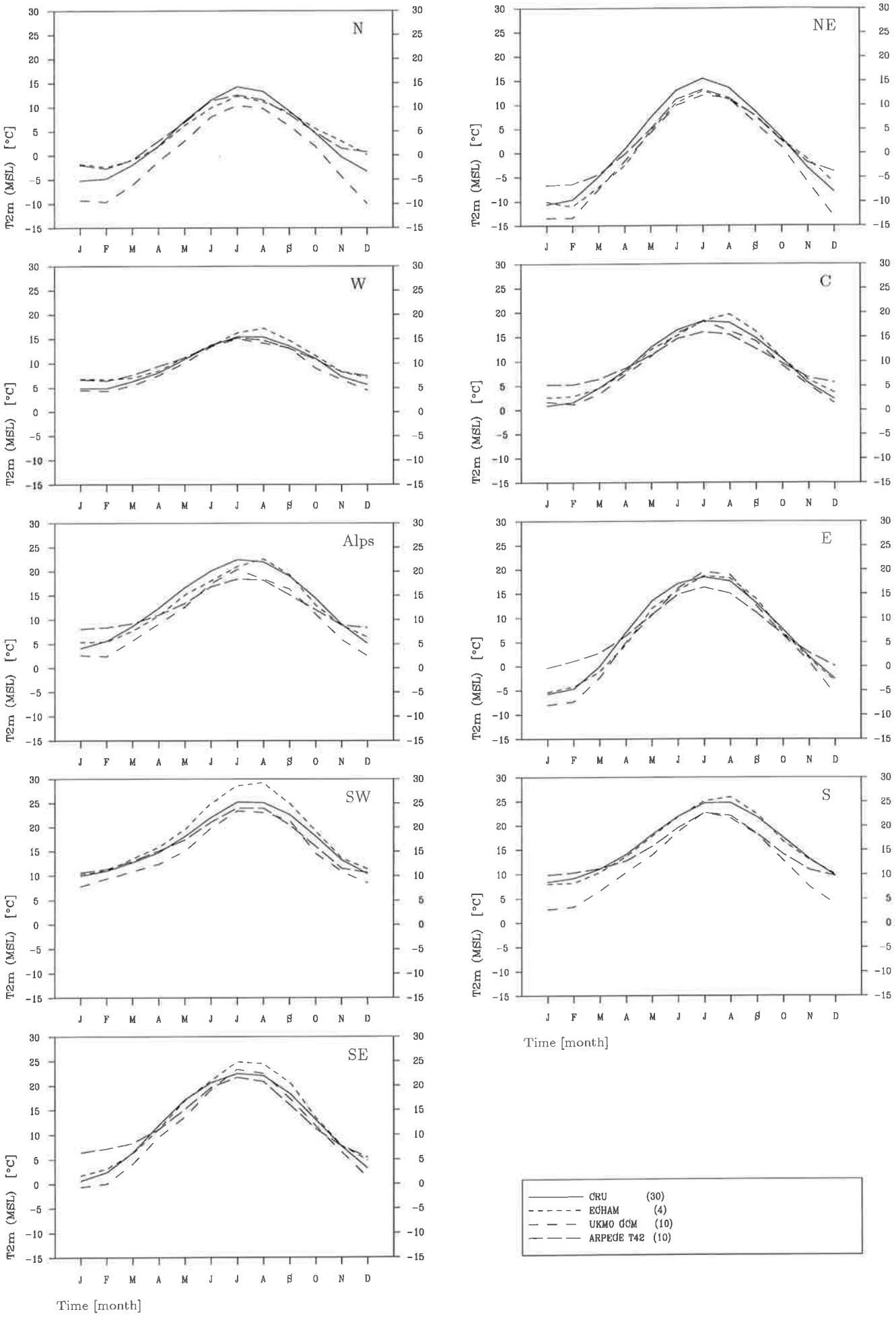

Figure5.4: Sub-area means of multi-year averaged monthly surface air temperature reduced to MSL [°C] for land points for CRU and GCM's.

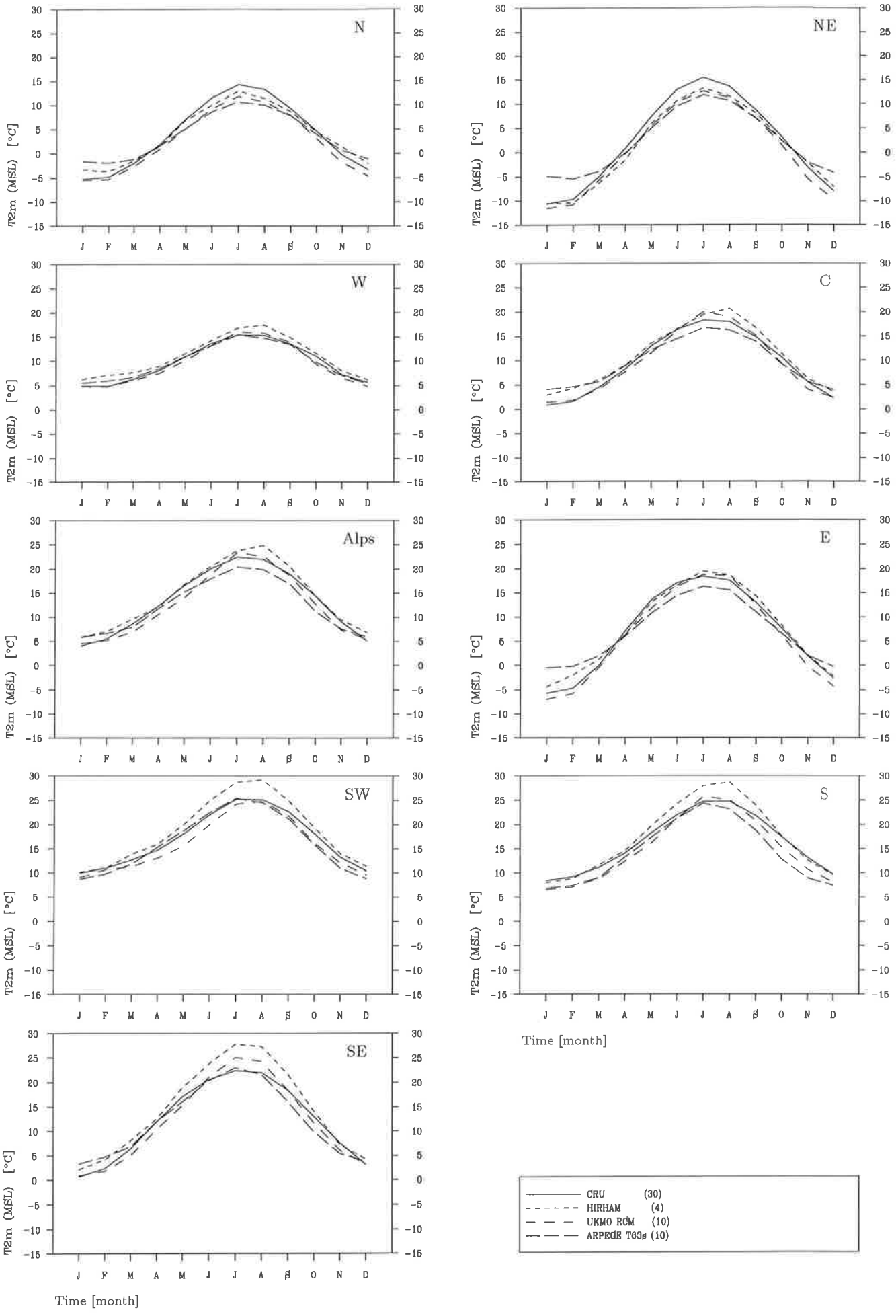

Figure5.5: Sub–area means of multi–year averaged monthly surface air temperature reduced to MSL [°C] for land points for CRU and RCM's.

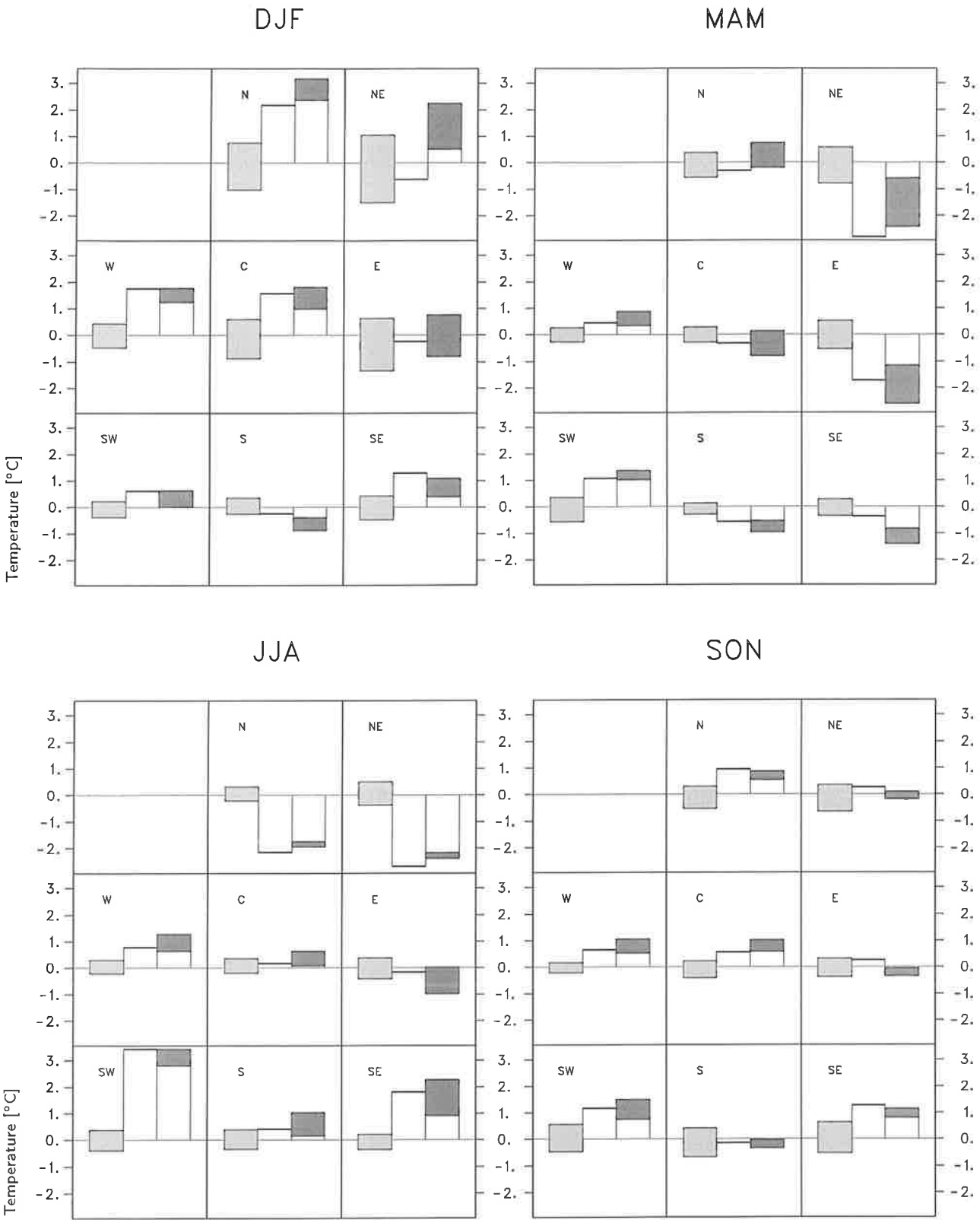

Figure 6.1: For each season and each sub-area (see Figure 5.1) temperature biases of the 46-months ECHAM3 simulation together with estimates of observed and modelled intervals of decadal variabilities. In each diagram the bar in the middle shows the bias of the 46-months simulation, the right hand bars show the minimum and maximum of the biases obtained in five different AMIP simulations and the left hand bars show the minimum and the maximum out of 21 observed 10-year averages. The intervals of decadal variability are shaded.

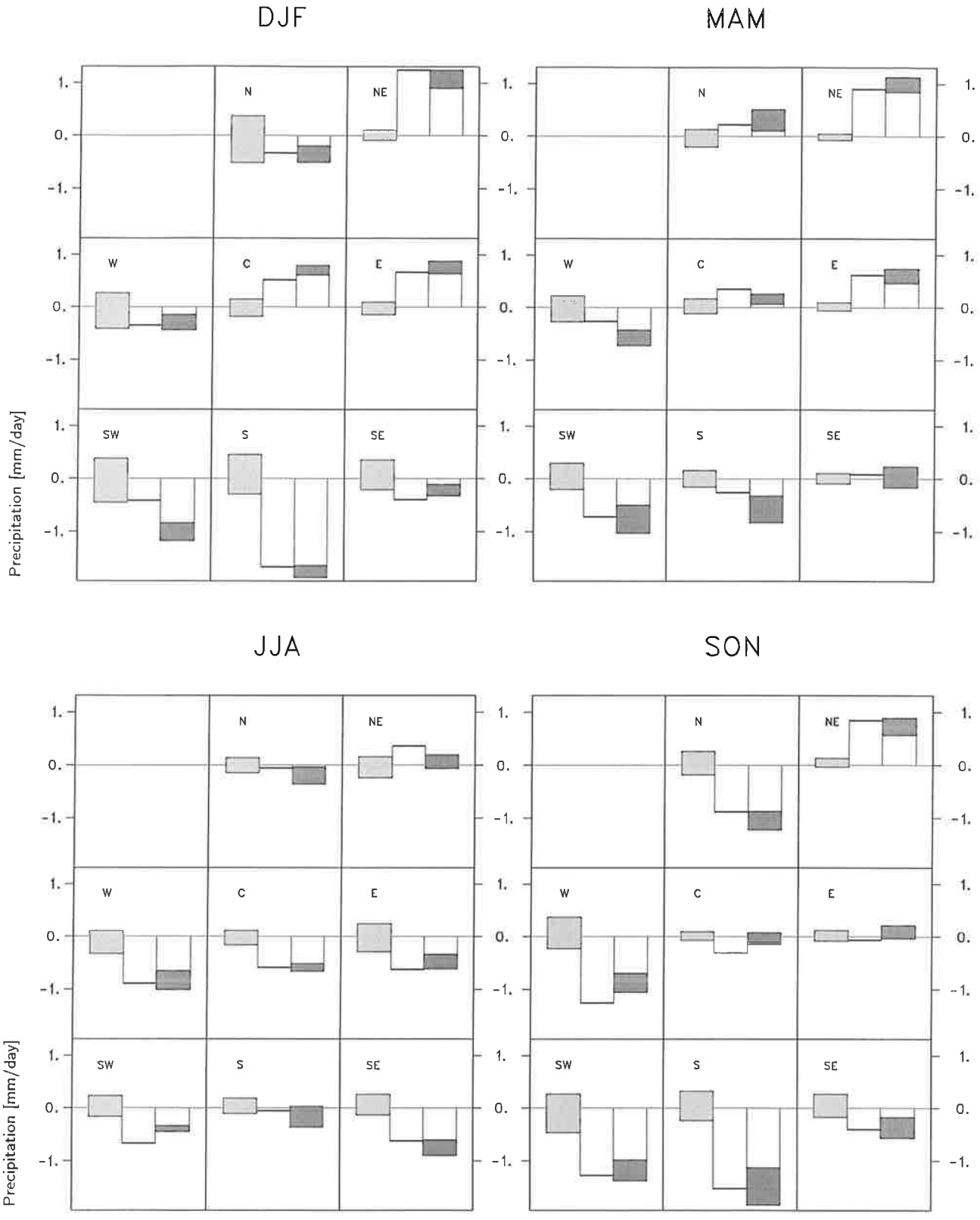

Figure 6.2: As Figure 6.1 except for precipitation.